Development and Characterization of circRNA sponges to functionally inhibit miR-122

Dissertation

vorgelegt von

Isabelle Jost

(Master of Science in Biology)

zur Erlangung des akademischen Grades

doctor rerum naturalium

(Dr. rer. nat.)

Justus-Liebig-Universität Gießen

FB 08 Biologie und Chemie

Gießen, Dezember 2017

Die vorliegende Arbeit wurde am Institut für Biochemie des Fachbereichs 08 der Justus-Liebig-Universität Gießen in der Zeit von September 2013 bis Dezember 2017 unter der Leitung von Professor Dr. Albrecht Bindereif angefertigt.

Dekan	**Prof. Dr. Volker Wissemann**
	Institut für Spezielle Botanik
	Fachbereich für Biologie und Chemie
	Justus-Liebig-Universität Gießen
1. Gutachter	**Prof. Dr. Albrecht Bindereif**
	Institut für Biochemie
	Fachbereich für Biologie und Chemie
	Justus-Liebig-Universität Gießen
2. Gutachter	**Prof. Dr. Michael Niepmann**
	Biochemisches Institut
	Fachbereich Humanmedizin
	Justus-Liebig-Universität Gießen

I. TABLE OF CONTENTS

II. ABSTRACT

Recent advances in RNA sequencing (RNA-seq) techniques and sequence analysis methods have led to the discovery of thousands of exonic circular RNAs (circRNAs), expressed in many species. These covalently closed RNA circles were assumed to be alternative products of pre-mRNA processing by the spliceosome. Being investigated more extensively only during the last five years, few circRNA candidates were characterized, and the understanding of their global biological relevance is still very limited. The currently best investigated circRNA is *CDR1as*/*ciRS-7,* which contains more than 70 miR-7 binding sites. It is thought to function as a microRNA (miRNA) sponge by competing for miR-7 binding with its targets. Due to their elevated stability compared with linear RNAs, circRNAs are particularly attractive for biotechnological and therapeutic applications.

In order to experimentally substantiate the hypothesis that circRNAs are processed by the spliceosome, plasmid-encoded circRNA splicing reporters (minigenes) were generated. Sequence elements of the natural gene context were gradually removed and a detailed mutational analysis of splice signals was performed. The minigene derivatives were then transfected into cells and processing products were detected via RT-PCR. With this approach, the requirement of fundamental splicing signals for efficient and precise exon circularization was demonstrated. The results provide valid evidence for the involvement of the spliceosome in circRNA biogenesis.

The very abundant and liver-specific miR-122 is an essential host factor in hepatitis C virus (HCV) infection. Miravirsen, which sequesters miR-122, is the first locked nucleic acid (LNA)-modified antisense oligonucleotide (oligo) drug for HCV treatment that has entered clinical trials. Based on the concept of the natural *CDR1as*/*ciRS-7* miRNA sponge, artificial circRNA sponges for functional sequestration of miR-122 from HCV RNA were designed. The artificial circRNAs were synthesized *in vitro* by enzyme-based transcription and ligation of eight consecutive binding sites, followed by gel-purification of the circular miRNA sponges. The *in vitro* generated circRNAs were transfected into cells and analyzed with respect to their subcellular distribution and their stability. Functional inhibition of miR-122 by the circRNAs sponges was tested in three different HCV reporter systems. Efficacy of the miR-122 circRNA sponges was analyzed in comparison to an unspecific circRNA, to their linear counterparts, as well as to miravirsen. The designed circRNA sponges clearly and specifically caused HCV-adverse effects in all tested reporter systems, which is evidence for the functional sequestration of miR-122. This demonstrates the potential of circRNAs to extend the spectrum of RNA-therapeutics as pharmaceutical products in the future.

III. ZUSAMMENFASSUNG

Dank der die jüngsten Fortschritte bei RNA Sequenziermethoden und der Analyse von Sequenzierungsdaten wurden Tausende von exonischen zirkulären RNAs (circRNAs) in vielen Spezies entdeckt. Es wird angenommen, dass diese kovalent geschlossenen RNA-Zirkel alternative Produkte der mRNA Prozessierung durch das Spleißosom darstellen. Da sie erst seit den letzten fünf Jahren eingehender untersucht werden, wurden bisher nur wenige circRNA Kandidaten funktionell charakterisiert, und das Verständnis für ihre übergreifende biologische Relevanz ist begrenzt. Die derzeit am besten untersuchte circRNA ist *CDR1as*/*ciRS-7*, die mehr als 70 miR-7 Bindestellen enthält. Es wird vermutet, dass *CDR1as*/*ciRS-7* wie ein mikroRNA (miRNA) Schwamm wirkt, also um die Bindung von miR-7 mit den Ziel-mRNAs konkurriert. circRNAs sind, durch ihre erhöhte Stabilität verglichen mit linearen RNAs, besonders attraktiv für biotechnologische und medizinische Anwendungsgebiete.

Um die Hypothese, dass circRNAs vom Spleißosom generiert werden, experimentell zu untermauern, wurden Plasmide mit circRNA Spleiß-Reportern (Minigen-Konstrukte) hergestellt. Zuerst wurden Sequenzelemente aus dem Kontext des natürlichen Gens schrittweise entfernt, um dann eine detaillierte Mutationsanalyse der Spleißsignale durchzuführen. Die Minigen-Konstrukte wurden in Zellen eingebracht, und die Prozessierungsprodukte wurden mittels RT-PCR analysiert. Mit Hilfe dieser Vorgehensweise konnte gezeigt werden, dass die grundlegenden Spleißsignale für die effiziente und präzise Zirkularisierung von Exons notwendig sind. Diese Ergebnisse liefern stichhaltige Beweise für die Beteiligung des Spleißosoms bei der Biogenese von circRNAs.

Die sehr abundante und leber-spezifische miR-122 spielt bei der Infektion mit dem Hepatitis-C Virus (HCV) eine essentielle Rolle als Wirtsfaktor. Miravirsen sequestriert miR-122 und wurde als erstes LNA-modifiziertes Antisense-Oligonukleotid zur Behandlung von HCV in klinischen Studien geprüft. Basierend auf dem Konzept von *CDR1as*/*ciRS*-7 als miRNA Schwamm, wurden artifizielle circRNAs konzipiert und hergestellt, um miR-122 zu blockieren und dadurch HCV zu hemmen. Die Synthese von artifiziellen circRNAs erfolgte durch enzym-basierte Transkription und Ligation von acht aufeinanderfolgenden Bindestellen, gefolgt von einer Gel-Aufreinigung. Die circRNAs wurden dann transfiziert, um sie hinsichtlich ihrer Lokalisierung und Stabilität innerhalb der Zelle zu untersuchen. Die funktionelle Inaktivierung von miR-122 durch die circRNAs wurde mit drei verschiedenen HCV Reporter Systemen getestet. Dabei wurde die Wirksamkeit der zirkulären miRNA Schwämme, mit einer unspezifischen circRNA, dem jeweiligen linearen Gegenstück und miravirsen verglichen. Die circRNA Schwämme haben deutliche und spezifische HCV-hemmende Effekte, was ein Indiz dafür ist, dass miR-122 erfolgreich inaktiviert wurde. Dadurch konnte gezeigt werden, dass circRNAs das

Potenzial haben als pharmazeutisches Produkt zukünftig zur Erweiterung des Spektrums von RNA-Therapeutika beizutragen.

1 INTRODUCTION

1.1 Central Dogma

Almost 60 years ago, Sir Francis Crick stated, what he called the central dogma, and postulated the flow of genetic information from DNA over RNA to protein, which represent the three most important macromolecules in the cell. The genetic information is stored in DNA molecules and is encoded by its sequence. This information can either be replicated to ensure sustainability, or the information is passed via RNA molecules for decoding into a polypeptide chain, which folds into a functional protein. However, genetic information cannot be transferred from a given protein to nucleic acids, or to another protein (Crick, 1970). The central dogma, which was at that time rather hypothetical, was proven and represents the basic principle of gene expression, today. Many discoveries between 1958 and today, have changed the understanding of a gene product. The potential of RNA goes far beyond being only a messenger molecule or template for protein synthesis.

1.2 Eukaryotic gene expression and pre-mRNA processing

Eukaryotic gene expression starts with transcription of a given gene by RNA polymerase II (RNAP II) in the nucleus. With the aid of transcription factors and the mediator complex, RNAP II initiates at the promoter region and starts transcribing the gene at the transcription start site (TSS). In order to generate a functional mRNA, the precursor-mRNA (pre-mRNA) undergoes three major maturation steps: 1) capping, 2) splicing and 3) polyadenylation (**Figure 1**). The capping machinery is recruited co-transcriptionally by the carboxy-terminal domain (CTD) of RNAP II. It adds a N7-methyl-guanosine 5'-triphosphate (m^7Gppp) to the 5' carbon of the first nucleotide of the nascent transcript.

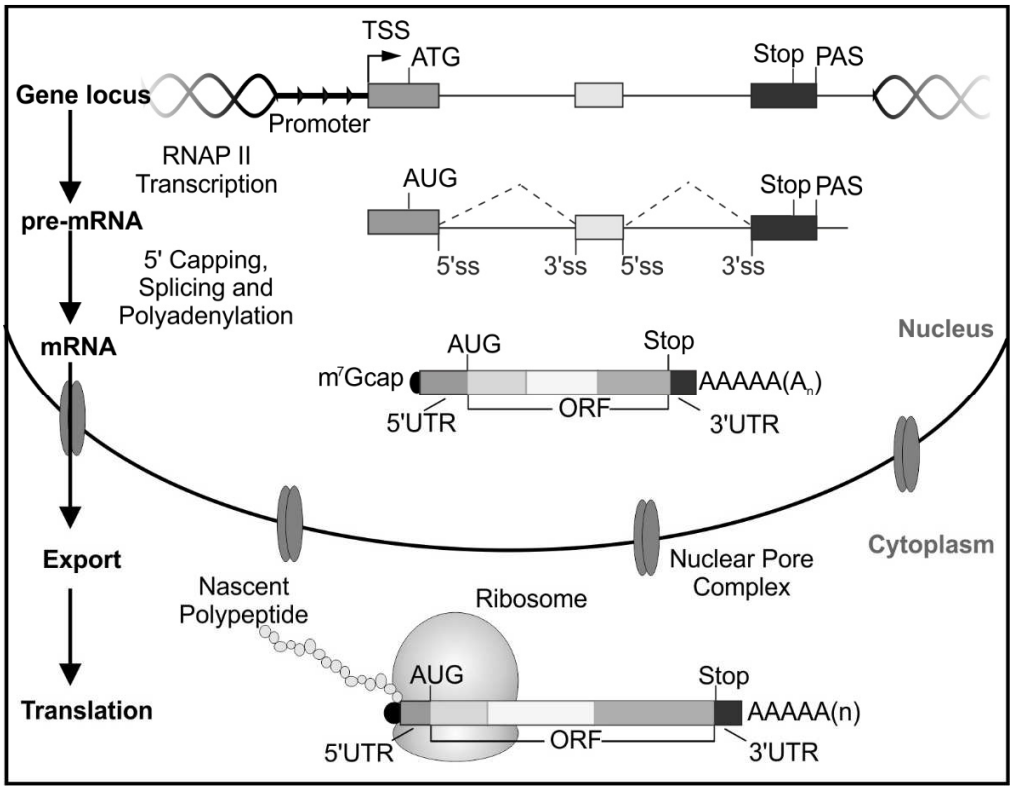

Figure 1 Eukaryotic gene expression.
Eukaryotic gene expression starts in the nucleus by RNAP II transcription at the gene locus. The newly synthesized pre-mRNA is co-transcriptionally modified by the capping machinery, which adds a m^7G cap at the 5'end. Introns (depicted as a line) are removed, and the exons (represented by boxes) are ligated during splicing, which is executed by the spliceosome. 5' and 3' splice sites (ss) define the intron/exon boundaries. The polyadenylation signal (PAS) marks the end of the transcript. At this position it is cleaved and a poly(A)-tail is added. The mature mRNA is exported through the nuclear pore complex (NPC) to the cytoplasm, where it is translated into a polypeptide chain, which then folds into a functional protein. The protein-coding region of the mRNA is signified by the start codon (AUG) and a stop signal. This region is translated by the ribosome and is called open reading frame (ORF). The ORF is flanked by 5' and 3' untranslated regions (UTRs), which regulate translation efficiency and mRNA stability.

After the RNAP II has passed the PAS, the primary transcript is cleaved, and the poly(A) polymerase adds approximately 200 adenosine residues, termed poly(A)-tail. The cap structure and poly(A)-tail are important for export to the cytoplasm, recognition by the translational machinery and mRNA stability. Transcription, capping, splicing and polyadenylation are coupled processes, which regulate each other (reviewed in Moore & Proudfoot, 2009; Bentley, 2014).

1.2.1 The molecular mechanism of splicing

Protein-coding genes in eukaryotes consist of expressed sequences (exons), which are interrupted by intervening sequences (introns) (Sharp, 1994). In order to provide a mature mRNA, the introns, are removed from the pre-mRNA by a process termed splicing (Moore & Sharp, 1993). It occurs co-transcriptionally and is executed by a macromolecular complex, the spliceosome. For correct excision of introns, which can be several kilobases (kb) long, sequence elements and splicing signals that specify the intron/exon boundaries are required (Lim & Burge, 2001) (**Figure 2**). Although introns in higher eukaryotes are much longer and more frequent, the consensus sequences in yeast are more conserved compared to human. This is attributed to the fact, that splicing in man is more complex.

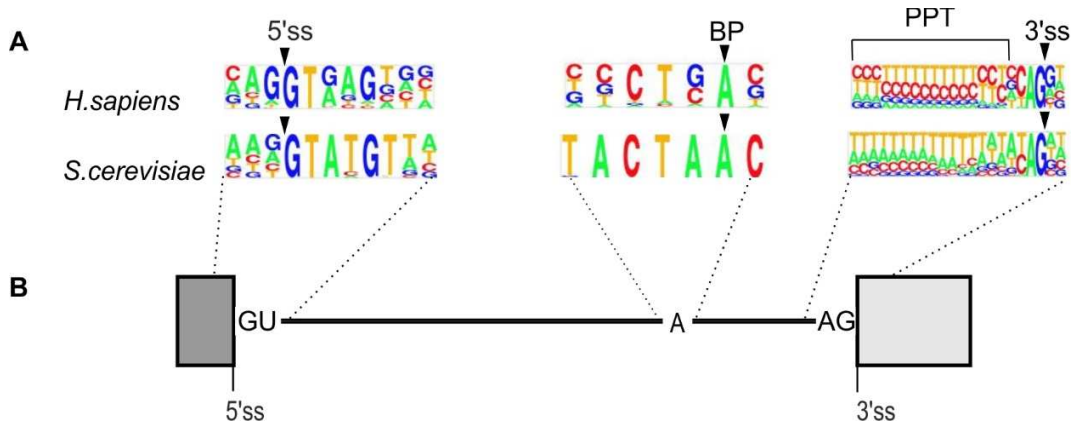

Figure 2 Splicing signals are conserved from yeast to man.
Consensus sequence motifs of *S.cerevisiae* and *H.sapiens* (**A**).
The 5'ss is defined by two universally conserved intronic GU nucleotides (nt). The 3'ss is defined by an almost invariant AG dinucleotide. A pyrimidine-rich region, which is termed polypyrimidine tract (PPT) is located directly upstream of the 3'ss. The BP adenosine (A) is located approximately 100 nt upstream (**B**) (modified after Lim & Burge, 2001; Patel & Steitz, 2003).

The spliceosome is a large and dynamic macromolecular machinery composed of five uridine-rich small nuclear RNAs (U snRNAs) and about 300 proteins in humans. The snRNAs U1, U2, U4, U5

and U6 are present as pre-assembled small nuclear ribonucleoprotein (snRNPs) complexes (Wahl et al, 2009; Will & Lührmann, 2011; Nguyen et al, 2016 and references therein). Each snRNP has a set of individual proteins, but they share a set of seven common core proteins, the Sm proteins (SmB, SmD1, SmD2, SmD3, SmE, SmF and SmG). These shared proteins assemble in a characteristic heptameric ring structure on a conserved region of the snRNAs, which is termed Sm site (Kambach et al, 1999). Assembly of the spliceosome occurs stepwise on the pre-mRNA substrate, and the four major building blocks U1 snRNP, U2 snRNP, tri-snRNP U5-U4/U6 and the nineteen complex (NTC) sequentially enter and leave spliceosome in a cycle (Jurica & Moore, 2003) (**Figure 3**).

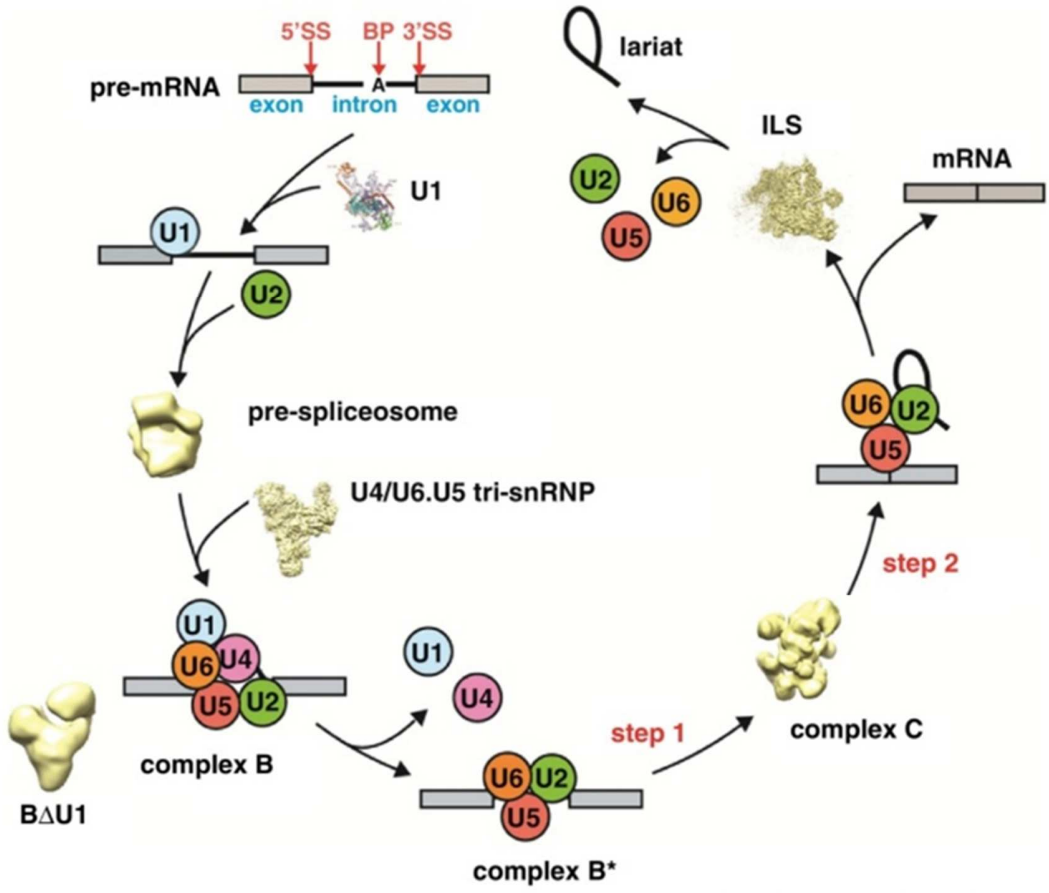

Figure 3 Spliceosome assembly.
The spliceosome assembles step-wise on its pre-mRNA substrate, and recognizes the 5'ss, 3'ss and the BP (red arrows). The five snRNPs (U1, U2, U4, U5, and U6) sequentially enter and leave the spliceosome. Discrete assembly steps were captured by electron microscopy (EM) and cryoEM, revealing the shape of the spliceosome at different stages, such as complex B, BΔU1, B*, C and the post-catalytic intron lariat spliceosome (ILS) (Nguyen et al, 2016).

The first step in spliceosome assembly is recognition of the 5' splice site (ss) by U1 snRNA. This interaction is mediated by base-pairing with the 5'end of the snRNA and the consensus sequence

of the substrate (complex E). Then transition to complex A is accomplished by binding of U2AF auxiliary factor to the BP and recruitment of the U2 snRNP. Complex B is generated, when U4/U5/U6 tri-snRNP enters. Thereby U1 snRNP leaves, and its interaction with the 5'ss is replaced by U6 snRNP. Then U4 snRNP is released and the NTC complex, which is a pre-assembled protein complex named after Prp19, joins. Moreover U6 and U2 snRNA undergo structural rearrangements, forming the catalytically active complex B* and thereby bring the 5'ss and 3'ss in close proximity. Chemically, splicing occurs in a two-step S_N2 transesterification (**Figure 4**). The 2' OH of the BP attacks the phosphate of the 5'ss, which results in release of the 5' exon. Further conformational changes lead to formation of complex C, accompanied by the second transesterification reaction. The free 3' OH of the 5' exon attacks the phosphate of the 3'ss, and both exons are covalently connected. The intron is released as a lariat together with U2, U5 and U6 snRNPs, and the snRNPs are recycled for further splicing reactions.

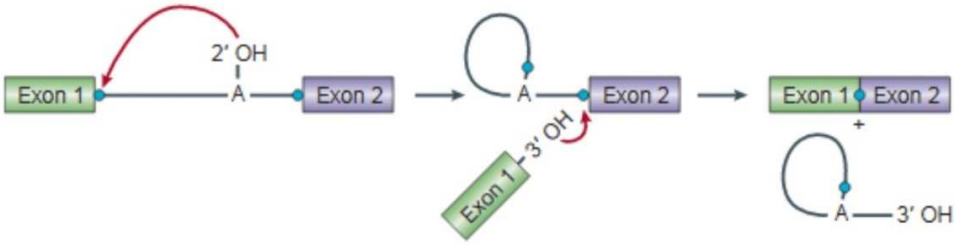

Figure 4 The chemical mechanism of pre-mRNA splicing.
Splicing occurs in two consecutive transesterification reactions. The phosphate of the 5'ss is attacked by the 2' OH of the BP adenosine (A). Thereby the first exon is released, and the free 3' OH of the 5'ss attacks the phosphate of the 3'ss. Both exons are ligated, and the intron is released as a lariat linked by a 2'-5' phosphodiester bond (Patel & Steitz, 2003).

Besides the snRNPs and their associated proteins, several other splicing factors e.g. RNA helicases and RNA binding proteins (RBPs) enter and leave the spliceosome. For a long time it was an open question, if the catalytic reaction is executed by protein or RNA components of the spliceosome. In 2013 Fica and coworkers were able to show that U6 snRNA catalyzes both splicing reactions, by forming a triple helix, which is similar to the tertiary conformation of autocatalytic group II introns. U6 positions two catalytic metal ligands that directly interact with the scissile phosphates (Fica et al, 2013; Fica et al, 2014).

1.2.2 Regulation of splicing and alternative splicing

The evolution of introns has one major advantage: It increases complexity of the proteome by producing more than one protein from a given gene. This is accomplished by different modes of

alternative splicing: exon skipping, alternative 3'ss or 5'ss selection and mutually exclusive inclusion of exons or even retention of the intron. Deep sequencing analysis of the human transcriptome shows that about 95% of the approximately 20,000 protein-coding genes are alternatively spliced, giving rise to about 80,000 transcripts (GENCODE accessed 03.07.2017).

Alternative splicing is regulated by numerous RBPs. The two largest groups are the serine/arginine-rich (SR) protein family or the family of heterogeneous nuclear ribonucleoproteins (hnRNPs). These auxiliary factors bind to sequence elements clustered near or within exons, which either enhance or repress splicing. There are intronic splicing enhancers or silencers (ISE, ISS), as well as exonic splicing enhancers or silencers (ESE, ESS) (Matlin et al, 2005). The regulation of splicing is executed by a huge network of RBPs, which depending on their function are classified as activators or repressors. They compete with each other, act synergistically or are redundant (Fu & Ares, 2014). Basically, the splicing enhancer and silencer elements fine-tune the activity of the spliceosome by recruiting the exon definition or intron definition complex (Ast, 2004).

The consequences of alternatively spliced mRNAs are different protein isoforms. Despite of being alternatively spliced, mRNAs can result in exactly the same protein isoform. But alternatively spliced 5' or 3'UTRs can cause altered mRNA stability, localization or translation efficiencies, and thereby modulate gene expression.

1.3 microRNAs

Every cell of a given organism carries exactly the same genetic information. Especially in multicellular organisms, individual cells have diverse functions and can differentiate into specialized cell types with distinct protein compositions. This set of proteins is not rigid, but adaptable to external influences and stimuli. For this reason gene expression is a dynamic, but tightly controlled process with many layers of regulation. As described above, one possibility to modulate gene expression is the production of different mRNAs by alternative splicing. On the level of mature mRNAs, cells have the ability to fine-tune gene expression by microRNAs (miRNAs). Per definition, miRNAs are single-stranded RNAs with a length between 19 and 24 nt, which are processed from precursors with a hairpin structure by the RNase III type enzyme Dicer. miRNAs regulate gene expression by binding to mRNA targets, which typically results in reduced protein expression (Ambros, 2003).

1.3.1 miRNA biogenesis and decay

The primary miRNA transcript (pri-miRNA) is generated by RNAP II transcription in the nucleus. It is 5' capped, spliced and polyadenylated, and because miRNA loci are sometimes arranged in polycistronic clusters, a pri-miRNA can give rise to several miRNAs. The pri-miRNA is then processed by the microprocessor complex, consisting of the core components Drosha and DGCR8 (Perron & Provost, 2008). These proteins recognize primarily the typical hairpin structure, which contain the mature miRNA. The important elements of this structure are the terminal loop, and an approximately 65 nt long stem, which is flanked by single stranded basal segments. Drosha, which is bound at the basal site of the stem, excises the hairpin miRNA intermediate termed pre-miRNA. Subsequently the pre-miRNA is exported by XPO5 and Ran-GTP to the cytoplasm, where the second maturation step occurs (Leisegang et al, 2012). A 19-24 nt long miRNA duplex with 2 nt 3' overhang is cut from the pre-miRNA by the endonuclease Dicer. Then one strand is loaded onto an Argonaute protein (AGO), forming the effector complex, also known as RNA-induced silencing complex (RISC) (for review Bartel, 2004; Ha & Kim, 2014; Daugaard & Hansen, 2017). Typically the strand, which is less extensively base-paired at its 5'end will become guide strand. The guide incorporates into RISC, while the passenger strand gets degraded (**Figure 5**).

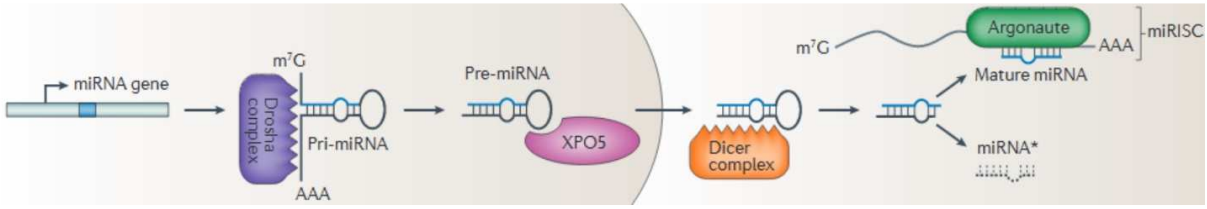

Figure 5 miRNA biogenesis.
In the nucleus, the pre-miRNA is excised from the pri-miRNA by Drosha complex, and is exported by XPO5. In the cytoplasm, Dicer complex processes the miRNA precursor into a 19-24 nt miRNA duplex. The guide strand is bound by AGO to form the miRISC, which executes mRNA silencing for gene expression regulation (Pasquinelli, 2012).

Analysis of miRNA sequencing data showed that a fraction of the expressed miRNAs have additional nucleotides mainly at their 3'end, which are not encoded by their gene. These non-templated nt arise from post-transcriptional 3'end processing and alter miRNA stability. The addition of non-templated nucleotides is termed tailing and in case of miRNA degradation one speaks of trimming. Adenylation or uridylation is the most frequently observed mode of tailing and conserved across *Drosophila* and vertebrates (Ameres et al, 2010; Burroughs et al, 2010; Wyman et al, 2011). First evidence that a miRNA target induces tailing and thereby destabilizes the miRNA was observed for a murine cytomegalovirus (MCMV) derived transcript (m169). Having several miR-27a/b binding sites, this transcript induces tailing of the interacting miRNAs, which leads to their degradation (Buck et al, 2010; Marcinowski et al, 2012). This is not an exclusively viral phenomenon, highly complementary target mRNAs also induce tailing and trimming of miRNAs. In neuronal cells, this process of target-directed miRNA degradation (TDMD) is highly efficient, but only minor tailing and trimming was observed in non-neuronal cells (La Mata et al, 2015). There are also post-transcriptional 3'end modifications which enhance miRNA stability (Katoh et al, 2009). In general miRNA decay is less extensively investigated compared to miRNA biogenesis.

1.3.2 Regulation of gene expression by miRNAs

The miRNA component of RISC functions as a guide and mediates mRNA interaction by base-pairing, while AGO induces silencing of the mRNA target. In humans four AGO proteins were identified, which associate with the same set of miRNAs (Azuma-Mukai et al, 2008). Nevertheless, only AGO-2 is catalytically active and can perform cleavage of a target RNA. Cleavage occurs when the miRNA is perfectly complementary to its target RNA (Jinek & Doudna, 2009; Schirle et al, 2014). This process is very similar to the mRNA silencing pathway by miRNAs in plants. Although in animals it is more common, that mainly bases 2-8 of the miRNA known as seed region interact with the mRNA. Additional base-pairing of 3-4 bases in the 3' region (nucleotides 13-16)

of the miRNA is possible. These supplementary 3' interactions enhance affinity for the target, therefore increase specificity, and efficient binding to the target mRNA (Wee et al, 2012; Schirle et al, 2014; Moore et al, 2015). Upon RISC binding, AGO recruits cofactors, which promote deadenylation and accelerate degradation of the target or interfere with translation (Bartel, 2009; Pasquinelli, 2012; Jonas & Izaurralde, 2015 and references therein). In general, miRNAs have only moderate effects on expression, most protein levels decrease only 2-fold upon miRNA targeting. It is very common, that mRNAs have four to five conserved target sites for different miRNAs, and binding of multiple miRNAs increase the repression (Selbach et al, 2008). The majority, about 32% of miRNA binding sites are located in the 3'UTR of mRNAs, but they are also found about 25% in ORF's (Chi et al, 2009).

The discovery of miRNAs and also other non-coding RNAs with a function in regulation of gene expression have reshaped the view on the central dogma and on genomes itself. A gene product is not necessarily a protein, and the genetic information in regions, which do not code for proteins are not necessarily just "junk DNA".

1.4 Hepatitis C virus

A virus is not a living organism, since it has no biochemical metabolism. It needs a host cell for its reproduction, and it utilizes cellular host factors for replication, synthesis of its components, as well as for virus particle assembly. Therefore it is well known and very common that viruses hijack cellular proteins. However, Hepatitis C virus (HCV) uses besides many cellular proteins a quite unusual host factor, the cellular microRNA 122 (miR-122) (reviewed in Sarnow & Sagan, 2016). This miRNA is essential for HCV propagation, and with approximately 120,000 copies per cell it is the most abundant miRNA in liver cells (Jopling et al, 2005; Jopling et al, 2006; Denzler et al, 2014). The liver tropism of HCV is thought to be at least partially related to the specific and exceptional high expression of miR-122 in liver cells.

Approximately 71 million people world-wide are chronically infected with HCV and many more do not even know they are infected (WHO, accessed 28.07.17). The HCV infection is symptomless for several years, but if not treated, HCV causes severe liver diseases such as fibrosis, cirrhosis and hepatocellular carcinoma (HCC) (Tsai et al, 2012; Hsu et al, 2012). Until now seven HCV genotypes have been identified. They have a remarkable genetic diversity, which is one important aspect why no HCV vaccine is available so far (Tarr et al, 2015). Nevertheless, potent direct acting antiviral (DAA) drugs against HCV have been launched in 2013 with a cure rate approaching 100% (Burstow et al, 2017).

1.4.1 HCV life cycle

HCV belongs to the family of *Flaviviridae*, and its propagation is driven by a plus strand RNA genome of 9.6 kb, which is not capped or polyadenylated (reviewed in Scheel & Rice, 2013; Paul et al, 2014; Popescu et al, 2014; Sarnow & Sagan, 2016). It encodes a polyprotein ORF, from which ten mature proteins are generated via cleavage by viral and host proteases. The core protein, envelope glycoprotein E1 and E2, are designated as structural proteins. E1 and E2 are incorporated into the envelope, whereas the core protein forms the nucleocapsid, which carries the viral genome. NS2, which is a protease and the ion channel p7 are not incorporated into the viral particle. They function in envelope formation (Popescu et al, 2011). The proteins NS3-NS5B represent the replicase complex and are sufficient for HCV replication (Lohmann, 1999). NS3 is associated with the NS4A cofactor. NS3 itself is a bipartite protein with a protease and a helicase domain. NS4B mediates alterations of the endoplasmatic reticulum (ER) membranes and formation of vesicles. NS5A is a phosphoprotein, which is required for virus assembly. The NS5B protein is the viral RNA-dependent RNA polymerase (RdRp) and is involved in synthesis of the

viral RNA (Behrens et al, 1996; Lohmann et al, 1997). The HCV ORF is flanked by highly structured 5' and 3'UTR's, with an internal ribosome entry site (IRES) located in the 5'UTR. The IRES element recruits ribosomes to the genome, and as a plus strand RNA, it can directly serves as template for translation (**Figure 6**) (reviewed in Niepmann, 2013).

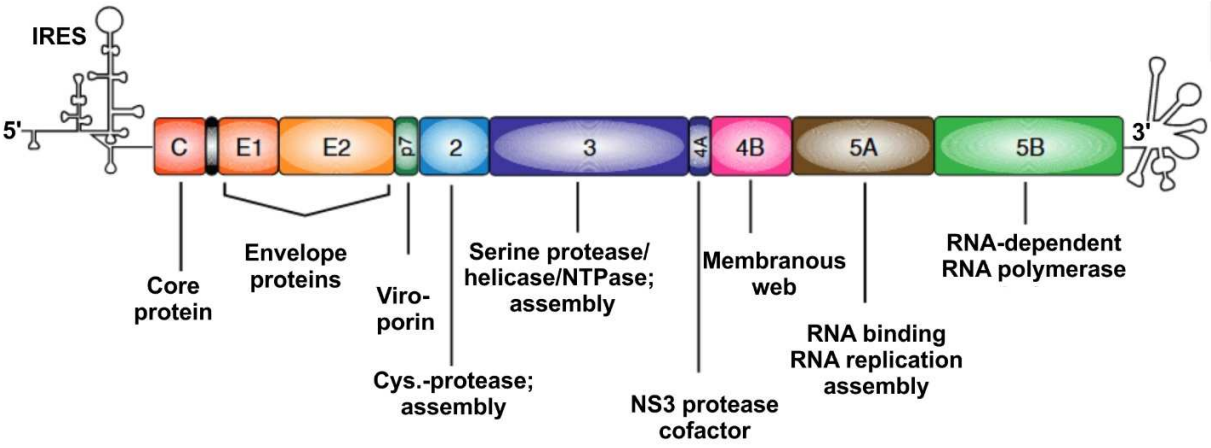

Figure 6 HCV genome organization.
The HCV genome is a single stranded RNA with positive polarity. The HCV 5'UTR encodes an IRES, which recruits ribosomes to the viral genome for polyprotein translation. Ten mature proteins are generated via cleavage from the polyprotein by cellular and viral proteases. The HCV proteins and their function are indicated below (modified after Bartenschlager et al, 2011).

HCV contacts the surface of liver cells via scavenger receptor B1 and CD 81 and travels to the tight junctions. There it binds to claudin1 and occludin, which induce receptor- and clathrin-mediated endocytosis of the HCV particle (Dubuisson & Cosset, 2014). Upon entry, the viral genome is released from the capsid to the cytosol, where ribosomes are recruited to the IRES for polyprotein translation. The signal sequence at the 5'end of the polyprotein mediates targeting to the translocon in the membrane of the ER. This is important because the mature HCV proteins are all membrane-associated. The non-structural proteins induce rearrangements of the ER membrane and accumulation of multi-membrane vesicles. These ER membrane alterations are termed membranous web and are hallmark of HCV infection (Egger et al, 2002). It is thought that the vesicles are coated at the inside with many copies of the non-structural proteins and that they are the site of replication. Inside the vesicles the viral RNA is protected from proteases and nucleases, but it is thought that they have an opening where NTPs can enter (Romero-Brey et al, 2012).

After synthesis of large amounts of non-structural proteins, the negative strand of the HCV genome is generated by NS5B. It then serves as template for production of many plus strand molecules. These are engaged either in translation, replication or they are packaged in virus

particles. The NS5A protein is believed to deliver the RNA genome to the core proteins, which assemble the nucleocapsid from ER-derived membranes. Accumulation of NS2, p7, E1 and E2, as well as host factors such as apolipoprotein E induce envelope formation. The nascent viral particles bud into the ER lumen and shuttle via the cellular secretory pathway to the cell surface, where they are released by exocytosis (Dubuisson & Cosset, 2014).

1.4.2 miR-122 and HCV infection

The liver-specific miR-122 enhances HCV accumulation and is essential for virus viability, but the underlying biochemical mechanism is not completely understood (Sarnow & Sagan, 2016). There are two miR-122 binding sites at the very 5'end of the HCV genome (Jopling et al, 2005; Jopling et al, 2006; Jopling et al, 2008). Additional miR-122 sites in the NS5B coding region and the 3'UTR are relevant for replication efficiency and regulation of viral translation, but the main fraction of miR-122 binds in the 5'UTR (Gerresheim et al, 2017; Luna et al, 2015). These sites in the 5'UTR are well conserved between the genotypes, which indicate their important role in HCV life cycle (**Figure 7**) (Shimakami et al, 2012b). Indeed, occupancy of both binding sites has greater impact on HCV accumulation, as when bound alone (Nieder-Röhrmann et al, 2017). However, binding of miR-122 to the first site contributes to higher degree to the positive effects on HCV accumulation (Jopling et al, 2008; Thibault et al, 2015; Shimakami et al, 2012b). In addition to genetic evidences, the direct interaction of miR-122 with the HCV binding sites was shown by biochemical and biophysical experiments. Both binding sites are simultaneously occupied *in vitro*, but they are bound with different affinities (Mortimer & Doudna, 2013). It is assumed that binding of miR-122 influences the secondary structure of the HCV 5'UTR (Díaz-Toledano et al, 2009; Mortimer & Doudna, 2013).

It is likely that miR-122 acts at different stages of the HCV life cycle. There is evidence that miR-122 affects viral translation initiation, replication and stabilizes the HCV genome by protecting the 5'end from exonucleolytic degradation by XRN-1 or XRN-2 (Henke et al, 2008; Roberts et al, 2011; Shimakami et al, 2012a; Sedano & Sarnow, 2014; Thibault et al, 2015; Li et al, 2015). Additionally, miR-122 is believed to influence translation and thereby the switch of the viral RNA from being a translation template to being the template for replication (Gerresheim et al, 2017). AGO-1 and AGO-2, are recruited by miR-122 to the HCV 5'UTR. However, it is not clear if AGO is only required to efficiently deliver miR-122, or if AGO remains bound in order to enhance HCV RNA accumulation (Berezhna et al, 2011; Shimakami et al, 2012a; Conrad et al, 2013; Luna et al, 2015).

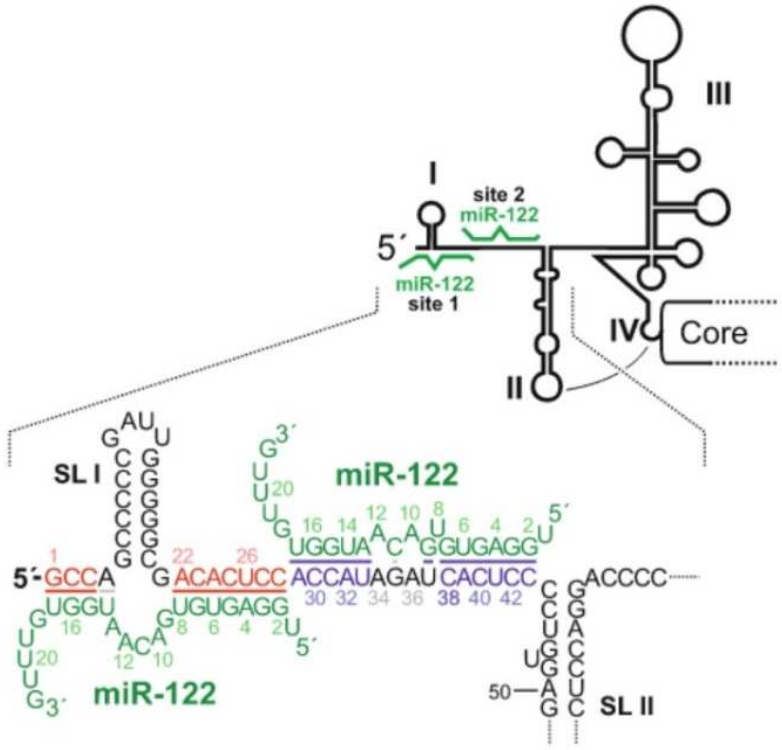

Figure 7 miR-122 interaction with the HCV 5'UTR.
The HCV 5'UTR has two miR-122 binding sites located directly at the very 5'end of the viral RNA. Site 1 resides at the base of stem loop (SL) I and site 2 is located upstream of SL II. Both sites show the typical seed interaction of nucleotides 2-7/8 of the miRNA. At site 1 the 3' supplementary base-pairing of the miRNA (15-17nt) with the HCV 5'UTR (1-3nt) creates a 3' overhang of the miRNA. The interaction with site 1 resembles the canonical miRNA:target interaction, whereas site 2 has extensive downstream miRNA base-pairing (nucleotides 13-17) with the HCV 5'UTR (Conrad & Niepmann, 2014).

Interestingly, miR-122 is post-transcriptionally monoadenylated by the non-canonical cytoplasmic poly(A) polymerase GLD-2. This monoadenylation stabilizes miR-122 (Katoh et al, 2009). The HCV core protein modulates miR-122 levels through inhibition of GLD-2, which leads to destabilization of miR-122 and reduced HCV levels. This finding might be indicative for a miR-122-driven negative feedback loop of HCV replication (Kim et al, 2016).

In liver cells, miR-122 regulates differentiation, the cholesterol metabolism, is involved in fatty acid oxidation and the lipid metabolism, as well as in regulation of systemic iron homeostasis (Sarnow & Sagan, 2016). Thus miR-122 is a key regulator of many important liver functions. In addition to that, miR-122 is frequently downregulated in HCC, and thought to act as tumor-suppressor in healthy liver. For example miR-122 regulates the WNT/β-catenin pathway via targeting BCL9. A de-repression of BCL9, which is a key target with seven miR-122 binding sites, was implicated in poor HCC outcome (Luna et al, 2017). In fact, HCV is suspected to cause HCC not only by

HCV-induced inflammation but also by sequestration of miR-122 from cellular mRNAs (Luedde & Schwabe, 2011; Luna et al, 2015).

HCV dependence on miR-122 led to the development of miR-122 antagonists (antagomiRs) for HCV treatment. Miravirsen (Santaris), which is a locked nucleic acid (LNA)-modified antisense oligo and RG-101 (Regulus) a *N*-Acetylgalactosamine (GalNAC)-conjugated antisense oligo, bind the mature miR-122 with high affinity. In consequence availability of miR-122 for binding to the HCV RNA is reduced. Additionally, miravirsen decreases miR-122 levels by interfering with its biogenesis (Gebert et al, 2014). Both miR-122 antagonists, miravirsen and RG-101 were able to reduce HCV levels in patients temporarily to non-detectable levels (Janssen et al, 2013; van der Ree et al, 2017).

1.5 Circular RNAs

1.5.1 Rediscovery of circRNAs

Recent discoveries show that many RNAs may also, contrary to the common belief occur as circular and not exclusively as linear molecules in the cell. The single-stranded and covalently closed RNA genome of viroids were the first reported circular RNAs (Sanger et al, 1976). After their discovery in 1976, few candidates, *DCC*, *ETS-1*, *SRY*, *cytochrome P450 2C24* and *cANRIL* were found (Nigro et al, 1991; Cocquerelle et al, 1992; Capel et al, 1993; Zaphiropoulos, 1996; Burd et al, 2010). Until 2013, they were underestimated as rare events with questionable biological relevance (Cocquerelle et al, 1993). Recent advances in RNA sequencing (RNA-seq) techniques have led to the identification of thousands of human exonic circular RNAs (circRNAs) (Jeck et al, 2013; Memczak et al, 2013; Salzman et al, 2013; Salzman et al, 2012).

Until now, five different types of circular RNAs were found. 1) circular RNA genomes, such as viroids and Hepatitis δ. 2) circular intronic RNAs (ciRNAs), which are byproducts of group I or group II intron self-splicing, as well as of spliceosomal splicing. 3) Processing intermediates for example during tRNA or rRNA maturation, which are mainly found in archaea. 4) circular non-coding RNAs, as snoRNAs or RNase P in some archaea. 5) Exonic circRNAs, which are produced by the spliceosome and consist of exons (Lasda & Parker, 2014 and references therein).

Exonic circRNAs are currently the best investigated of the described circRNA species (Hentze & Preiss, 2013; Jeck & Sharpless, 2014; Lasda & Parker, 2014). They were found in many eukaryotic organisms: yeast (*S. saccharomyces*, *S. pombe*), plant (*O. sativa*, *A. thaliana*), fly (*D. melanogaster*) worm (*C. elegans*), mouse and human (Barrett et al, 2015; Lu et al, 2015a; Wang et al, 2014; Westholm et al, 2014; Ivanov et al, 2015; Guo et al, 2014; Memczak et al, 2013; Jeck et al, 2013). In yeast, only few circRNAs were identified, mainly because few genes have introns (Barrett et al, 2015; Spingola et al, 1999). In contrast to that, by mid 2013 approximately 2,000 circRNAs were found in mouse and over 25,000 circRNAs were found in human, whereof 69 are conserved (Jeck et al, 2013). The number of identified circRNAs has increased further and a database of circRNAs from different cell lines, tissues and species was created (Glažar et al, 2014). For computational prediction of circRNAs, different strategies of sequence analysis and sample preparation were used. It is not trivial to reliably predict circRNAs, because *trans*-spliced RNAs, genomic rearrangements (e.g. exon duplications), or simply reverse transcriptase (RT) errors hamper the analyses. Most circRNAs are not very abundant, that's why a greater sequencing depth or enrichment of circRNAs is required. For enrichment, enzymatic methods as RNase R exonuclease treatment was applied (Jeck et al, 2013). Likewise depletion of the poly(A)

fraction leads to circRNA enrichment (Salzman et al, 2012; Salzman et al, 2013; Zhang et al, 2014). Various strategies for the identification of splice junctions in non-linear order (e.g. mapping to annotated genes, or mapping to AG/GU junctions) were applied (Memczak et al, 2013; Jeck et al, 2013; Guo et al, 2014; Szabo et al, 2015). The combination of these approaches and to a large extend the enhanced sequencing depth led to the discovery of the new class of circRNAs, which were missed in RNA-seq analyses before.

1.5.2 circRNA properties

The computational analyses of identified circRNAs show that they are diverse, conserved, but most of them are not very abundant. Approximately 14% of actively transcribed human genes produce circRNAs, mainly arising from the 5'end of these genes. They contain at least one exon, but in most cases not more than five exons. Their length is between 0.1-4 kb with a median length of 547 nt. A given gene can give rise to several circRNA isoforms (Jeck et al, 2013).

The majority of the identified circRNAs is not very abundant (0.1-10%) compared to the associated mRNA (Guo et al, 2014). Nevertheless, some circRNA candidates are highly abundant and even more highly expressed then the corresponding linear mRNA. For example, in HeLa cells 25 copies of the circular *CAMSAP1* isoform were detected per cell, whereas only eight copies of the linear mRNA were found (Starke et al, 2015). In platelets the *SMARCA5*-derived circRNA is 151-times higher expressed compared to the parental mRNA (Maass et al, 2017).

Many circRNAs are flanked by long introns, which frequently have ALU repeats or similar elements (e.g. short interspersed nuclear elements) (Jeck et al, 2013; Ivanov et al, 2015). They are arranged in reverse complementary orientation and thus exhibit base-pairing ability. It was suggested that these elements promote exon circularization by bringing the splice sites in close proximity. The stimulatory effect of reverse complementary elements was experimentally confirmed by several groups (Zhang et al, 2014; Liang & Wilusz, 2014; Starke et al, 2015).

Moreover, endogenously expressed circRNAs associate with protein factors and exist as circRNA-protein complexes (circRNPs) in the cell (Schneider et al, 2016; Chen et al, 2017; Li et al, 2017). circRNAs were found to be predominantly cytoplasmic, and there are hints that circRNAs are actively exported, although the export mechanism is still elusive (Salzman et al, 2012; Jeck et al, 2013; Guo et al, 2014). Mass spectrometry analysis of co-precipitated proteins revealed that export factors as DDX93B, THOC4 and XPO5 crosslink to circRNAs (Chen et al, 2017).

The majority of circRNAs is not associated with ribosomes. Therefore circRNAs are not thought to be translated in general. But there is evidence, that some circRNAs are translated (Legnini et

al, 2017; Pamudurti et al, 2017; Yang et al, 2017b). Furthermore circRNAs were found to have half-life times of over 48 h, which was much more stable than their associated mRNAs (~20 h) (Cocquerelle et al, 1993; Jeck et al, 2013; Memczak et al, 2013; Liang & Wilusz, 2014).

1.5.3 circRNA biogenesis

Apparent from sequence analyses, most circRNAs exhibit circular junctions, which map to annotated splice sites. This suggests the involvement of the spliceosome in circRNA biogenesis (Memczak et al, 2013; Jeck et al, 2013). Even before their rediscovery, circRNAs were suggested to be generated by the spliceosome, however they were thought to be splicing errors (Cocquerelle et al, 1993; Capel et al, 1993; Pasman et al, 1996; Braun et al, 1996). The involvement of the spliceosome in circRNA production was recently demonstrated by using mutational analysis of splice sites and other splicing signals in minigene constructs (Ashwal-Fluss et al, 2014; Starke et al, 2015; Wang & Wang, 2015).

During canonical splicing, the upstream 5'ss attacks to the downstream 3'ss of the following exon, thereby releasing the intron as a lariat. The proposed mechanism for circularization of one or several exons is the linkage of the 5'ss with an upstream 3'ss. This mode of splicing is inverse compared to canonical splicing, and is often referred to as backsplicing (Lasda & Parker, 2014; Chen & Yang, 2015). It is thought that circularization occurs, because 5'ss and 3'ss are brought in close proximity. This can be achieved by interactions of complementary sequence elements or is mediated by protein-protein interactions (Zhang et al, 2014; Liang & Wilusz, 2014; Ashwal-Fluss et al, 2014; Conn et al, 2015). The circularization efficiency and production of different circRNA isoforms is influenced by competing interactions of reverse complementary repeats (RCR) (Zhang et al, 2016a; Liang & Wilusz, 2014)(**Figure 8**).

Furthermore, A-I conversions mediated by ADAR-1 modulate these RCR interactions, weaken the base-pairing and thereby antagonize circularization (Ivanov et al, 2015; Rybak-Wolf et al, 2015). The protein factors NF90/NF110 were recently found to enhance circRNA formation, by binding to RCR elements, which flank circularizing exons. NF90/NF110 are thought to regulate circRNA production in response to viral infection (Li et al, 2017).

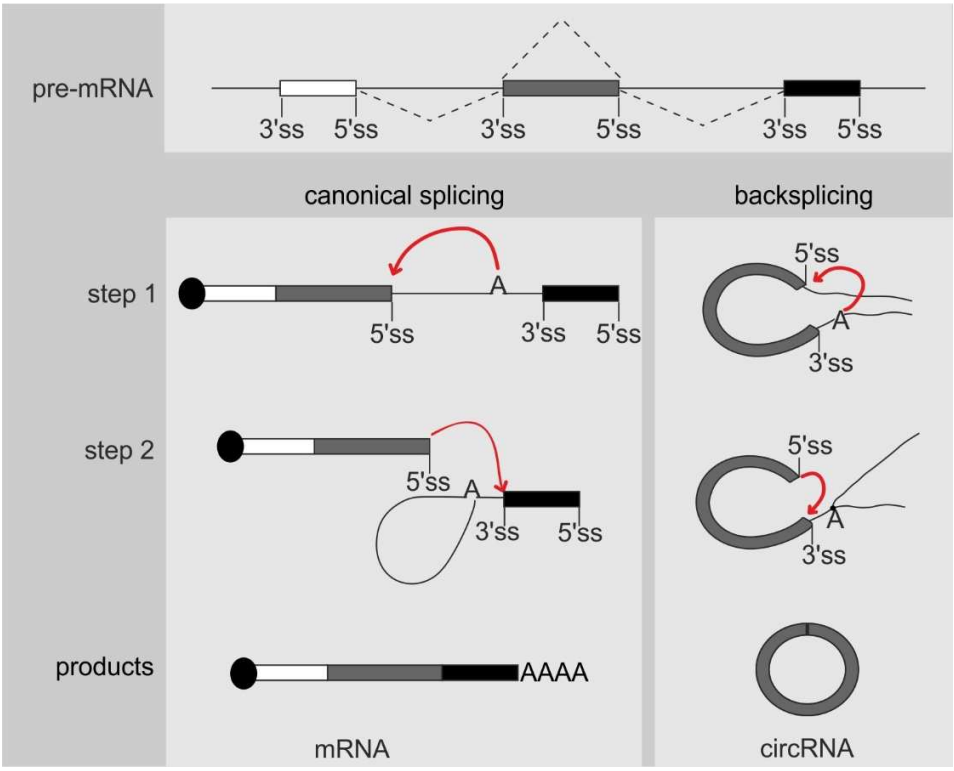

Figure 8 Mechanism of canonical pre-mRNA splicing and backsplicing.
Splicing occurs via two sequential transesterification steps. In the first step the BP adenosine (A) attacks the 5'ss. In the second transesterification step, the 3'ss is attacked by the 5'ss. The stable products of canonical splicing and backsplicing are a mature mRNA with 5'cap and poly(A)-tail and a circRNA, respectively.

There is evidence that circularization is regulated by additional protein factors independent from RCR elements. The splicing factor *muscleblind (*MBL*)* regulates the production of a circRNA from its own mRNA by binding in the flanking introns (Ashwal-Fluss et al, 2014). Comparable effects were observed for the titin (*TTN*) gene and Rbm20, which is a regulator of alternative splicing. Rbm20 binding sites are enriched in circRNA flanking introns of the *TTN* gene. Moreover, Rbm20 is crucial for the formation of a subset of *TTN*-derived circRNAs (Khan et al, 2016). *Quaking* (QKI) has also been implicated to be involved in biogenesis of circRNAs by binding to intronic sequences near the splice sites, thereby promoting circularization (Conn et al, 2015) (**Figure 9 A**). Additional splicing factors have been implicated in regulation of exon circularization. In *Drosophila* the knockdown (KD) of splicing factors (Hrb27C, Hrb78F, SRSF1, SRSF11 and SRSF 6) led to altered circularization efficiencies (Kramer et al, 2015). Altered ratios between linear and circular splicing were observed by overexpression of splicing factors (SRSF 1, hnRNP H, RBM4 and DAZAP1) in combination with ESE and ESS elements in human cell culture system (Wang & Wang, 2015).

Backsplicing is frequently observed for alternatively spliced exons, leading to the second hypothesis that the skipped exon is circularized in a second step from the exon-containing lariat

(Zaphiropoulos, 1996; Zhang et al, 2016a; Barrett et al, 2015) (**Figure 9 B**). For alternatively spliced exons, a slow polymerase rate enhances exon inclusion and reduces circRNA production from these exons in *Drosophila* (Ashwal-Fluss et al, 2014). These findings are in line with canonical alternative splicing, support the hypothesis that the second mechanism exists and provide evidence, that exon circularization occurs co-transcriptionally (La Mata et al, 2003; Ashwal-Fluss et al, 2014). Views vary on whether backsplicing occurs co- or post-transcriptionally, in two studies backsplicing is claimed to occur post-transcriptionally (Liang & Wilusz, 2014; Zhang et al, 2016b).

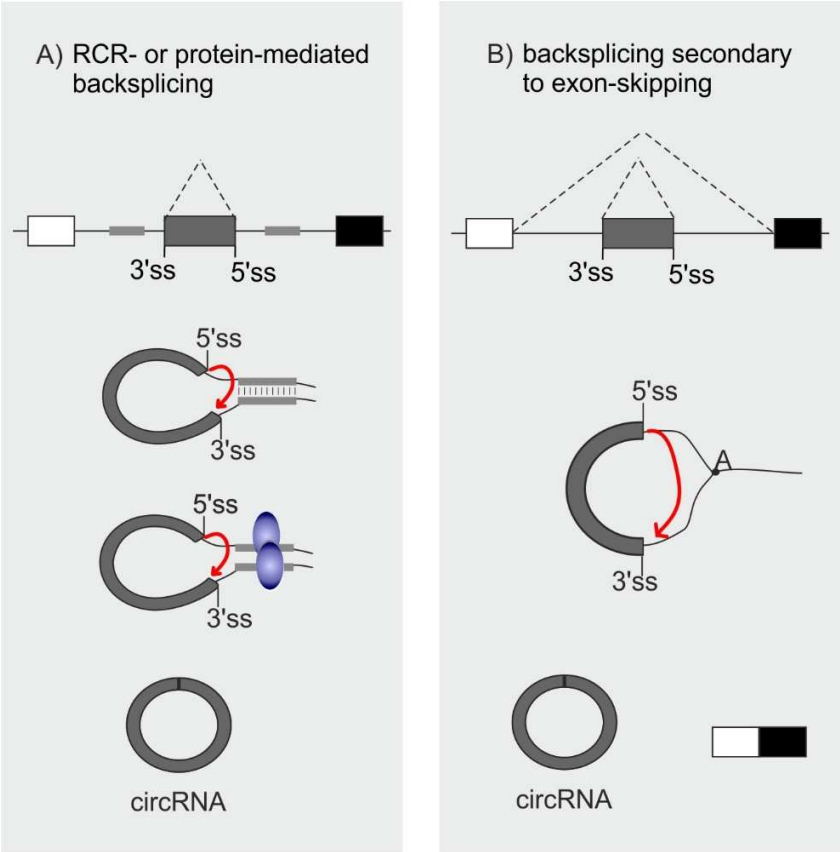

Figure 9 Different modes of circRNA formation.
Direct backsplicing is accomplished by interactions of the flanking introns. These interactions are either thought to be mediated by RCR elements, which base-pair with each other, or by protein-protein interactions (**A**). Another hypothesis is, that some circRNAs are generated secondary to exon skipping from the exon-containing lariat (**B**).

1.5.4 Circularization strategies and circRNA synthesis

In order to elucidate circRNA functions, *in vivo* expression strategies and *in vitro* synthesis of circRNAs gain in importance (Petkovic & Müller, 2015 and references therein). Several groups

have designed or used circRNA expression vectors as reporters to study circRNA biogenesis, for overexpression or exogenous expression of specific circRNAs in different biological systems (Hansen et al, 2013b; Liang & Wilusz, 2014; Starke et al, 2015). Exon circularization is mainly achieved by construction of an expression vector containing one exon, which is flanked by introns with RCR regions. These circRNAs are generated endogenously by the spliceosome with the advantage that interacting protein factors possibly assembled during the natural pathway of circRNA biogenesis. But there are also alternative strategies to generate circRNAs spliceosome-independently, for example by tRNA splicing or genetically engineered autocatalytic group I introns (Umekage & Kikuchi, 2009; Lu et al, 2015b; Schmidt et al, 2016).

The heterologous expression of a circularized streptavidin aptamer in *E.coli* and subsequent purification was established by Umekage and coworkers (Umekage & Kikuchi, 2007; Umekage & Kikuchi, 2009). They used a group I intron self-splicing system termed PIE (**Figure 10**). The intron-exon structure of the *td* gene from T4 bacteriophage was converted, and PIE stands for permuted intron-exon structure (Puttaraju & Been, 1992). In the original *td* gene, the intron is excised and then circularized during the autocatalytic self-splicing process. By permutation of the intron-exon structure circularization of the exon is induced and circRNAs can be produced *in vitro* or *in vivo* for example in *E.coli* or in yeast (Ford & Ares, 1994).

Another option for *in vitro* synthesis of circRNAs is the enzymatic ligation of RNA substrates, which are produced either by synthetic oligomerization or *in vitro* transcription. By ligating the RNA substrate two products are generated. The intermolecular ligation, results in linear dimers and intramolecular ligation leads to circularized products (Petkovic & Müller, 2015). Immediate vicinity of the 5’ and 3’ends of the RNA substrate enhance the circularization reaction. There are different strategies to use DNA oligos, eg. splint oligos or helper hairpins to enhance circularization. Moreover structure elements in the substrate itself, such as a terminal stem or dumbbell structure, can favor the circularization. There are several enzymes available (e.g. T4 DNA ligase, T4 RNA ligase 1 and T4 RNA ligase 2), with different specificities (reviewed in Petkovic & Müller, 2015).

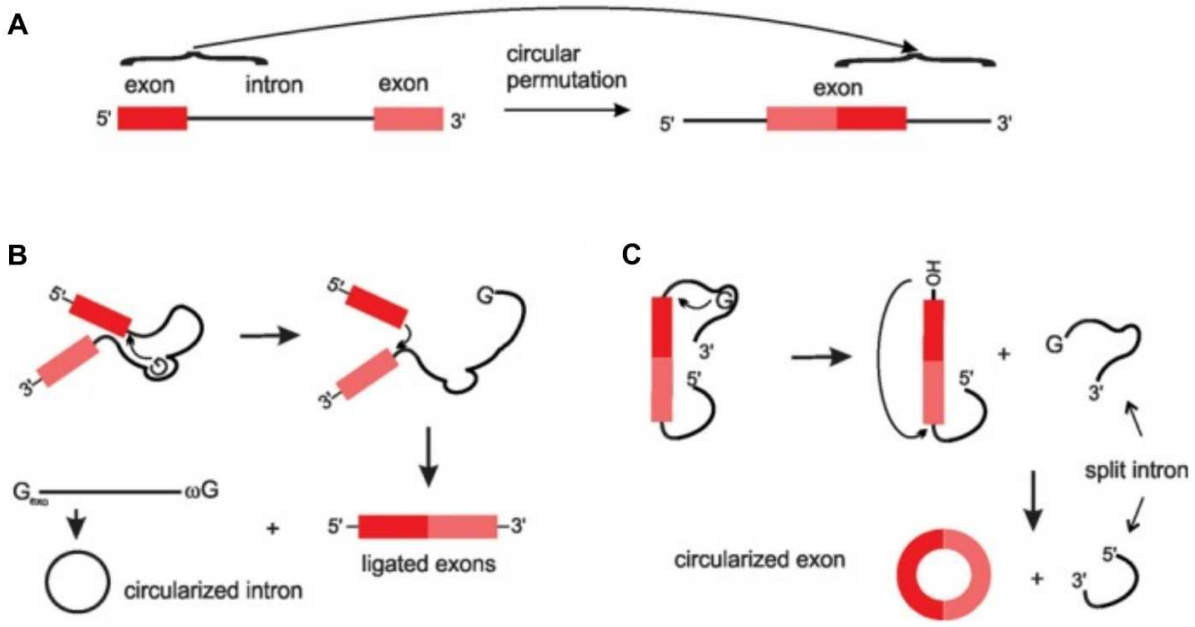

Figure 10 Group I intron self-splicing mechanism of the *td gene* and the permutated *td gene*. Original gene structure of T4 bacteriophage *td* gene, and after permutation of the intron-exon structure (**A**). Group I intron self-splicing mechanism of the *td* gene (**B**) in comparison to the mechanism of the *td* gene with permutated intron-exon structure (**C**) (modified after Petkovic & Müller, 2015).

1.5.5 Biological relevance of circRNAs

Although thousands of circRNAs have been identified, the functions of most of them are still unknown. There are proper arguments for their functionality, as circRNAs are developmentally regulated, expressed in a cell-type- or tissue-specific manner, and conserved across species. It appears, that circRNAs are particularly abundant in the nervous system. In fly heads and in mouse brains circRNA expression changes upon neuronal development and is upregulated in the ageing nervous system (Rybak-Wolf et al, 2015; Gruner et al, 2016). circRNAs are not only time-dependent, but also tissue-specifically regulated in mouse, pig and human fetal brain (Rybak-Wolf et al, 2015; Venø et al, 2015; Szabo et al, 2015; Barrett et al, 2015; You et al, 2015; Gruner et al, 2016). Furthermore, there is evidence that circRNAs might function in neuronal plasticity (You et al, 2015).

The most prominent and currently best investigated circRNA is *CDR1as*, produced from the antisense strand of cerebellar degeneration-related protein 1. *CDR1as* has more than 70 miR-7 binding sites and is co-expressed with miR-7 in neocortical and hippocampal neurons (Hansen et al, 2013a; Memczak et al, 2013). miR-7 inhibitory effects were observed in *CDR1as* overexpression experiments in zebrafish (Memczak et al, 2013). Interestingly, *CDR1as* has

besides the miR-7 sites one almost perfectly complementary binding site for miR-671, which induces cleavage of the circRNA by the RNA-induced silencing complex (RISC) (Hansen et al, 2011). *CDR1as* is thought to be an inhibitor by competing for miR-7 binding with the miR-7 targets. Therefore it is also known as circular RNA sponge for miR-7 (*ciRS-7*) (Hansen et al, 2011; Hansen et al, 2013b; Memczak et al, 2013). Recent data show downregulation of miR-7 and upregulation of miR-671 in neurons of *CDR1as*/*ciRS-7* KO mice, suggesting a stabilizing effect of miR-7 upon interaction with *CDR1as*/*ciRS-7*. Additionally, loss of *CDR1as*/*ciRS-7* caused increased synaptic vesicle release and neurophysiological alterations, which are correlated to several neuropsychiatric disorders (Piwecka et al, 2017). These results indicate a major role of *CDR1as*/*ciRS-7* in brain function. In line with that, decreased *cDR1as*/*ciRS-7* levels in brain samples from Alzheimer disease patients were observed (Zhao et al, 2016). Besides its role in brain function, *CDR1as*/*ciRS-7* is linked to modulation of insulin secretion in pancreatic β cells (Xu et al, 2015).

Moreover, the circRNA originating from the sex determination region Y (*SRY*), which is highly expressed in mouse adult testis, has 16 binding sites for miR-138. SRY is also likely to function as miRNA sponge (Capel et al, 1993; Hansen et al, 2013b). *CDR1as*/*ciRS-7* and circSRY seem to be the exception, since the majority of the identified circRNAs do not have several miRNA binding sites. This argues against the theory, that endogenous circRNAs act as miRNA competitors in general (Guo et al, 2014). Nevertheless, a circRNA derived from the HIPK3 gene has been implicated in binding of different miRNAs and thereby influencing cell proliferation (Zheng et al, 2016). It still needs to be shown whether a larger fraction of the newly identified class of circRNAs is involved in miRNA sequestration or regulation (Denzler et al, 2014).

Two very recent studies show the involvement of circRNAs in cellular antiviral immune response (Chen et al, 2017; Li et al, 2017). The protein factors NF90/NF110 modulate production of 250 circRNAs by stabilizing the interaction of RCR elements in the circRNA flanking introns. Both proteins are complexed with circRNAs and are released upon viral infection, where they interact with the viral mRNA to inhibit replication (Li et al, 2017). By transfection of *in vitro* produced circRNAs Chen et al. (2017) recognized increased protection against viral infection. Exogenous circRNAs, but not the endogenous circRNAs activate the RIG-I pathway, which stimulates the cellular immune response. The foreign circRNAs are thought to be detected by lack of bound protein factors. Whereas the endogenous circRNPs are identified as self-circRNAs, probably due to bound proteins. These proteins are thought to assemble during circRNA biogenesis, because the protein composition of circRNPs is influenced by their flanking introns (Chen et al, 2017).

There are many different ways how circRNAs could hypothetically influence gene expression or function in the cell (Hentze & Preiss, 2013). They are speculated to serve as miRNA or protein vehicles, possibly even releasing their cargo by cleavage through a perfectly complementary miRNA (Hentze & Preiss, 2013). Since circRNAs were shown to be complexed with diverse protein factors they could not only compete for miRNA binding, but also for interaction with RBPs (Schneider et al, 2016; Chen et al, 2017; Li et al, 2017). Moreover they could bind to mRNAs, regulate gene expression by sequence interactions, aid the assembly of large RBP complexes, or even be translated (Hentze & Preiss, 2013).

During the last 5 years, prediction, detection, validation and synthesis methods for circRNAs were established and improved. Thus many circRNAs were identified, few were characterized but their global impact and biological function remained elusive, so far. However, the elevated stability of circRNAs is an attractive characteristic for biotechnological and therapeutic use.

1.6 Aim of this work

In the first part of my thesis I focused on the characterization of circRNA biogenesis. The involvement of the spliceosome in circRNA biogenesis was already speculated in the early 2000's, when the first exonic circRNAs were discovered. This hypothesis was substantiated, when computational analysis of sequencing data showed that the vast majority of the identified circRNAs map to annotated splice sites. But to that date no conclusive studies were available, which showed that circRNAs are generated by the spliceosome. To address this issue, I first aimed to recapitulate circRNA expression from plasmid-derived minigenes. These minigenes served as reporter system to elucidate minimal requirements for circRNA expression. Moreover, a comprehensive mutational analysis of the splice signals was performed to clarify the role of the spliceosome in circRNA biogenesis. Exonic splice enhancers (ESEs) are sequence elements, which increase processing efficiency of linearly spliced exons. They promote exon inclusion by recruiting proteins, which positively modulate splicing. Finally, the impact of ESEs on circRNA formation in competition with linear splicing was investigated.

In the second part of my work I designed artificial circRNAs for miRNA sequestration. It had been shown that the endogenous circRNA *CDR1as*/*ciRS-7* binds miR-7. Initially, it was thought to function as miRNA sponge, competing with endogenous targets for miRNA binding. For the development of artificial circRNA sponges, high-affinity miRNA binding sites were designed and experimentally validated. Then, synthesis and purification methods suitable for production of the designed circRNA sponges were examined and established. The artificial circRNA sponges were transfected into cells and their subcellular localization, as well as their half-life was analyzed. The very abundant liver-specific miR-122 was targeted for proof of the concept that artificial circRNA sponges can be used to inactivate miRNAs. miR-122 is not only essential for HCV propagation, but the inhibition of miR-122 by LNA-modified or GalNAC-conjugated antisense oligos (miravirsen and RG-101) was shown to reduce HCV levels in patients drastically. Thus, functional inhibition of miR-122 by circRNA sponges was tested in different HCV reporter systems.

2 RESULTS

2.1 circRNA biogenesis

2.1.1 Identification and characterization of the *CNTROB*-derived circRNA

The computational analysis of circRNA sequencing data showed that most circRNA junctions exhibit annotated splice sites. Therefore circRNAs are thought to be generated by the spliceosome. The aim was to experimentally address the question if circRNAs are products of pre-mRNA processing by the spliceosome. Thus, biogenesis of circRNAs was analyzed by minigene splicing assays. A minigene is a splicing reporter, which contains the minimal requirements for processing by the spliceosome. For linear splicing it is well-known that most of the important intronic regulatory sequence elements are in proximity of the exon. In minigenes used to analyze linear splicing, the introns are often shortened, leaving 300-500 bp upstream or downstream of the exon of interest intact. For circRNA generation few information of sequence requirements were available. For this reason I wanted to start with the recapitulation of a single-exon circRNA from the natural gene context. This included the partial upstream and downstream exon leaving the neighboring splice sites intact, full length introns and the circularizing exon. The *CNTROB* gene was selected by Lee-Hsueh Hung from circRNA expression data in fibroblasts, because of the relatively short introns, surrounding the predicted circularizing exon (**Figure 11 A**) (Jeck et al, 2013).

Initially, expression and splicing pattern of the predicted circRNA and its neighboring exons were analyzed in HeLa cells using RT-PCR. The linearly spliced junctions were detected via conventional convergent primers located in exons 12-14. For detection of the circular isoform divergent primers within the circularizing exon 12 were used. This results in a PCR product, if the 3'ss of the exon is linked to its upstream 5'ss. Convergent primers located in exon 13, were designed to measure total levels, including linearly and circularly spliced, or unprocessed isoforms. In addition, skipping of exon 13 was analyzed using primers in exon 12 and 14. PCR products of expected size were obtained for total levels (E13 total), the linearly spliced mRNA (E12-13, E13-14 and E12-14) and for the circular splice junction (E13 circular). Skipping of exon 13 was not confirmed, because only the product which includes exon 13 was detectable (E12-14) (**Figure 11 B**).

Furthermore, the application of column-based RNA purification (Qiagen RNeasy kit) for circRNA analysis was examined, to ensure that circRNAs were not retained in the matrix of the column. Thus equal amounts of RNA, which were either isolated by Trizol and EtOH precipitation or which were additionally column purified, were subjected to RT-PCR. No difference in the abundance of

the PCR products was observed between both purification methods, suggesting a quantitative purification of circRNAs by column-based RNA isolation (**Figure 11 B**).

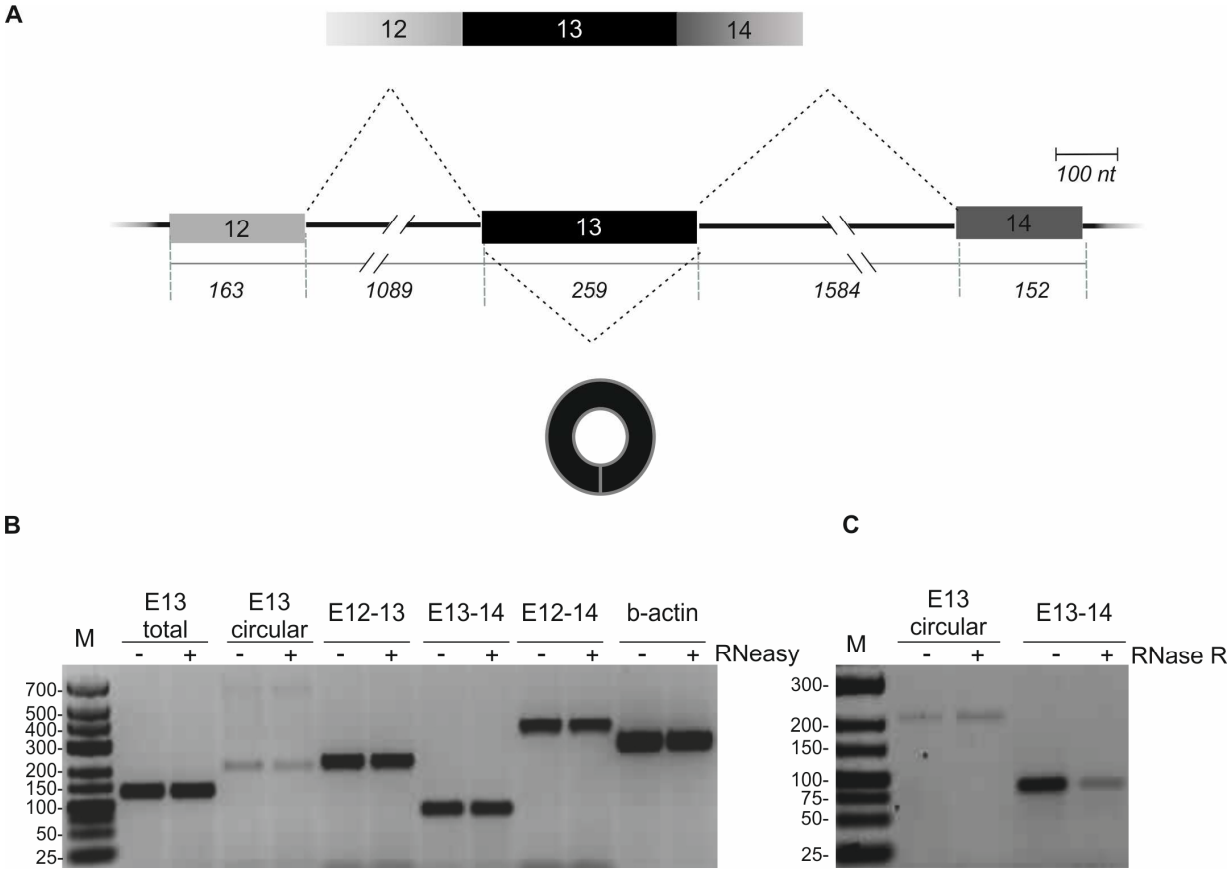

Figure 11 Expression and splicing pattern of *CNTROB* circRNA.
Schematic representation of the *CNTROB* intron exon structure adjacent to the circularizing exon 13. The exons are depicted as boxes, introns as lines and the numbers below indicate the length in nt. The precursor can be processed into a linearly spliced mRNA (partially shown at the top) or the middle exon is circularized (bottom) (**A**).
The splicing pattern of *CNTROB* in HeLa cells was analyzed by semi-quantitative RT-PCR using HeLa total RNA, which was extracted with Trizol (-) or was additionally column purified (+). For detection of the linear splice junctions (E12-13, E13-14, and E12-14), and for total levels of exon 13 (E13 total) convergent primers were used. The circular isoform of exon 13 was detected with divergent primer pairs. The β-actin mRNA (b-actin) served as loading control (**B**).
In (**C**) 1 µg of HeLa total RNA was incubated with (+) 5 u RNase R for 3 h and for control treatment without RNase R (-). Then the samples were analyzed by RT-PCR detecting the circular splice junction (E13 circular) and the downstream linear splice junction (E13-14). PCR products were separated by 2% agarose gel electrophoresis and visualized with ethidium bromide (EtBr).

To confirm that the detected PCR product (E13 circular) originates from a circRNA, additional validations were necessary. The splice junction of a circRNA equals the junction of *trans*-spliced RNAs, where the exon 13 of two different pre-mRNA molecules was spliced in tandem. HeLa total

RNA was treated with 5'-3' exonuclease RNase R, which digests linear RNAs, and reanalyzed. The RT-PCR signal of the linear splice junction decreased upon RNase R treatment, whereas the signal for the circular splice junction remained stable, supporting circularity of the detected RNA (**Figure 11 C**).

2.1.2 Recapitulation of *CNTROB*-derived circRNA processing with minigenes

Four *CNTROB*-based minigene constructs were generated, gradually removing sequence elements of the natural gene context. The intention was to determine the minimal requirements for circRNA production, and to create a minimal circRNA expression vector. In the first construct *CNTROB* Long, which was the basis for the following constructs, the natural context was maintained. The circularizing exon, flanked by its original introns and a small part of the neighboring exons were cloned into pcDNA3 vector backbone. This encodes the cytomegalovirus (CMV) promotor and a bovine growth hormone (BGH) polyadenylation signal. It allows the expression of minigenes in cells. After expression RNAs were isolated and the processing products were analyzed by RT-PCR. In the second construct *CNTROB* Short, the contribution of the flanking exons to circRNA production was studied, by deleting the flanking exons and truncating the introns. Both minigenes, contained a sequence tag added within exon 13 to distinguish plasmid-derived circRNAs from endogenous circRNAs.

Introns next to circularizing exons frequently contain ALU repeats and it was suspected that they facilitate circularization by base-pairing (Jeck et al, 2013). For *CNTROB* such base-pairing regions were not present in the natural introns adjacent to the circularized exon. In order to investigate the influence of such base-pairing regions a reverse complementary repeat (RCR) was introduced into RCR-CL B and RCR-CL Delta constructs. A fragment of the upstream intron (221 nt) was inserted in reverse complementary orientation downstream of the exon. The RCR region was designed to leave the PPT, as well as the predicted BP unpaired to prevent interference with splice signals. Then, most of the natural *CNTROB* exon sequence was substituted by external sequences. In RCR-CL B the natural exonic sequence was substituted by 384 nt of HNRNP L intron 6, which contains several hnRNP L binding sites. The RCR-CL Delta construct contains 308 nt from the plasmid pCR2.1 (**Figure 12**).

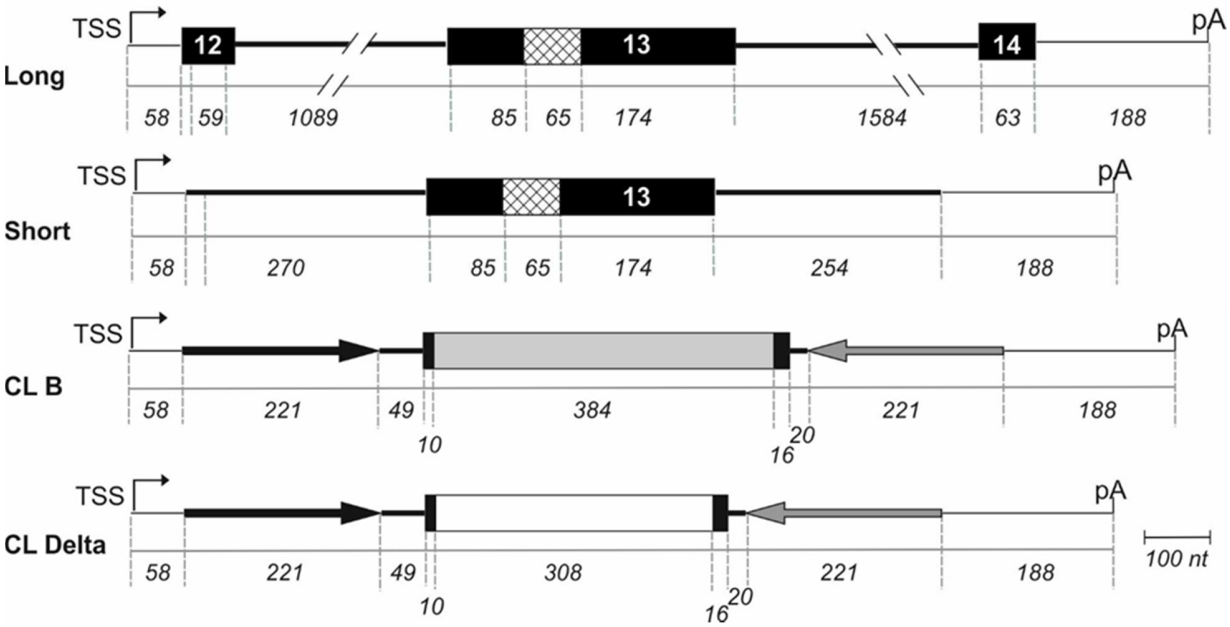

Figure 12 Minimal requirements for circRNA expression.
CNTROB-derived minigene constructs, where exons are represented as boxes and introns as bold lines. The transcription start site (TSS) and the polyadenylation site (pA) are encoded by the vector backbone. *CNTROB*-derived sequences are shown in black, the shaded area indicates a sequence tag that identifies the exogenous expressed circRNA. In the CL B and CL Delta constructs most of the exon was substituted by extrinsic sequences CL B is marked in light grey and originates from intron 6 of the *HNRNP L* gene, containing several hnRNP L binding sites. The CL Delta sequence was taken from the plasmid pCR2.1 and is depicted in white. This construct was named RCR-CNTROB in (Starke et al, 2015). In both constructs a reverse complementary repeat (RCR) region was created, by cloning 221 nt of the upstream *CNTROB* intron in reverse orientation downstream of the exon (grey arrow).

The described minigenes were transfected into HeLa cells and after 16 h of expression, isolated RNAs were analyzed by RT-PCR, comparing the production of circular RNAs from these constructs. For all minigenes the corresponding circular isoforms were detected, although circRNA levels derived from CNTROB Short were much lower compared to CNTROB Long minigene (**Figure 13 A-C**). The expression of the pre-mRNA from the minigenes was monitored by amplifying total levels of the circularizing exon (**Figure 13 A, B**). In case of RCR-CL B the linear isoform was detected using primers in the 5' and 3'end of the unprocessed transcript (**Figure 13 C**).

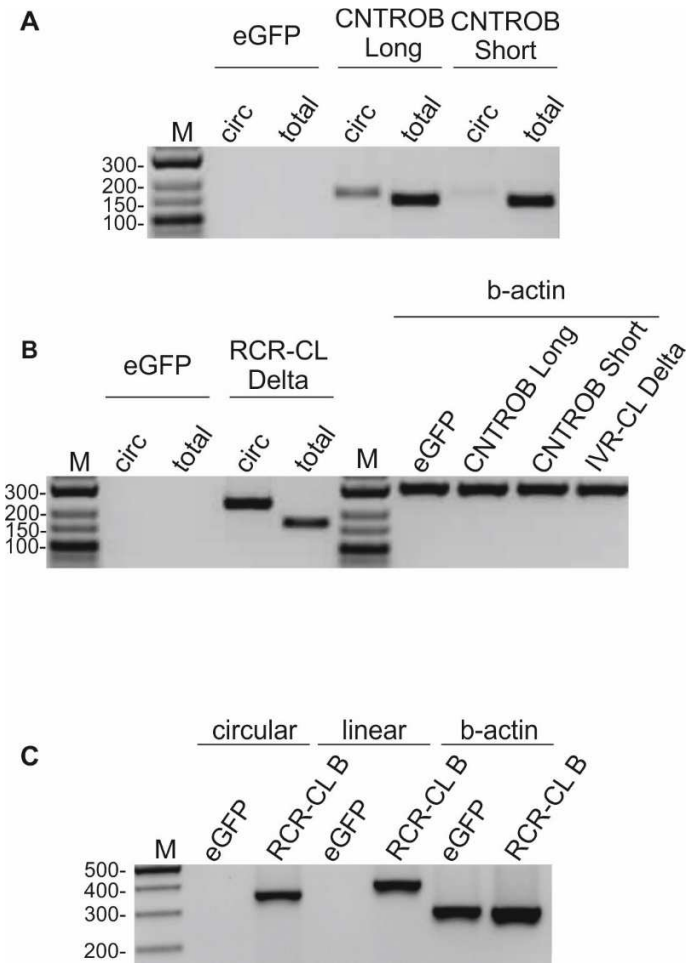

Figure 13 Expression of minimal circRNA expression constructs in HeLa.
CNTROB-derived minigene derivatives (see **Figure 12**) or eGFP, which served as negative control, were transfected into HeLa cells and expressed for 16 h. RNAs were isolated and analyzed by RT-PCR, using divergent primers for detection of the circular isoform or convergent primers to detect total levels of the circularized exon (**A, B**). In (**C**) convergent primers specific for the linear transcript were used. β-actin served as loading control.

2.1.3 Northern blot analysis of circRNAs generated from *CNTROB* minigenes

In order to validate circular conformation of the expressed RNAs, northern blot analysis was performed. It has been shown before that circRNAs migrate slower in denaturing polyacrylamide (PAA) gels compared to linear RNAs of the same length (Tabak et al, 1988). This effect is not observed in agarose gels. Consequently comparison of the running behavior of circRNAs in the different gel systems can be used to demonstrate circularity. In addition, the experimentally verified circRNA expression vector *ciRS-7*, which was used to express a circular miR-7 sponge was modified and co-analyzed with RCR-CL B (Hansen et al, 2013a). The miR-7 sponge sequence of *ciRS-7* was substituted by the CL B sequence leaving the original 5'ss and 3'ss, as

well as the RCR region intact (ciRS-7-CL B). Then RCR-CL B and ciRS-7-CL B were transfected into HeLa cells, and the isolated RNAs were analyzed by two different northern blot techniques. RNAs were either subjected to denaturing 6% PAA gel electrophoresis, then transferred by electroblotting, or RNAs were resolved by denaturing 1.2% agarose gel electrophoresis and transfer was accomplished by vacuum blotting (**Figure 14 A, B**). For circRNA detection two different probes were tested. The junction probe was specific for the circular isoform, and hybridized across the circular junction, whereas the exon probe was designed to detect the CL B sequence. Expressed circRNAs were detected at the expected size in the agarose gel (ciRS-7 CL B 555 nt, RCR-CL B 410 nt), whereas aberrant running behavior of the circRNAs was observed in PAA northern blots (**Figure 14 A, B**). Moreover PAA northern blot analyses revealed, that a fraction of the detected circRNAs run at their expected size. This product corresponded to the linearized circRNA (**Figure 14 A**). Note that the junction probe detected the expressed circRNAs more efficiently compared to the exon probe.

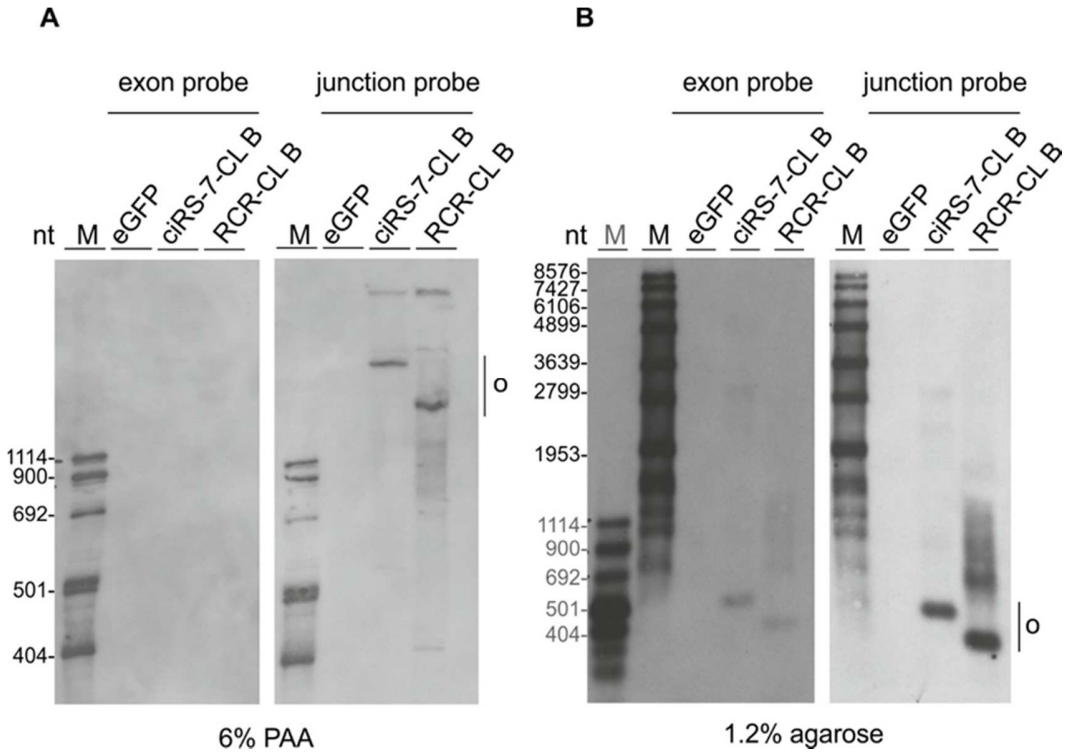

Figure 14 Northern blot analysis of circRNA expression.
HeLa cells were transfected with ciRS-7-CL B, RCR-CL B or eGFP and total RNA was isolated after 16 h. Samples were analyzed by 6% denaturing polyacrylamide (PAA) gel electrophoresis (**A**) or 1.2% denaturing agarose gel electrophoresis (**B**) and northern blot. The DIG-labelled RNA probes hybridize across the splice junction (junction probe) or span the exon (exon probe). circRNAs expressed from ciRS-7-CL B (555 nt) and RCR-CL B (410 nt) were detected by northern blot and are labelled with a circle.

2.1.4 Mutational analysis of RCR-CL Delta

Next the involvement of splice signals and consensus sequence elements in circRNA biogenesis were addressed. Thus mutant derivatives of the minimal circRNA expression constructs RCR-CL B (see Appendix **Figure A1**) and RCR-CL Delta were established. Sequence elements like the PPT, 3'ss and 5'ss or the branch point were manipulated (summarized in **Figure 15**). The mutations were designed on the basis of sequence analyses using Human Splicing Finder along with MaxEntScan (Desmet et al, 2009; Yeo & Burge, 2004). These tools predict the location and strength of the splice sites or helped to identify potential branch points.

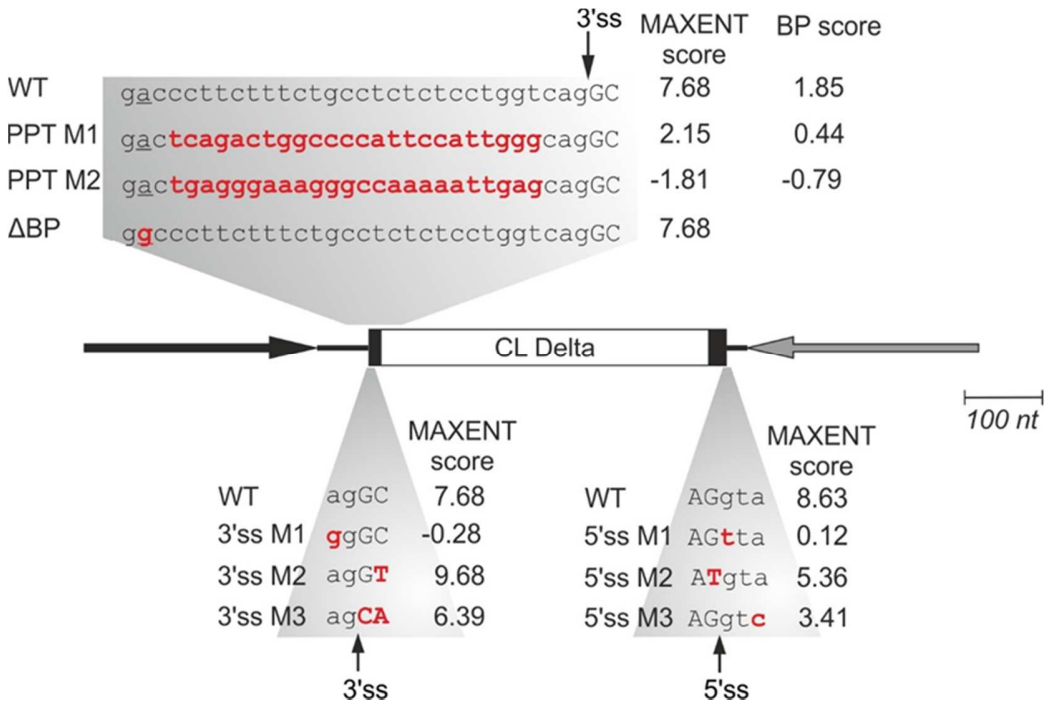

Figure 15 Mutational analysis of RCR-CL Delta minimal circRNA expression construct.
The RCR-CL Delta minigene construct and introduced mutations (M) are schematically illustrated. *CNTROB*-derived sequences are depicted in black, a box symbolizing the exon, bold lines represent the introns and the RCR region is indicated by arrows, facing each other. Mutated nucleotides are highlighted in red, the predicted branch point (BP) is underlined, intronic sequences are shown in lowercase letters and exonic sequences in capital letters. Sequence elements like the polypyrimidine tract (PPT), the BP or 3'ss and 5'ss were mutated. The splice site strength was predicted using MAXENT score and the branch point strength was modeled using the BP score (Yeo & Burge, 2004).

The mutated minigenes were transfected into HeLa cells and circRNA synthesis was analyzed by RT-PCR and northern blot using primers and probes indicated in (**Figure 16 A**). In the RT-PCR analysis, the circular isoform produced from the mutated plasmids was compared to wildtype (WT) levels (**Figure 16 B**). The inactivation of the 3'ss (3'ss M1) abolished circRNA production,

whereas, the other 3'ss mutations (3'ss M2 and M3) did not substantially change splicing efficiency.

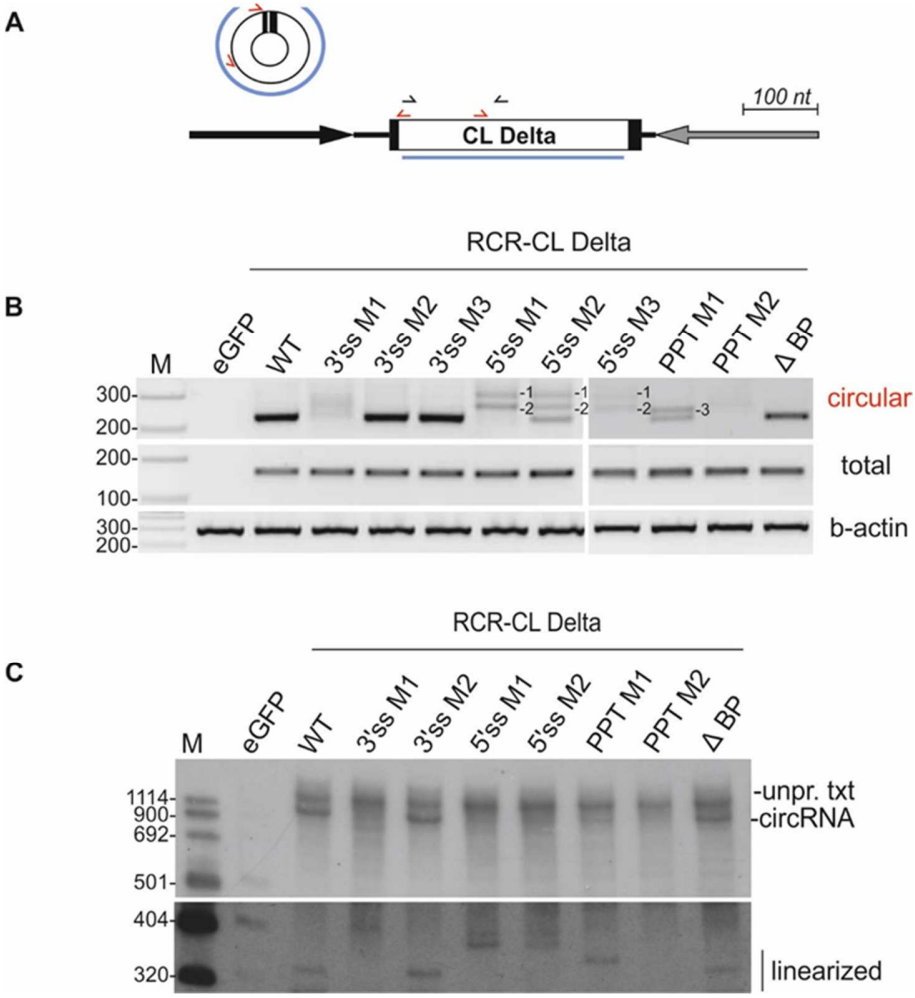

Figure 16 The circRNA biogenesis requires common spliceosomal sequence elements.
RCR-CL Delta minigene constructs shown in (**Figure 15**) and eGFP for controls, were transfected into HeLa cells. The RNA was isolated and analyzed by semi-quantitative RT-PCR (**B**) or northern blot (**C**). The position of primer pairs amplifying the circular junction (red arrow), detecting total levels (black arrow) and the northern probe (blue line) are indicated in the graphic on top (**A**).
The RT-PCR changes in the splicing pattern were monitored by comparing the expression of RCR-CL Delta total levels with the expression of the circular isoform, β-actin (b-actin) served as loading control (**B**).
For northern blot the RNA was separated on a 6% denaturing PAA gel and RCR-CL Delta expressed RNAs were detected using a DIG-labelled RNA probe. The unprocessed transcript (unpr. txt) is approximately 1170 nt long and the WT circRNA has a length of 335 nt. The panel at the bottom shows the linearized circRNA at a longer exposure (**C**). The northern blot was performed by Oliver Rossbach.

All alterations in the 5'ss lead to noticeable changes in exon circularization. For the minigene constructs with 5'ss M1 and M3 a PCR product for the circRNA with expected size was not detected, but two larger PCR products (1 and 2) appeared. The mutated 5'ss M2 lead to reduced levels in WT-length circRNA. The additional PCR products observed for 5'ss M1 and M3, were

detected as well. The mutations of the PPT did also reduce splicing efficiency drastically. The PPT M2 abolished production of the circRNA, whereas for PPT M1 low levels of the WT circRNA were detected, together with an additional PCR product (3). Substitution of the predicted BP did not reduce the circularization efficiency.

In addition to RT-PCR, northern blot analysis of was performed for selected minigene derivatives (**Figure 16 C**). The expressed circRNAs were detected by using a probe, which hybridized in the CL Delta sequence (see **Figure 16 A**). The circular isoform (335 nt) identical to the circRNA expressed from the parental plasmid (RCR-CL Delta WT) was detected only for the 3'ss M2 and Δ BP, although the unprocessed transcript (~ 1170 nt) was expressed from all constructs. The lower panel in **Figure 16 C** shows a longer exposure of the northern blot to visualize the linearized circRNAs.

Finally the relevance of the RCR regions for circRNA biogenesis was investigated. For this purpose additional minigene derivatives of RCR-CL Delta were generated (**Figure 17 A**). The RCR region located downstream of the exon was deleted (Δ 3'), or substituted by a vector sequence (sub. 3'). In order to restore base-pairing ability the upstream intron was partially replaced by the reverse complement of the vector sequence (sub. 3'-5'). This set of minigenes was expressed in HeLa cells, total RNA was isolated and analyzed by RT-PCR. Deletion of the 3' RCR region or its substitution led to decreased circRNA levels, but circRNA synthesis was not abolished. By restoring the interaction of the flanking introns circRNA levels were increased (**Figure 17 B**).

The data obtained from the mutational analysis of RCR-CL Delta are summarized in **Table 1**. In most cases the circRNA synthesis from plasmids carrying the mutations matched the predicted splicing efficiencies (MaxEnt Score) (Yeo & Burge, 2004). An exception is the deletion of the predicted BP (Δ BP), which did not result in reduced circRNA levels. Interestingly, mutations of the 5'ss (5'ss M1-M3) and of the PPT (PPT M1) lead to PCR products, which did not match the expected size. These products were further analyzed by cloning and sequencing. Sequence analysis of the cloned PCR products revealed usage of cryptic splice sites.

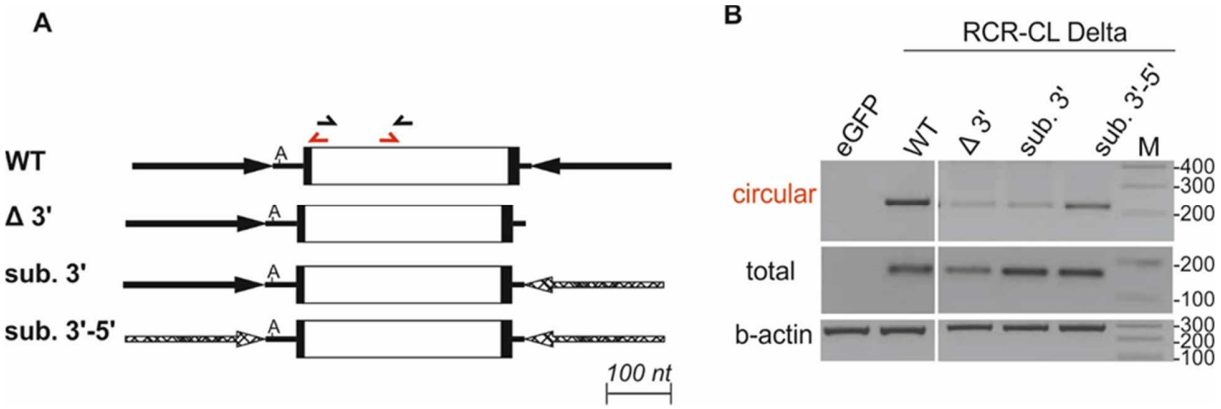

Figure 17 Reverse complementary repeats are stimulatory but not essential for circularization.
RCR-CL Delta minigenes with manipulated RCR regions are schematically shown in the left panel (**A**). *CNTROB*-derived sequences are marked in black and the RCR substitution is labelled by shaded arrows. The base-pairing ability of the RCR region was disrupted by deleting the 3' RCR (Δ 3'), by substitution of the 3' RCR with a vector sequence (sub 3'). RCR base-pairing was restored by substitution of the 3'- and 5' RCR region (sub 3'-5') (**A**).
The RCR-CL Delta repeat mutants were transfected in HeLa cells, and circularization efficiency of the constructs was analyzed by RT-PCR (**B**). For negative controls eGFP was transfected. Position and orientation of the primers used for circRNA detection (red) and total expression levels (black) are shown in the diagram (**A**). The β-actin (b-actin) levels were examined to control for equally loaded amounts.7

For the mutations in the 5'ss two aberrant circular isoforms (1 and 2) were generated. In isoform 1 a 5'ss with a score of 2.37, which was located 39 nt downstream of the original splice site was used. Astonishingly, in isoform 2 not only the 5'ss (-3 nt), but also the 3'ss (-20 nt) changed. In the aberrant circRNA isoform 3, which was generated from RCR-CL Delta PPT M1 minigene a cryptic splice site with a score of 5.76, 23 nt upstream relative to the original 3'ss was used. These spliced isoforms were also detected by northern blot (see **Figure 16 C**, lower panel with the linearized circRNAs). This was indicative that the aberrant PCR products originated most probably from the circularized exon and not from a *trans*-spliced junction.

Table 1 Summary of RCR-CL Delta mutational analysis.
PCR products obtained from experiments shown in **Figure 16** and **Figure 17** were cloned via TOPO-TA cloning kit, sequenced and analyzed. The positions of the 3'ss and 5'ss were determined, and splice site strength was predicted. The circRNAs which were spliced using the original splice sites, although they were mutated were termed WT circRNA. Three aberrant spliced circRNA isoforms were found (1, 2, and 3), using cryptic splice sites. The relative position of cryptic splice sites to the WT splice site is depicted and the corresponding splice site score was predicted. The alternatively spliced circRNAs and their splice site positions are marked in red. For two constructs no PCR product was obtained; these are indicated by N/A.

RCR-CL Delta	circRNA	3'ss position	3'ss score	3'ss relative to WT	5'ss position	5'ss score	5'ss relative to WT
WT	WT	282	7.68	0	634	8.63	0
3'ss M1	N/A	/	-0.28	/	/	/	/
3'ss M2	WT	282	9.68	0	634	8.63	0
3'ss M3	WT	282	6.39	0	634	8.63	0
5'ss M1	1	282	7.68	0	673	2.37	39
	2	262	-9.67	-20	637	-28.7	3
5'ss M2	WT	282	7.68	0	634	5.36	0
	1	282	7.68	0	673	2.37	39
	2	262	-9.67	-20	637	-28.7	3
5'ss M3	1	282	7.68	0	673	2.37	39
	2	262	-9.67	-20	637	-28.7	3
PPT M1	WT	282	2.51	0	634	8.63	0
	3	258	5.76	-23	634	8.63	0
PPT M2	N/A	/	-1.81	/	/	/	/
ΔBP	WT	282	7.68	0	634	8.63	0
Δ3'repeat	WT	282	7.68	0	634	8.63	0
sub3'repeat	WT	282	7.68	0	634	8.63	0
sub3'-5' repeat	WT	282	7.68	0	634	8.63	0

Initially, the mutational analysis of splice signals was performed with RCR-CL B minigene (see Appendix **Figure A1**). In this minigene most of the original *CNTROB* exon was replaced by a sequence with several hnRNP L binding sites. In order to prevent interference of hnRNP L binding with the mutational analysis, an unspecific vector sequence was used in RCR-CL Delta. Nevertheless, the results from RCR-CL B mutational analysis coincide to a large extent with the results from RCR-CL Delta.

2.1.5 Influence of ESEs on circRNA splicing

With the preceding experiments involvement of splice signals in circRNA biogenesis was demonstrated. In the following the impact of exonic splice enhancer (ESE) elements on circRNA synthesis was investigated. These sequence elements were found to mediate fine-tuning of the spliceosomal machinery and influence constitutive as well as alternative splicing (Matlin et al, 2005). In a study from Fairbrother et al (2002) a computational analysis allowed the prediction of short sequences with ESE activity. A set of the predicted ESE elements and inactive point mutants thereof were validated using a splicing reporter (Fairbrother et al, 2002). Two of these identified ESE sequences from the study, and the corresponding inactive mutant as well as a neutral sequence were cloned into the minigene construct *LPAR1* (Starke et al, 2015). This construct was derived from the *LPAR1* gene, which gives rise to a circular RNA consisting of exon 2 and 3. The intron between these exons was removed and replaced by a multiple cloning site (MCS), which was then used to insert the ESEs. Flanking introns were shortened and a fragment of the neighboring exons was included, to study the competition between linear and circular splicing (**Figure 18 A**). Then, the minigenes were transfected into HeLa cells and produced circRNA levels were analyzed by RT-PCR. The inserted ESE sequences and according controls did not affect circularization efficiency of exon 2 and 3, nor was any effect on linear splicing or exon skipping observed (**Figure 18 B**).

The mutational analysis of circRNA minigenes (RCR-CL Delta and RCR-CL B) showed, that fundamental splicing signals such as the PPT, 3'ss and 5'ss were required for efficient and precise exon circularization. Further the impact of RCR elements was investigated, showing that RCRs promote circRNA formation, but they are not essential for circularization. By studying the impact of ESEs in circRNA biogenesis, the aim was to find potential splicing factors or sequence elements, which either enhance or decrease circRNA production. At least the ESEs used in these experiments do not affect circRNA production or linear splicing in HeLa cells in the *LPAR1* minigene.

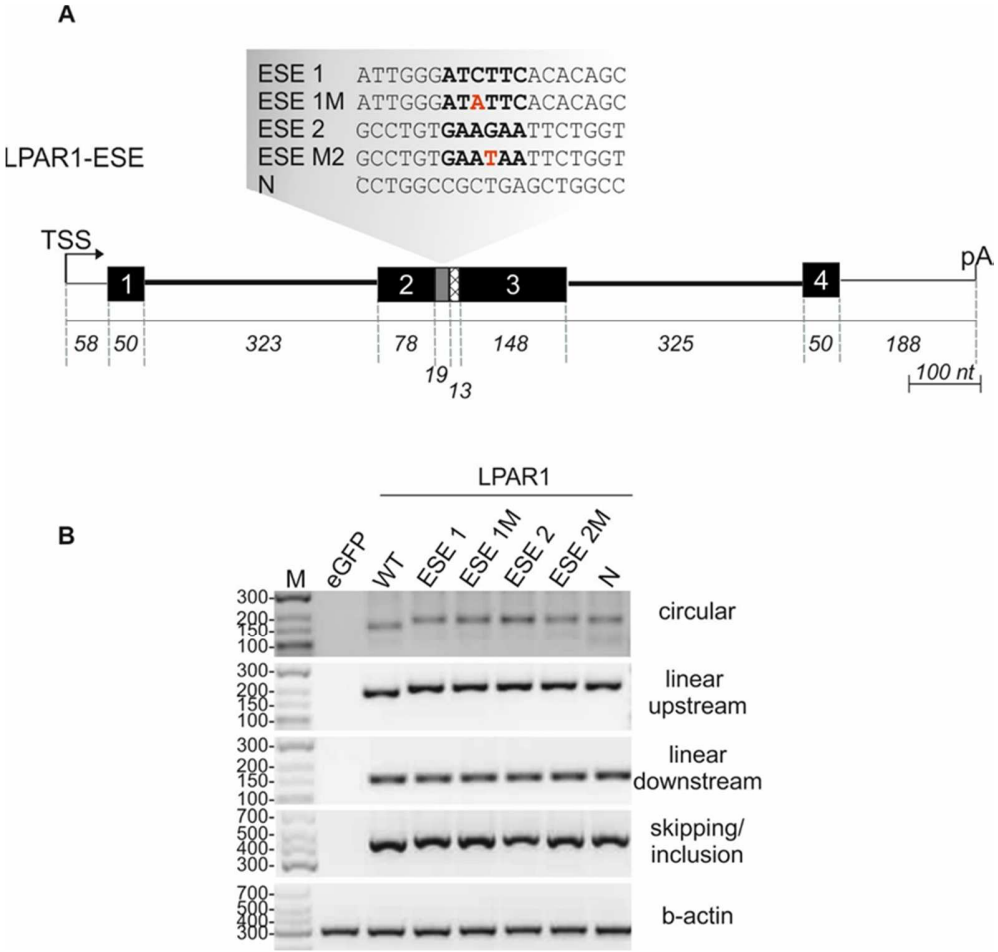

Figure 18 *LPAR1* minigene splicing is not affected by exonic splice enhancer motives.
The *LPAR1* minigene is depicted schematically, as described before. The intonic sequence between exon 2 and 3 was deleted and a MCS was added, which additionally served as sequence tag (shaded box). Two different exonic splice enhancer motives (ESE1, ESE2), its corresponding inactive mutant (M) and a neutral sequence (N) of the same length (grey box) were inserted leaving only a small part of the original tag sequence (Fairbrother et al, 2002). The sequences of the ESE motives are shown in bold letters and the mutated nucleotides are highlighted in red (**A**).
The minigenes were transfected into HeLa cells and the splicing pattern was analyzed by semi-quantitative RT-PCR. The circular isoform, the upstream and downstream splice junction were analyzed. Skipping of exon 2 and 3 was monitored by using primers at the 5' and 3'end of the precursor. For negative controls eGFP was transfected and β-actin (b-actin) was used as loading control (**B**).

2.2 Design and characterization of high-affinity miR-122 binding sites

HCV propagation is strongly dependent on the liver-specific miR-122. In order to prove the concept of circular miRNA sponges, artificial circRNAs were created to sequester miR-122 from HCV. High abundance of miR-122 and the high-affinity of the HCV binding sites, required development of a very potent sponge, to be able to compete for binding. In this chapter strong miR-122 binding sites were developed and the interaction of miR-122 with the binding sites was validated by luciferase and pulldown assays.

For miR-122 interaction studies pmirGLO Dual-Luciferase expression vector was used. The vector has a Firefly luciferase gene with a MSC in its 3'UTR, where miRNA target sites were inserted. The Firefly luciferase is the primary reporter, reacting with decreased translation or reduced transcript stability upon miRNA interaction with the target sites. By measuring the Firefly luciferase activity miRNA binding can be monitored indirectly. The Renilla luciferase gene serves as control reporter, it is constitutively co-expressed and thus used for normalization (**Figure 19**).

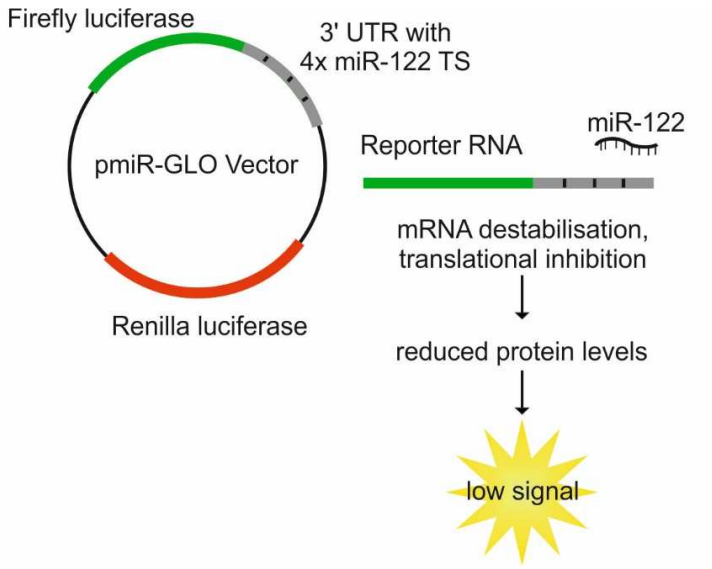

Figure 19 miRNA interaction studies using pmirGLO Dual-Luciferase expression system.
Graphic representation of the experimental setup for miR-122 interaction studies with selected target sites (TS). The target sites (4-times) or control sequences of similar length were inserted into the 3'UTR of the Firefly luciferase gene. Upon expression of the Firefly luciferase mRNA, miR-122 interacts with the target sites, which leads to destabilization of the reporter mRNA or its translational repression. This results in reduced luciferase levels and bioluminescence signals. The Renilla luciferase gene is constitutively expressed and used for normalization.

A functional miRNA sponge requires high-affinity binding sites to efficiently sequester the miRNA molecules. Three miR-122 binding sites were selected and cloned into the Firefly 3'UTR of the

Dual-Luciferase expression vector, to experimentally test them in luciferase assays (**Figure 20**). One endogenous miR-122 binding site from the *IGF1R* mRNA was chosen because it had already been experimentally validated (Bai et al, 2009). The *IGF1R* binding site was discovered by searching the miRNA interaction database miRTarBase (Chou et al, 2016). The other two target sites were designed based on the structural model of miRNA targeting to mediate particularly strong interaction with miR-122 (Schirle et al, 2014). The artificial target site named *bulge* exhibits complementarity to miR-122, except nucleotides 10-12. The second artificial target site was designed to be perfectly complementary to miR-122 and was abbreviated *perfect*. This target site was thought to be cleaved by the RISC complex (Jinek & Doudna, 2009; Schirle et al, 2014). For each of the three described target sites, seed mutants were designed (**Figure 20**). The miR-122 target sites and mutants were selected and designed by Oliver Rossbach.

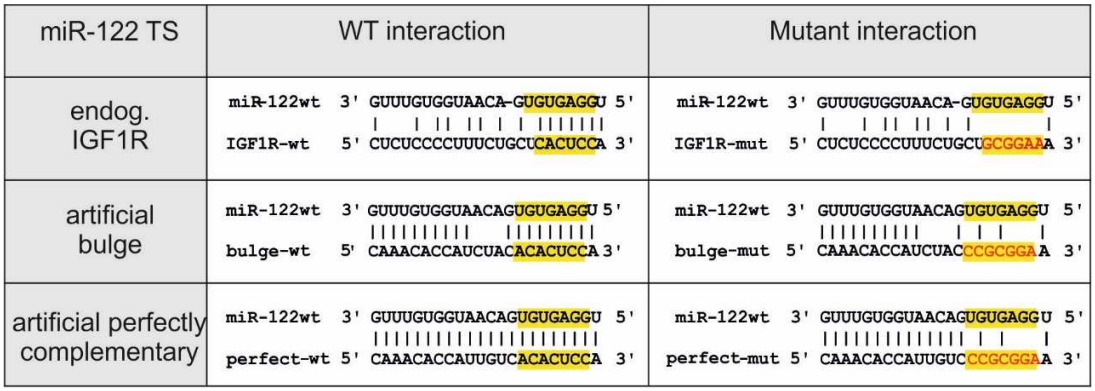

Figure 20 Predicted interaction of miR-122 with high-affinity target sites.
Three different target sites were chosen and validated for miR-122 binding. One endogenous (endog.), already experimentally validated miR-122 target site from the *IGF1R* mRNA and two artificial target sites: *bulge* and perfectly complementary (*perfect*). For each of these target sites a seed mutant was generated. The interaction of the target sites (left) or its seed mutants (right) with miR-122 are illustrated. The seed region is colored in yellow and mutated nucleotides are highlighted in red.

Four consecutive target sites or four-times the mutated binding site with four nt spacing were cloned into the 3'UTR of the Firefly luciferase gene. First, the pmirGLO Dual-Luciferase reporter system was tested in HeLa cells, which express miR-122 only at very low levels. The pmirGLO reporter constructs with the *bulge* or *perfect* binding sites, together with controls (empty vector and seed mutants) were co-transfected with a miR-122 expression vector. By transfecting increasing amounts of the miR-122 expression vector, the quantitative impact of miR-122 on the luciferase activity was monitored. A miR-122 dose-dependent reduction of the relative luciferase activity was observed for the reporters harboring the *bulge* and *perfect* binding sites (**Figure 21**). The relative luciferase activity from the reporters with mutated binding sites and the empty vector

control were not affected by the expression of miR-122. Even without exogenous expression of miR-122, a minor reduction in relative luciferase activity with the *bulge* and *perfect* target sites was observed, indicating that miR-122 was present in HeLa cells (**Figure 21**).

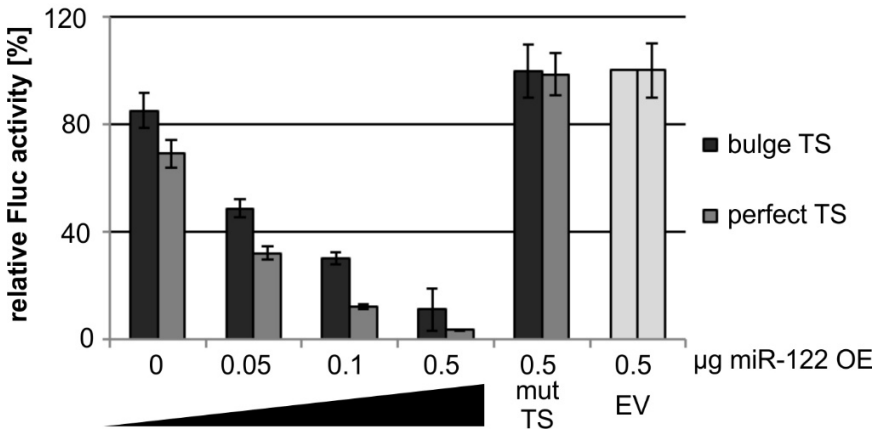

Figure 21 Analysis of miR-122 effects on pmirGLO-Dual Luciferase reporter system.
HeLa cells were transfected with the pmirGLO Dual-Luciferase reporters, containing four times the bulge and perfect target sites (TS) in their 3'UTR. For controls the respective seed mutant (mut TS) or the empty vector without insertion in the 3'UTR (EV) were transfected. Increasing amounts of miR-122 expression vector (OE) (0, 0.05, 0.1 and 0.5 µg) were co-transfected. Firefly luciferase activity was measured after 16 h of expression, normalized to Renilla luciferase activity and to the EV control. Error bars represent the standard error of the mean (SEM) from three technical replicates.

Next the complete set of miR-122 binding sites *IGF1R*, *bulge*, *perfect* and the corresponding seed mutants were analyzed by luciferase assays in Huh7.5, which highly express miR-122. For negative controls, fragments of comparable length from *LAPTM4A*, *HNRNPK* and *KPNB1* 3'UTR were inserted into the 3'UTR of the reporter. These control reporters do not exhibit miR-122 target sites. The experiments were performed in triplicates and normalized to luciferase activity of the *LAPTM4A* negative control. A strongly and significantly reduced relative luciferase activity was measured for the *bulge* and *perfect* target sites (**Figure 22 A**). The control reporter with the insertion from *KPNB1*, showed only moderate but significant reduction in luciferase activity. Interestingly, the seed mutant of the *perfect* binding site also showed significantly reduced luciferase activity relative to *LAPTM4A*. No decrease in luciferase activity was observed for the reporter with the *IGF1R* binding sites.

In addition to luciferase assays, the influence of the described target sites on the reporter RNA stability was determined by RT-PCR (**Figure 22 B**). Here the reporter RNAs with the *bulged* and *perfect* miR-122 binding sites showed reduced steady state levels compared to the mutated binding sites. The reporter RNA levels with the *IGF1R*-derived target sites were slightly decreased compared to its seed mutant.

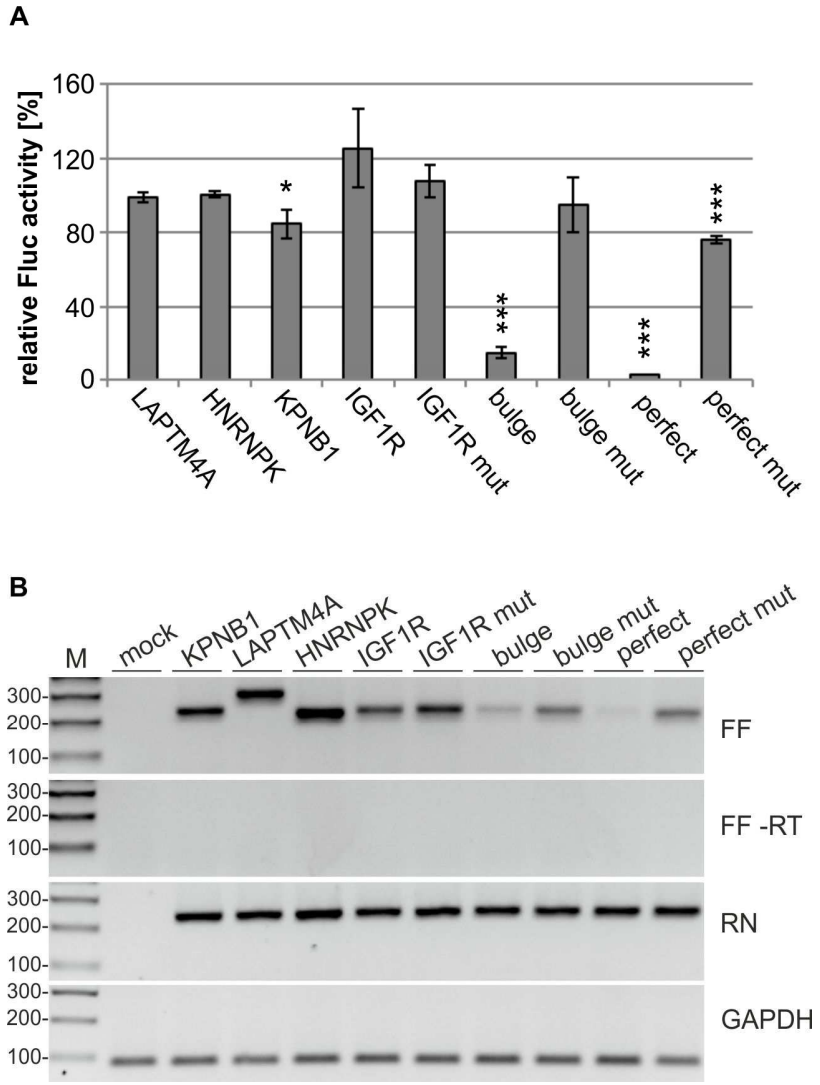

Figure 22 *In vivo* miR-122 binding site analysis and reporter RNA stability.
Huh7.5 cells were transfected with pmirGLO Dual-Luciferase reporters, containing the *IGF1R*, *bulge* and *perfect* binding sites, or the respective seed mutants (mut) (see **Figure 20**)**.** pmirGLO Dual-Luciferase reporters, containing insertions from *LAPTM4A*, *KPNB1* or *HNRNPK* 3'UTRs of the same length, were used for control transfections (**A**, **B**).
Firefly luciferase activity was measured, normalized to Renilla luciferase activity and to *LAPTM4A* negative control. Error bars represent the standard deviation (SD) from three replicates. Statistical analysis by t-test with * $p<0.05$; *** $p<0.001$ (**A**).
For analysis of the reporter RNA stability total RNA was isolated and subjected to RT-PCR detecting Firefly (FF), Renilla (RN) and *GAPDH* mRNAs. A minus RT control was performed using the same primers as for Firefly mRNA detection (FF-RT) (**B**).

In order to acquire additional evidence for miR-122 binding to the designed target sites, direct interaction was assayed by *in vitro* pulldown assays. *In vitro* generated and biotinylated transcripts containing four consecutive binding sites were used as bait. The transcripts were bound to beads, and incubated with Huh7 extracts. After selection and purification, miR-122 molecules were detected by northern blot analysis (**Figure 23**). Efficient binding of miR-122 to the *bulge* and *perfect* target sites was confirmed by the pulldown assays. Furthermore, only low levels of miR-122 were recovered by the *IGF1R* target site, matching the preceding results. For the pulldowns with the mutated binding sites and specificity controls (*KPNB1* and minus RNA) no signal for miR-122 was observed.

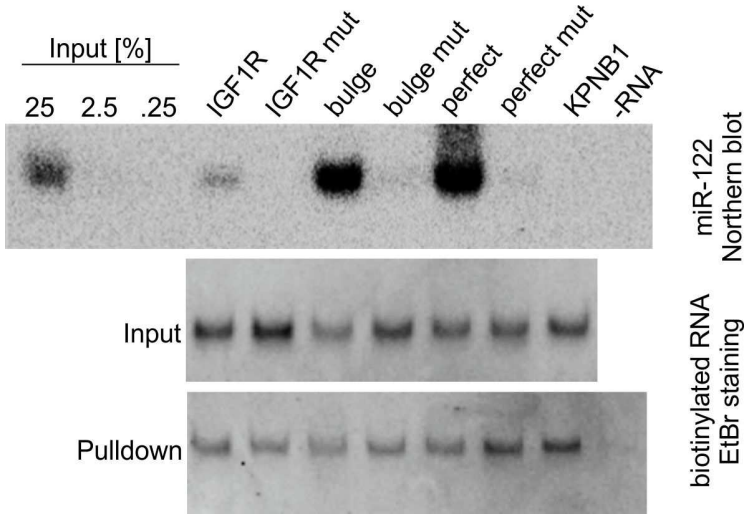

Figure 23 Characterization of miR-122 binding sites by *in vitro* pulldown assay.
In vitro transcribed and biotinylated target RNAs were generated, containing four copies of the miR-122 binding sites *IGF1R*, *bulge* and *perfect* or the related seed mutant (mut). Background binding was monitored with *KPNB1* 3'UTR fragment of the same length or minus RNA (-RNA) controls. The biotinylated target RNAs and *KPNB1* were bound to Neutravidin beads and incubated with Huh7 extracts. The bound RNAs were isolated and analyzed by northern blot using 5' ^{32}P labelled DNA probes directed against miR-122. For estimate of the pulldown efficiency 25, 2.5 or 0.25% of Huh7 extracts, were examined by northern blot. The biotinylated RNAs were analyzed before (middle panel) and after the pulldown (bottom) on 8% denaturing PAA gels and RNAs were visualized by EtBr.

The data obtained *in vivo*, by luciferase assays and RT-PCR supported the binding of miR-122 to the target sites *bulge* and *perfect*. Additionally, the direct interaction was confirmed by *in vitro* pulldown assays. Both experiments support strong and specific interaction of miR-122 to the WT binding sites *bulge* and *perfect*. For the *IGF1R* binding site, interaction with miR122 was much weaker compared to *bulge* and *perfect*. Interestingly, the *bulge* and *perfect* binding sites lead to destabilization of the luciferase reporter RNAs *in vivo*, but not in the *in vitro* pulldown experiment (see **Figure 22 B** and **Figure 23** panel Pulldown).

2.3 circRNA synthesis

The attempts to express circRNAs containing miR-122 binding sites via different expression plasmids, as they were used for investigations of circRNA biogenesis, failed. The circRNAs were either expressed at very low levels, or they did not produce circRNAs at all (data not shown). Then, two different methods have been used to produce artificial circRNAs, with the purpose to transfect them into cells. Besides *in vitro* circularization by using T4 RNA ligase 1, the group I self-splicing mechanism was used.

2.3.1 circRNA production by genetically engineered ribozyme self-splicing

The data presented in **Figure 24** show the *in vitro* self-splicing reaction of the permutated intron-exon (PIE) ribozyme. It was adapted from (Umekage & Kikuchi, 2009), where they expressed a circular streptavidin aptamer in *E.coli* and subsequently purified it from *E.coli* total RNA in large amounts (190 µg from 1L of *E.coli* culture). The original PIE ribozyme containing the streptavidin aptamer was used to establish the method in our laboratory.

2.3.2 *In vitro* self-splicing of the PIE ribozyme

The self-splicing mechanism is activated by GTP, releasing the downstream intron (99 nt). Next, the free OH of the exon attacks the 3'ss, which results in a circRNA (82 nt) and the release of the upstream intron (117 nt) (**Figure 24 A**). The precursor was synthesized by *in vitro* transcription and purified. Then the transcripts were incubated for 1 h or 3 h in self-splicing buffer at different concentrations (4, 8 and 100 µM) of GTP. The reaction was terminated by adding Formamide (FA) RNA loading buffer and heat denaturation at 85℃. T he analysis of the self-splicing reaction by native 2% agarose gel electrophoresis, showed the induction of self-splicing at 100 µM GTP. After 1 h a fraction of the unprocessed precursor was still present, but after 3 h it was completely consumed. The product detected beneath the 100 nt marker band matched the expected size of the circularized streptavidin aptamer (**Figure 24 B**). In order to obtain more evidence for the production of a circRNA by self-splicing, samples were analyzed on a denaturing 10% PAA gel (**Figure 24 C**). By comparing the running behavior of the self-splicing products in agarose and denaturing PAA gels, the retention of the circRNA in PAA gels should confirm its circular configuration. The *in vitro* transcription and self-splicing reaction were repeated under the same conditions as described before. However, the reaction without GTP yielded several products, contrary to the expectations of detecting only the precursor. Self-splicing buffer and transcription

buffer were almost similar, so self-splicing could already have occurred during the *in vitro* transcription.

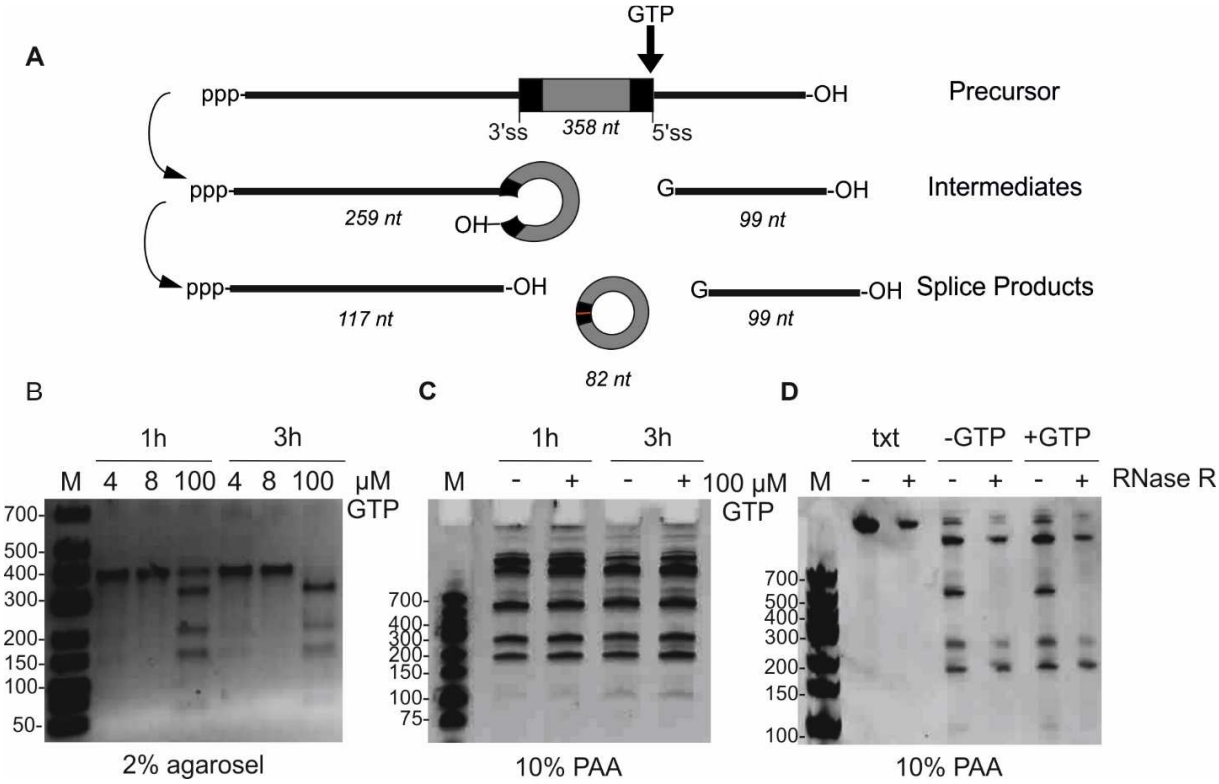

Figure 24 *In vitro* self-splicing reaction.
The self-splicing mechanism of the permuted intron exon (PIE) group I ribozyme, showing the nucleophilic attack of GTP, the precursor, intermediates, splice products and their respective length. The box colored in dark grey represents the streptavidin aptamer sequence and black indicates the natural ribozyme sequence (**A**).
The precursor was synthesized by *in vitro* transcription and 20 µg of transcript were incubated with self-splicing buffer containing 4, 8 or 100 µM GTP for 1 h or 3 h. After purification 600 ng of the RNA were analyzed on a 2% agarose gel (**B**).
The *in vitro* transcription and self-splicing reaction were repeated and 1.2 µg per sample was loaded on a 10% denaturing PAA gel (**C**). Samples incubated for 180 min from the 10% PAA gel (**C**) and the unspliced transcript (txt) from the agarose gel (**B**) were reanalyzed. 5 µg RNA were incubated with 1.25 u RNase R for 3 h and resolved by 10% PAA gel electrophoresis (**D**). RNA was visualized by EtBr staining.

Furthermore, several products showed aberrant mobility in the PAA gel, relative to their predicted sizes and considering the running behavior observed in the agarose gel. It was not clear which band corresponded to the circRNA or if it was produced at all. Consequently the samples were reanalyzed (**Figure 24 D**). In order to clarify which band corresponds to the circRNA, the samples were treated with RNase R. The unprocessed precursor (transcript; txt) from the reaction analyzed in **Figure 24 B**, was compared with the self-splicing reaction (3 h) analyzed in **Figure 24 C**. Although the electrophoresis was performed under denaturing conditions, the mobility of the

unprocessed transcript (358 nt) was unexpected slow (**Figure 24 D**). Besides, the RNA species differed in their sensitivity to RNase R treatment. Particularly resistant to RNase R treatment and possibly the circular isoform, were RNA species which migrated between marker bands 200 nt and 150 nt.

2.3.3 PIE ribozyme-generated circRNAs expressed in *E.coli* and Huh7

Next the PIE streptavidin aptamer was expressed in *E.coli*, and synthesis of the circRNA was monitored by RT-PCR. Divergent primers were used for detection of the circRNA, and convergent primers located in the introns to verify expression of the precursor (**Figure 25**). For that purpose the PIE streptavidin ribozyme was cloned into the pcDNA3 vector backbone. The construct was expressed, using *E.coli* KRX strain, which has a chromosomal rhamnose-inducible T7 RNA polymerase. Moreover the construct included the rrnC terminator to create 3'ends on the bacterial transcripts.

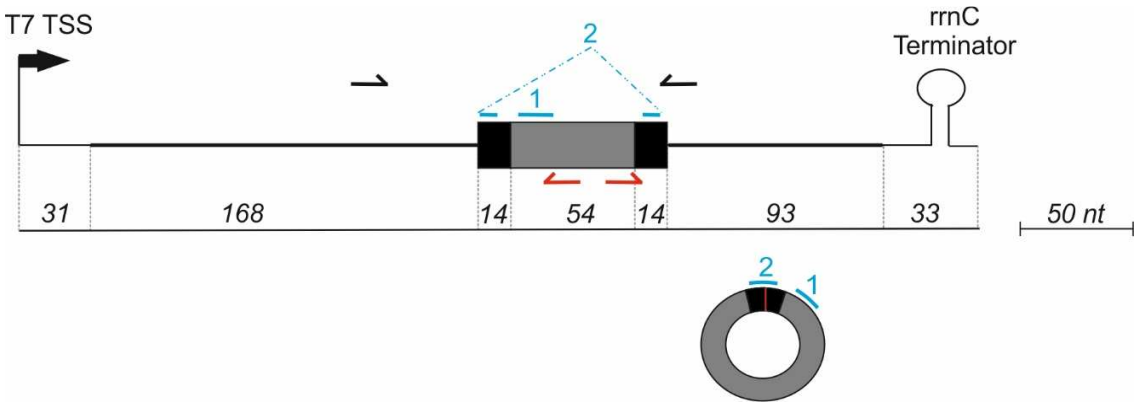

Figure 25 PIE circRNA expression construct.
The PIE ribozyme was cloned into pcDNA3 that allows eukaryotic expression driven by CMV promoter, as well as bacterial expression through rhamnose-inducible T7 polymerase expression. To stop bacterial transcription the rrnC terminator was inserted at the end of the construct. Expression can be monitored by RT-PCR detecting the circular isoform with divergent primers (red arrows) or the precursor using convergent primers (black arrows). For northern blot detection two probes indicated in blue were designed.

For the test expression, 15 ml of *E.coli* culture were incubated at 37℃, the expression was induced at OD_{600} of 0.7 by adding rhamnose (see **4.2.7.3**). A 2 ml sample was taken to measure pre-induced expression. After 2 h of expression at 30℃ cells were harvested and analyzed by RT-PCR (**Figure 26 A**). One sample per condition (induced and pre-induced) were subjected to lysis, prior RNA preparation by Trizol. The RNA from the other samples was isolated using Trizol only, but skipping the lysis step. Synthesis of the circRNA was observed for samples of the induced

cultures only. A signal for the precursor was detected for both conditions pre-induced and induced. The DNA template of the construct would result in an identical PCR product, considering that in pre-induced samples no circRNAs were detected, the signal probably resulted from residual plasmid DNA. The lysis did not substantially enhance circRNA recovery from bacterial culture (**Figure 26**).

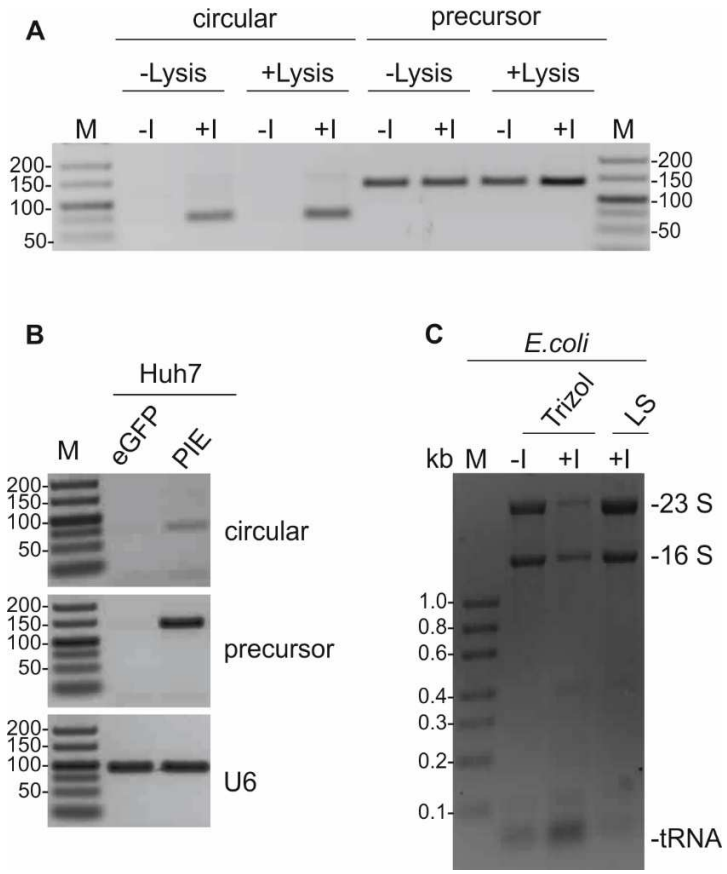

Figure 26 Test expression of the PIE ribozyme in *E.coli* and Huh7 cells.
E.coli were transformed with the PIE streptavidin expression vector and total RNA was isolated from 1 ml *E.coli* culture per condition. The samples were lysed with PK-buffer at 65℃ (+Lysis) or isolated with Trizol only (-Lysis) and the expression of the linear precursor or the circRNA were monitored by RT-PCR prior induction or 2 h post induction (-I/+I) (**A**).
The expression of the ribozyme-generated circRNAs was tested in Huh7 cells. After transfecting the expression plasmid for 16 h total RNA was isolated and analyzed by RT-PCR (**B**).
The PIE ribozyme was expressed in *E.coli* using two 200 ml cultures. RNA was isolated by hot phenol with an upscaled protocol. For quality control of the RNAs purified via large scale (LS) isolation, 1.2% denaturing agarose gel electrophoresis was performed. The RNA purified from 200 ml *E.coli* culture via LS isolation was compared to the RNA isolated via Trizol from 1 ml *E.coli* culture (**C**).

The PIE expression vector also contained a CMV promoter, which facilitates expression in eukaryotic cells. Thus it was tested, if the ribozyme-generated circRNA was expressed in Huh7 cells, with the result that self-splicing of the PIE streptavidin aptamer was confirmed by RT-PCR

(**Figure 26 B**). The signal for the circRNA, expressed in Huh7 was rather low. Due to the fact that RT-PCR is a very sensitive method, this was indicative that ribozyme-generated circRNAs were not expressed at high levels, as it is required for miRNA sequestration. For this reason, validation of the circular configuration of the PIE-derived RNAs in Huh7 was not pursued.

By expressing circRNAs in *E.coli*, large cultures volumes can be used and subsequently purified circRNAs can be transfected at higher amounts than they are expressed in the cell. Thus expression in a larger culture volume and enrichment of the circRNA via anion exchange chromatography was established. The expression of the PIE ribozyme in *E.coli* was tested using two 200 ml cultures, which were induced at OD_{600} of 0.7. Then bacteria were harvested after 2 h of expression at 30°C. Next, the RNA was purified by the hot phenol isolation method, which yielded approximately 10 mg RNA from 400 ml of *E.coli* culture. The RNA quality was monitored by inspecting integrity of the rRNAs via denaturing 1.2% agarose gel electrophoresis (**Figure 26 C**). Afterwards, the RNA was analyzed by northern blot, probing circRNA expression with 5' ^{32}P labelled DNA antisense oligos (**Figure 27**). The expression of PIE-generated circRNAs in *E.coli* was compared to the *in vitro* self-splicing reaction and RNA from pre-induced *E.coli* culture served as negative control. For detailed analysis, three gels were prepared in parallel. Two of them were used for northern blots, detecting the PIE ribozyme-derived circRNAs using two different probes. Probe 1 hybridized in the streptavidin aptamer sequence, detecting total levels and probe 2 was specific for the circular junction (see **Figure 25**).

The other gel was ethidium bromide (EtBr) stained. *In vitro* transcribed and unprocessed precursor (358 nt) was detected, as well as two signals for the *in vitro* self-splicing reaction. These products migrated at the approximate size of the circRNA, probably representing the circular isoform and its linearized counterpart. The expression of the precursor in *E.coli* was confirmed. It was detected by probe 1, which binds in the streptavidin aptamer sequence. Although RT-PCR analysis hints that the circRNA was expressed in *E.coli*, no signal was observed in the northern blot.

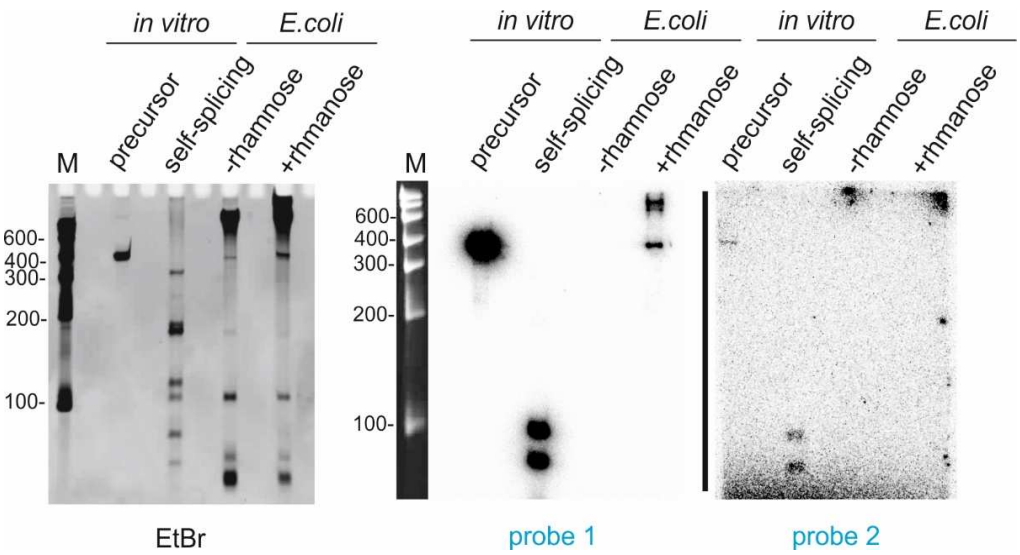

Figure 27 Analysis of PIE ribozyme-generated circRNAs by northern blot.
600 ng of the unprocessed precursor, the *in vitro* self-splicing reaction and 1 µg of the large scale RNA isolation from induced (+rhamnose) and pre-induced (-rhamnose) *E.coli* cultures were subjected to 8% denaturing PAA gel electrophoresis and EtBr stained. 5% of the samples were analyzed by northern blot using 5'- ^{32}P labelled DNA probes (**Figure 25**) which detect either total levels (probe 1) or the circular junction (probe 2).

2.3.4 Purification of ribozyme-generated circRNAs from *E.coli* total RNA

In order to enrich the in *E.coli* expressed and PIE-generated circRNAs, anion exchange chromatography was performed. For a first test run total RNA (1.6 µg) from uninduced *E.coli* culture was mixed with RNA (0.9 µg) of the *in vitro* self-splicing reaction. The RNAs were eluted using a linear gradient from 500-800 mM NaCl. Then the RNA was isolated and subjected to RT-PCR to determine the elution profile of the circRNA in comparison to its precursor (see Appendix **Figure A2**).

After the successful test run, the *E.coli* expressed and ribozyme-generated circRNAs were enriched by anion exchange chromatography using 100 µg RNA. The RNAs were eluted by a linear NaCl gradient from 500-700 mM, and the circRNA as well as the precursor were detected by RT-PCR (**Figure 28 A**). For further analysis northern blots were performed (as described above). Fractions were pooled using every second fraction in P1 (13-17), P2 (19-25) and P3 (27-33). The pooled fractions P1-P3 were compared to 2% input and RNA from the *in vitro* self-splicing reaction served as positive control. Contrary to the RT-PCR analysis the enrichment of circRNAs by anion exchange chromatography was not confirmed by northern blot (**Figure 28 B**). For further purification of the PIE-generated circRNAs a second purification step would comprise selection by antisense oligos. The antisense selection is based on the same region hybridizing to

an antisense oligo as it was used for detection by northern blot. Since this detection of PIE-generated circRNAs failed, the project was not continued.

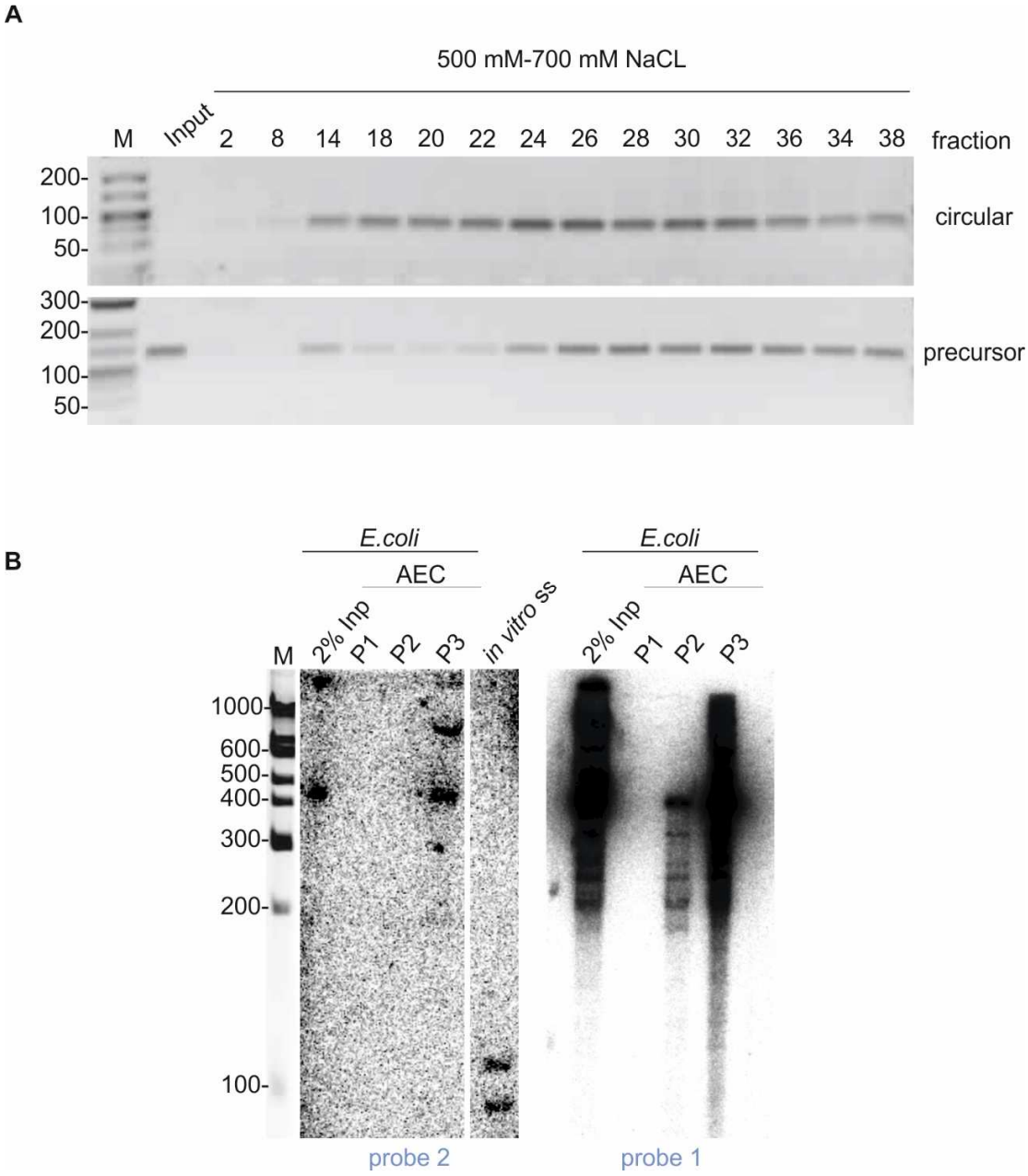

Figure 28 Purification of in *E.coli* expressed and PIE ribozyme-generated circRNAs by anion exchange chromatography.
100 µg RNA from PIE ribozyme expression in *E.coli* were separated by anion exchange chromatography (AEC) using a linear gradient from 500 mM to 700 mM NaCl. RNAs from fractions indicated, were purified and distribution of the circRNAs and the precursors was monitored by RT-PCR (**A**).
Fractions (13, 15, 17), (19, 21, 23, 25) and (27, 29, 31, 33) were pooled in P1, P2, P3 respectively. Pooled fractions, 2% input (2 µg) and 30 ng of the *in vitro* self-splicing (ss) reaction were loaded on a 7% denaturing PAA gel and were further analyzed by northern blot (probes as described in **Figure 25**) (**B**).

2.3.5 *In vitro* circRNA synthesis by ligation

2.3.5.1 Circularization and purification of miR-122 sponges

In close cooperation with Silke Schreiner and Oliver Rossbach a protocol for the *in vitro* synthesis of circRNAs by ligation and their preparation via gel-purification was established. This protocol provided for the first time the opportunity to circularize miR-122 sponges. The interaction studies represented in **Figure 22** and **Figure 23** showed that miR-122 was potently bound by the target sites *bulge* and *perfect*. For *in vitro* synthesis of circRNA sponges three constructs were designed. These constructs either contained eight consecutive *bulge* or *perfect* binding sites with 4 nt spacing between each binding site, along with a control sequence (*shuffle*). During optimization of the ligation protocol, it became apparent that repetitive sequences are problematic, in regards to detection methods and poor circularization efficiency. In order to evade these problems a non-repetitive sequence of 60 nt which was identical in all constructs was added at the 5'end and additionally served for northern probe detection. Moreover a stem of 11 nt followed by 5 unpaired nt at the outermost ends was created and was supposed to enhanced circularization efficiency (**Figure 29 A**). This stem structure with the unpaired ends was supposed to favor intramolecular over intermolecular ligation. The constructs were *in vitro* transcribed using a four-fold excess of GMP to obtain mainly monophosphorylated transcripts, which are required for the ligation reaction. These were purified and then ligated using T4 RNA ligase in 250 µl volume at 16℃ overnight. 5% of each reaction were analyzed on a denaturing 7% PAA gel, detecting linear monomers, and products of intermolecular ligation (linear dimer) or intramolecular ligation (circularized monomers). The circularization efficiency of the *shuffle* sequence was much higher compared to the constructs containing the *bulge* or *perfect* target sites (**Figure 29 B**). Less efficient circularization was probably caused by disadvantageous secondary structures due to the repetitive binding sites. For the purification step, the samples were separated by preparative denaturing 7% PAA gel electrophoresis and RNAs were visualized by UV shadowing (see Appendix **Figure A3**). The linear and circular monomers were cut from the gel, and purified. After their concentrations had been adapted they were re-examined by gel electrophoresis for quality control (**Figure 29 C**). Furthermore the purified RNAs were treated with RNase R and analyzed by denaturing 7% gel electrophoresis (**Figure 29 D**). The linear RNAs and also the linearized RNAs disappear upon RNase R treatment, whereas the circRNAs were stable.

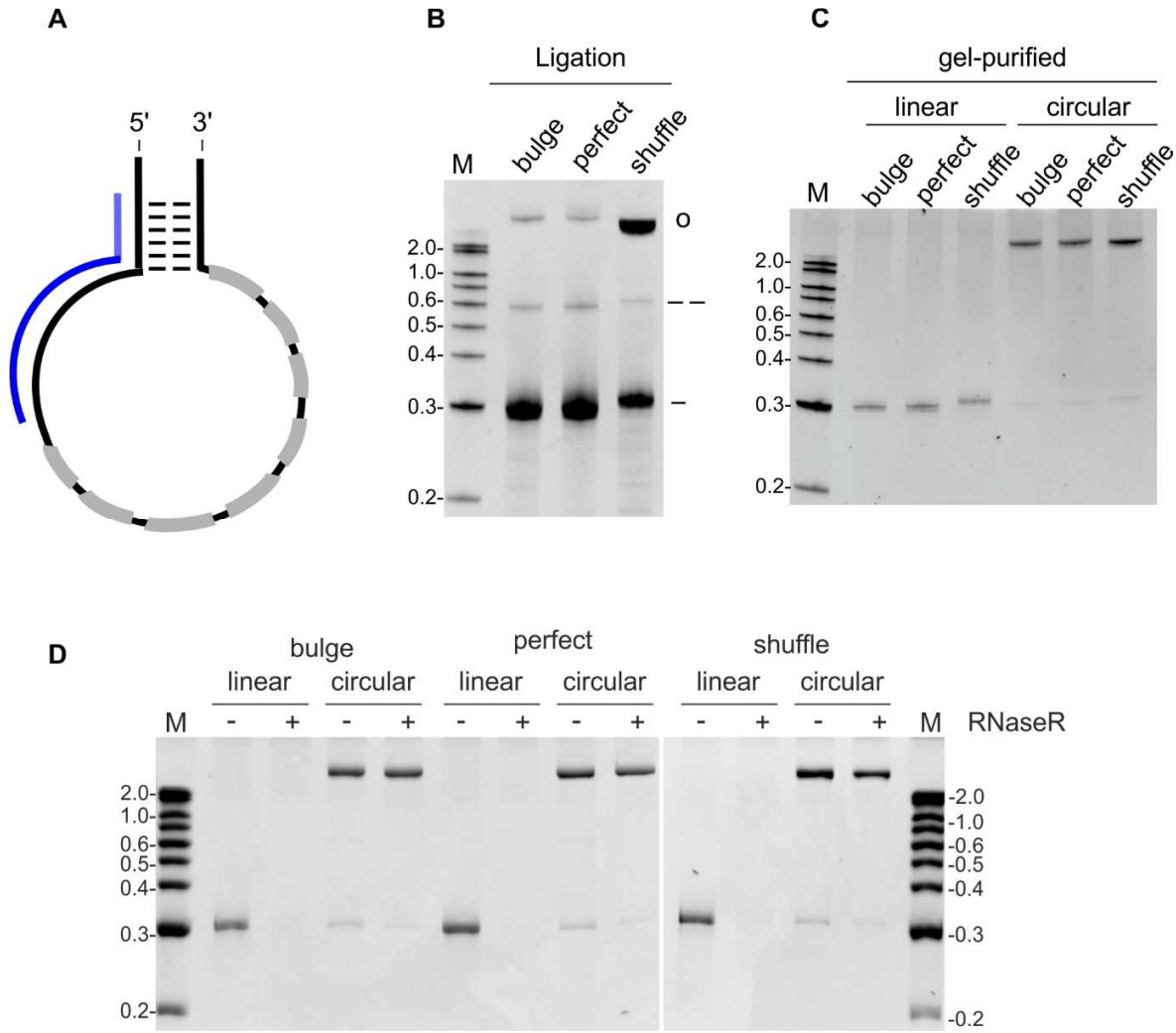

Figure 29 *In vitro* synthesis of circular miR-122 sponges.
Schematic representation of the miR-122 sponge constructs used for *in vitro* circularization by ligation. The transcripts contain eight miR-122 binding sites *bulge*, *perfect* (grey) or a *shuffle* control sequence of the same length. A stem of 11 nt was introduced, followed by 5 unpaired nt at each end. The first 76 nt at the 5'end of the constructs are identical between the different constructs and were used for northern probe hybridization (blue line) (**A**).
miR-122 sponge constructs described in **A** were synthesized by *in vitro* transcription, ligated by T4 RNA ligase and then analyzed on a denaturing 7% PAA gel. The RNA species present in the ligation reaction were: linear monomers (-), linear dimers (- -) and the circularized RNA (o) (**B**). The linear monomers and their circular equivalents were gel-purified and separated for quality control on a denaturing 7% PAA gel (**C**).
Then 100 ng of the gel-purified RNAs (*bulge*, *perfect* and *shuffle*) were treated with (+) or without (-) 0.5 u RNase R. 50% of the reaction were analyzed on a denaturing 7% PAA gel. RNAs were visualized by EtBr staining. Gels in **B** and **C** were kindly provided by Oliver Rossbach.

The yield of this method was limited, on the one hand caused by low circularization efficiency of the miR-122 sponge sequences, on the other hand by the gel-purification step. But it provided the opportunity to synthesize circRNAs containing miR-122 binding sites in amounts to be able to characterize them and to transfect them into cells.

2.3.5.2 Characterization of circular miR-122 sponges

In order to achieve functional sequestration of miR-122 and therefore inhibition of HCV propagation, cytoplasmic localization of the circRNA sponges is crucial. Both mature miRNAs as well as the HCV translation and replication reside in the cytosol, so the subcellular localization of *in vitro* synthesized and transfected circRNA sponges was determined. The linear and circular sponges *bulge* and *perfect*, together with the *shuffle* control sequence were transfected in Huh7.5 cells. After harvesting the cells, a cell fractionation was performed and RNAs were isolated form cytoplasmic and nuclear fractions. The localization was determined by northern blot, detecting the transfected RNAs with internally ^{32}P labelled RNA probes, which hybridized in the region identical between the constructs (**Figure 29 A**). For loading control between the samples U1 snRNA was co-analyzed. The transfected RNAs were equally distributed between the cytoplasm and nucleus. Moreover 10% of the lysates were saved, and analyzed by western blot, detecting hnRNP A1 (mainly nuclear) and GAPDH (cytoplasmic) to prove effective fractionation (**Figure 30**).

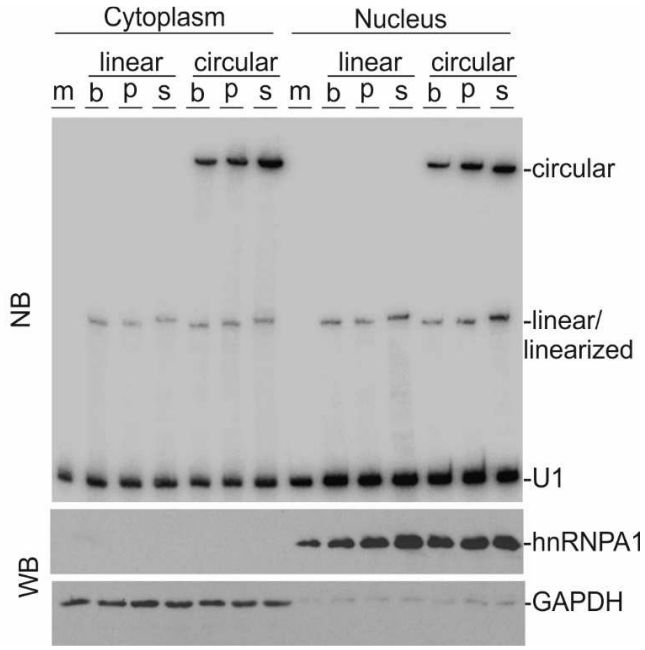

Figure 30 Transfected circRNAs are equally distributed between nucleus and cytoplasm.
Linear or circular gel-purified RNAs containing *bulge* (b), *perfect* (p) miR-122 binding sites or a *shuffled* sequence (s) were transfected into Huh7.5 cells. Mock (m) transfected cells served as negative control. After sub-cellular fractionation RNAs were isolated and analyzed by northern blot (NB), using a combined probe of ^{32}P internally labelled RNAs, detecting either the constant region of the transfected RNAs or the U1 snRNA. 10% of the lysates were subjected to western blot analysis (WB) probing the distribution of hnRNP A1 (almost exclusively nuclear) and GAPDH (cytoplasmic) to verify the fractionation. Western blots were performed by Oliver Rossbach.

Endogenous circRNAs exhibit greater stability compared to their parental mRNAs (Cocquerelle et al, 1993; Jeck et al, 2013; Memczak et al, 2013). It is thought they are resistant to exonucleases, because they lack 5' and 3' ends. The *in vitro* produced artificial circRNAs were resistant to RNase R in *in vitro* assays (**Figure 29**). For analysis of their stability in cells, the half-life times of the artificial circRNAs in comparison to their linear counterparts were examined.

For stability analysis, the *in vitro* synthesized circRNAs *bulge*, *perfect* and *shuffle* were transfected into Huh7.5 cells along with their linear analogs. The cells were harvested after 4, 8, 14, 24, and 32 h and RNAs were isolated. Then 20% of each sample was subjected to northern blot detecting the transfected RNAs and U1 snRNA. Data presented in **Figure 31** was exemplarily chosen from two replicates. The signals for the linear RNAs in **Figure 31** were too low for accurate measurement of the half-life. Northern blots were repeated using 30% instead of 20% of the isolated RNA (see Appendix **Figure A4**).

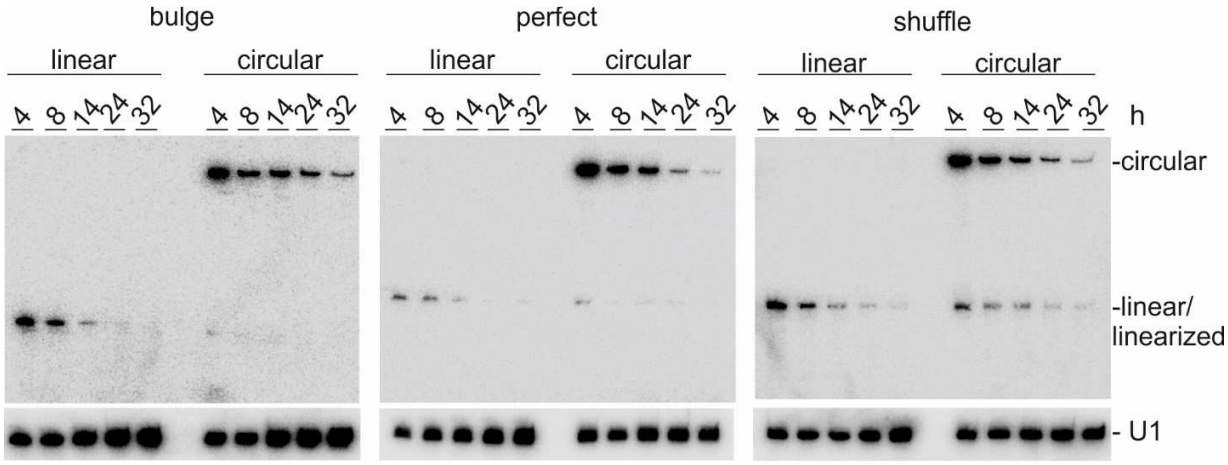

Figure 31 Stability analysis of *in vitro* generated circRNAs.
The gel-purified circular or linear RNAs were transfected into Huh7.5 cells and RNA was isolated at time points 4, 8, 14, 24 and 32 h. 20% of each sample was loaded and the transfected RNAs plus U1 snRNA were detected using a mixed ^{32}P internally labelled RNA probe (as described before). Due to high abundance, U1 snRNA is shown in the lower panel using a shorter exposure time.

For measurement of the half-life, signals from the transfected RNAs were quantified by (ImageQuant TL), averaged, normalized to the 4 h time point and fitted to *Equation 1* (see **4.2.7.13** and Appendix **Figure A5**).

For the *in vitro* synthesized circRNAs half-life times between 7 h to 9 h were determined. But only the circRNA with the *bulge* binding sites was significantly more stable in comparison to its linear counterpart. The circRNA with the *perfect* binding sites was not significantly less stable compared to the circRNA with the *bulge* binding sites (**Table 2**). This suggests that the *perfect* binding site was not cleaved by the RISC complex, as it had been assumed.

Table 2 Summary of the stability analysis of *in vitro* generated miR-122 sponges.
Half-life and values for the lower 95% confidence level (LCL) and upper 95% confidence level (UCL) of *in vitro* synthesized and transfected circRNAs, or the linear equivalent.

	t ½ [h]	LCL	UCL
linear bulge	5.4	4.4	6.4
circular bulge	9.3	6.7	11.9
linear perfect	8.2	6.0	10.7
circular perfect	7.8	6.4	9.1
linear shuffle	6.4	4.3	8.6
circular shuffle	6.7	6.5	7.1

2.4 Sequestration of miR-122 from HCV by circRNA sponges

With the preceding experiments, the production and purification of miR-122 circRNA sponges were established and optimized. Potent binding sites were identified and the *in vitro* generated circRNAs were further characterized, in terms of their stability and subcellular localization. In the following experiments the functional inhibition of miR-122 by circRNA sponges was examined, using different HCV reporter systems. HCV propagation is dependent on miR-122, which binds at two adjacent sites on the HCV 5'UTR. The bound miR-122 on the one hand protects the HCV genome from exonucleolytic decay and on the other hand promotes viral translation (Sarnow & Sagan, 2016).

The repression of viral translation due to miR-122 sequestration by circRNA sponges was investigated, using a HCV-Firefly luciferase reporter (HCV-FL) (**Figure 32 A**). It is composed of a Firefly luciferase ORF, flanked by the original HCV 5'UTR and 3'UTR (Henke et al, 2008). In order to ensure correct folding of the IRES element, a fragment (33 nt) of the core coding protein was included. The reporter was transfected as an *in vitro* transcript generated by T7 RNA polymerase from a PCR product. This ensured exact 5' and 3'ends and therefor correct folding, which is important for the authentic stability of the reporter.

The circRNAs *bulge*, *perfect*, *shuffle*, and their linear analogs together with miravirsen (200 ng/ml) were transfected into Huh7.5 cells. The HCV-FL reporter RNA was transfected the following day, and after 4 h of expression luciferase activity was measured. The experiment was performed in triplicates, obtained values were averaged and plotted (**Figure 32 B**). In comparison to the mock treated cells, linear and circular miR-122 sponges (*bulge* and *perfect*) significantly reduced luciferase activity of the HCV-FL reporter. Transfection of miravirsen led to reduced luciferase activity as expected. It served as positive control because HCV inhibition by targeting miR-122 with miravirsen was shown before (Lanford et al, 2010; Janssen et al, 2013). The *shuffle* control sequence, neither as linear RNA, nor as circRNA did affect luciferase activity. In order to confirm that the *shuffle* sequence was not specific for miR-122 *in vitro* pulldown experiments (data not shown) and pmirGLO Dual-Luciferase reporter assays were performed (see Appendix **Figure A6**).

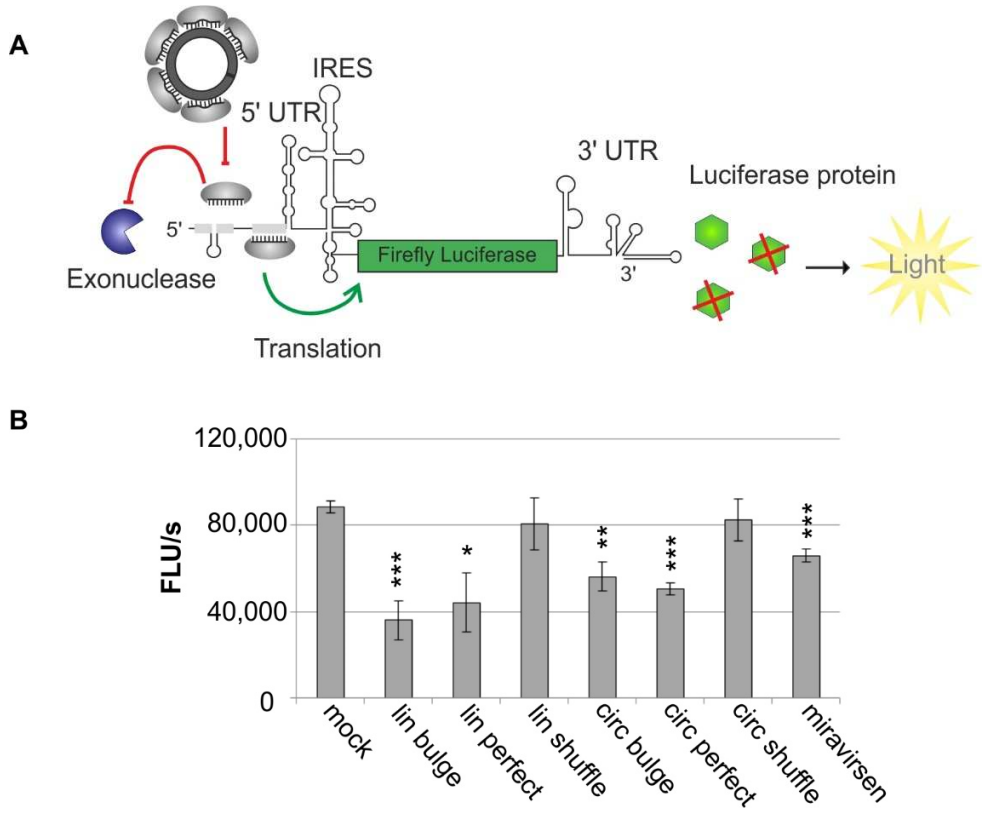

Figure 32 miR-122 sponges inhibit translation of HCV Firefly luciferase reporter.
The consequences of miR-122 inactivation were analyzed using HCV Firefly luciferase reporter (HCV-FL). Most of the viral ORF was substituted by a Firefly luciferase ORF leaving the original HCV 1b strain 5' and 3'UTR intact. The start codon and 33 nt of the core coding region are included. Both miR-122 binding sites on the HCV 5'UTR are indicated as grey boxes. Upon binding miR-122 protects the viral genome from exonucleolytic decay (red arrow) and promotes viral translation (green arrow). The miR-122 sponges compete with the HCV-encoded binding sites and inhibit miR-122 function (**A**).
200 ng/ml of gel-purified linear and circular RNAs (*bulge*, *perfect* and *shuffle*) or miravirsen were transfected into Huh7.5 cells. The next day the HCV-FL reporter was transfected as an *in vitro* transcribed RNA. After 4 h of expression luciferase activity was measured and plotted showing Firefly luciferase units per second (FLU/s) on the y-axis. The experiments were performed in triplicates and for statistical analysis a paired t-test for unequal variances was performed comparing mock transfection with each condition *p<0.05; **p<0.01; ***p<0.001 (**B**).

HCV-FL reporter expression for 4 h is perfect to study mainly the effect of miR-122 inhibition on translation. The destabilization of the HCV reporter RNA due to reduced or absent miR-122 binding would become apparent at later time points (Conrad et al, 2013). Thus HCV-FL levels were measured by RT-PCR to ensure that reduced luciferase activity was not caused by lower transfection efficiency.

The experiment was performed as described above with the exception that 150 ng/ml of miravirsen, linear or circRNA were transfected into Huh7.5 cells. From three of the replicates total RNA was isolated and RT–PCR was performed (**Figure 33 A**). The remaining three replicates

were used to determine luciferase activities (**Figure 33 B**). There was no distinct difference in HCV-FL RNA levels between the samples, but luciferase activity was significantly lower for transfections with circular or linear RNAs containing *bulge* or *perfect* binding sites. Consequently, the minor but significant reduction in luciferase activity can be attributed to translational inhibition and therefore miR-122 sequestration.

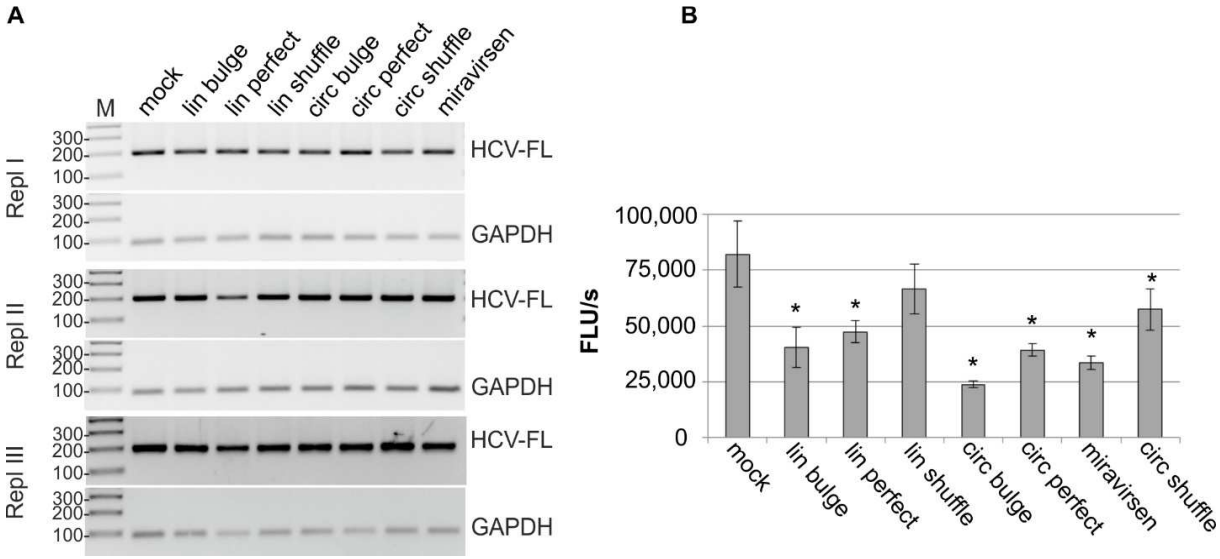

Figure 33 HCV-FL reporter RNA stability upon transfection of miR-122 sponges.
For analysis of reporter RNA stability 150 ng/ml of the gel-purified linear and circular RNAs (*bulge*, *perfect*, *shuffle*), as well as miravirsen were transfected into Huh7.5 cells one day before HCV-FL reporter RNA transfection. After 4 h of expression 3 replicates were used for RNA isolation and stability analysis by RT-PCR, using primers in the 5'UTR of the HCV-FL reporter and primers to detect the *GAPDH* mRNA (**A**). The other 3 replicates were used for measurement of the luciferase activity and plotted showing FLU/s on the y-axis. The statistical analysis was performed as described before *p<0.05 (**B**).

Moreover, different doses of miR-122 sponges (linear and circular) or miravirsen were transfected and the inhibitory effect on HCV-FL translation was determined (**Figure 34**). In this experiment miravirsen did not affect HCV-FL translation. But a reduced translation of the HCV-FL reporter was observed for circular and linear miR-122 sponges containing *bulge* and *perfect* binding sites. Nevertheless, there was no dose-dependent decrease of luciferase activity. For the linear miR-122 sponges *bulge* and *perfect* the effect on HCV-FL translation was comparable at 100 ng/ml and 400 ng/ml. The transfection of higher amounts of circRNA sponges showed even less reduction in luciferase activity. It might be the case that, with 100 ng/ml the maximal effect was already reached. Alternatively, the transfection for higher amounts might be less efficient.

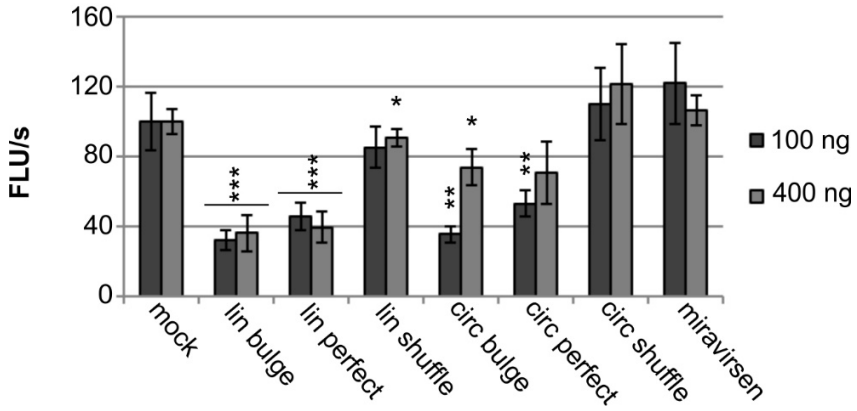

Figure 34 No enhanced inhibitory effect on HCV-FL with increasing amounts of miR-122 sponges. The experiment was performed as described before, transfecting circular or linear miR-122 sponges (*bulge*, *perfect* and *shuffle*) and miravirsen. By comparing the transfection of 100 ng/ml or 400 ng/ml per condition, the inhibitory effect on HCV-FL translation with increasing amounts of miR-122 sponges was examined. The experiments were performed in triplicates and statistically analyzed as described before *p<0.05; **p<0.01; ***p<0.001.

For additional evidence of miR-122 inactivation by circRNA sponges, experiments using the stable cell line Huh-luc/neo NS3-3'ET were performed. This cell line carries an autonomously replicating HCV reporter RNA. It is bicistronic and encodes a luciferase ORF, HCV non-structural proteins NS3-NS5B and neomycin phosphor-transferase, which is used for selection (Lohmann, 1999). Expression of the first cistron, which is used to monitor replication and translation efficiency via luciferase activity is driven by the HCV IRES located in the 5'UTR. The non-structural proteins required for replication are expressed via the strong IRES of encephalomyocarditis virus (EMCV) (**Figure 35 A**). This reporter system resembles the actual situation in HCV infected cells much better than the HCV-FL reporter system. On the one hand HCV translation and replication are already in progress and on the other hand the membranous web, where HCV replication takes place, is formed. This reporter system is an appropriate method to study the effects of HCV therapeutics on replication and translation efficiency under biosafety level (BSL)-1 conditions (Lohmann, 1999). However, in this experimental setup the effects on translation and replication cannot be examined separately.

The inhibition of miR-122 was studied by transfecting 200 ng/ml of circRNAs *bulge*, *perfect* and *shuffle* along with miravirsen into the stable replicon cell line Huh-luc/neo NS3-3'ET. Cells were harvested 4, 12, 24 and 48 h after transfecting the circRNAs or miravirsen, and luciferase activity was measured. A significant downregulation of the luciferase expression was observed for circRNAs *bulge* and *perfect* from 4 to 24 h. After 48 h, a significant reduction in luciferase activity was observed only for cells treated with the circRNAs containing the *bulge* binding sites. The

luciferase values for control transfections with the *shuffle* circRNA were not significantly reduced compared to values obtained from mock transfected cells. Conversely, miravirsen did also not affect the luciferase activity (**Figure 35 B**).

Moreover the dose-dependent response of the replicon cell line to the circRNA with the *bulge* binding sites was studied. Huh-luc/neo NS3-3'ET cells were transfected with either 40 ng/ml or 200 ng/ml of the *bulge* circRNA and harvested after 4 and 24 h (**Figure 35 C**). For controls, cells were mock treated or transfected with 200 ng/ml of the *shuffle* circRNA. The luciferase values of mock treated cells and cells transfected with the *bulge* circRNA were compared. A significant reduction in luciferase activity was observed for 4 h and 24 h using the high dosage (200 ng/ml).

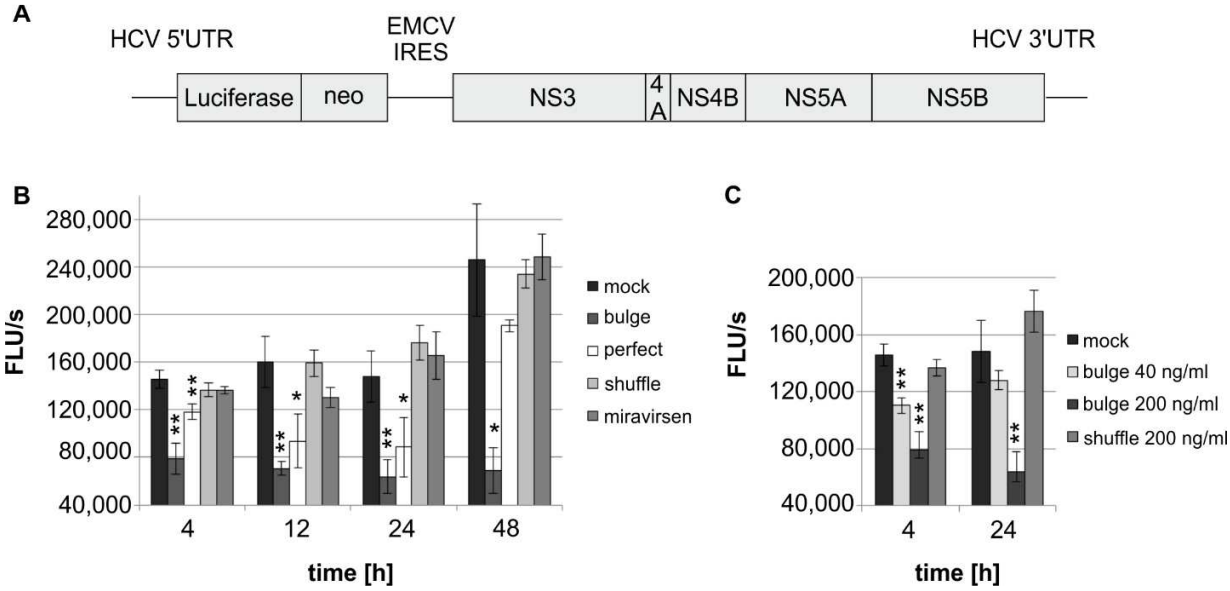

Figure 35 Time course and dose-dependency analysis in HCV replicon cell line.
Schematic representation of the HCV reporter RNA, autonomously replicating in the stable cell line Huh-luc/neo NS3-3'ET. The first cistron of the reporter is under control of the HCV 5'UTR, encodes a luciferase gene and the selection marker, which is neomycin phosphor-transferase (neo). The second cistron is driven by the EMCV IRES, followed by viral proteins NS3-NS5B and the HCV 3'UTR (**A**).
Huh-luc/neoNS3-3'ET cells were transfected with 200 ng/ml of *in vitro* generated and gel-purified circular RNAs (*bulge*, *perfect* and *shuffle*) or miravirsen. Cells were harvested after 4, 12, 24 and 48 h (**B**).
In (**C**) mock and control circRNA (shuffle) transfections were compared to transfections with different amounts (40 ng/ml or 200 ng/ml) of the circular RNA containing the *bulge* binding sites. Cells were harvested after time points 4 h and 24 h. The luciferase activity was measured and FLU/s were plotted against the time [h]. The transfections were performed in triplicates and statistical analysis was performed as described before *p<0.05; **p<0.01.

With 40 ng/ml the luciferase activity was significantly lower in comparison to mock treated cells after 4 h, but not after 24 h. Furthermore the difference in luciferase activity between 40 ng/ml and 200 ng/ml treatment was significant with p> 0.05 for the 4 h time point and for the measurement

after 24 h significant with p> 0.01. Thus the circRNA sponge with the *bulge* binding sites inhibits the luciferase activity of the HCV replicon reporter in a dose-dependent manner (**Figure 35 C**).

Ultimately, the influence of the miR-122 sponges was studied using an infective HCV cell culture system. Transfection of the full-length JC1 HCV RNA leads to autonomous replication and generation of infective virus particles in cell culture. JC1 is a chimeric clone composed of structural proteins form HCV clone J6 and non-structural proteins derived from HCV clone JFH1. The linear and circular RNAs *bulge*, *perfect* and *shuffle* were co-transfected with the JC1 HCV RNA. Then the lysates were analyzed by western blot 5 days post transfection (**Figure 36**). Synthesis of viral proteins was monitored by detection of the HCV core protein and NS3. The linear and circular miR-122 sponges *bulge* and *perfect*, as well as treatment with miravirsen abolished synthesis of the core protein and of NS3. Transfection of the *shuffle* sequence as a circular or linear RNA did not affect viral protein synthesis. This clearly showed a specific inhibition of HCV by miR-122 sponges with the *bulge* and *perfect* binding sites (**Figure 36**). Transfections and western blots were performed in the BSL-3 facility by Lyudmila Shamalova from the Michael Niepmann group (Institut für Biochemie, FB 11).

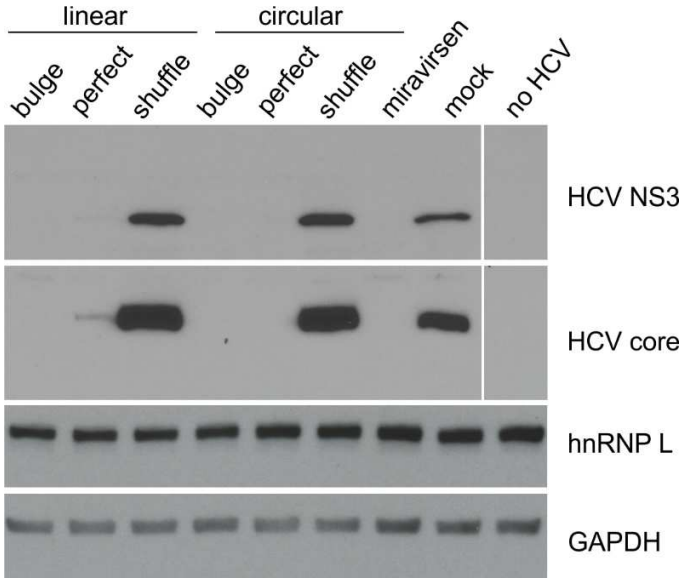

Figure 36 miR-122 circRNA sponges eliminate viral protein synthesis in a full-length infective HCV cell culture system.
Huh7.5 cells were co-transfected with full-length JC1 HCV RNA and 130 ng/ml of *in vitro* generated and purified linear or circular RNAs *bulge*, *perfect*, *shuffle*. For positive control 130 ng/ml miravirsen were used. For further controls mock treated cells and cells without transfection of HCV RNA were analyzed. Cells were harvested after 5 days and lysates were subjected to western blot, detecting viral proteins HCV NS3 and HCV core, together with hnRNP L and GAPDH as loading controls. This experiment was performed by Lyudmila Shalamova.

RESULTS

The functional inhibition of miR-122 by circRNA sponges was assayed with different HCV reporter systems. In all experiments, a specific and significant reduction of the HCV reporter was observed upon transfection of circular or linear sponges containing miR-122 binding sites. Efficacy of miR-122 sponges was tested in HCV infected cells, as well as in Huh-luc/neo NS3-3'ET cells, whereupon the latter mimics the situation of a full-blown infection. Additionally, dose-dependent HCV-adverse effects for the circRNA sponge with *bulge* binding sites was observed in experiments using the replicon cell line Huh-luc/neo NS3-3'ET.

3 DISCUSSION

With the discovery of thousands of circRNAs in human cells, a new class of non-coding RNAs was founded. The comprehensive analysis of circRNA expression via RNA-seq has identified circRNAs in many cell types, tissues and across various species. Being discovered only recently, the class of circRNAs is not well characterized yet, and functionally largely unexplored. In my work I approached the question how circRNAs are generated, and tested the involvement of the spliceosome in circRNA biogenesis. Moreover, I developed artificial circRNAs for miRNA sequestration. The inactivation of miR-122 by circRNA sponges was validated with different HCV reporter systems.

3.1 circRNA biogenesis

3.1.1 circRNAs are processed by the spliceosome

In the first part of my work, I experimentally approached the mechanism of circRNAs biogenesis. Therefore, a minimal circRNA expression vector was designed, based on the gene context of *CNTROB* exon 13, which was predicted to circularize in fibroblasts. The enrichment of sequence reads for the *CNTROB* exon 13 in RNase R treated samples indicated its circular configuration in fibroblasts (Jeck et al, 2013). Initially, the expression pattern of *CNTROB* exon 13 was analyzed in HeLa cells in comparison to its linearly spliced neighboring exons (**Figure 11 B**). The circular junction was less abundant compared to the splice junctions of the neighboring exons, nevertheless circularity of *CNTROB* exon 13 was confirmed by RNase R treatment (**Figure 11 B, C**). The production of circRNAs from minigenes was maintained, although most of the natural gene context was deleted or substituted, leaving only the splice signals intact (**Figure 13 and Figure 14**). Then, basal sequence elements required for processing by the spliceosome were mutated. As expected the disruption of splice signals (3'ss, 5'ss and PPT) abolished circRNA generation. Mutations which decreased splice site strength lead to reduced efficiency in circRNA processing or aberrant splicing (**Figure 16**). These observations are in line with what is known from linear splicing and are evidential for the involvement of the spliceosome in circRNA production (Shirley et al, 2013; Daguenet et al, 2015). In related experiments using minigenes derived from other genes several groups could also show that 5'ss and 3'ss are required for circRNA biogenesis (Zhang et al, 2014; Liang & Wilusz, 2014; Starke et al, 2015).

Astonishingly, in experiments with the minimal circRNA constructs (RCR-CL Delta and RCR-CL B), mutation of the predicted BP did not interfere with circRNA biogenesis. My colleagues

Stefan Starke and Tim Schneider designed a three-exon construct (*LPAR1* minigene) (Starke et al, 2015). This minigene was based on the results from the mutational analysis of the minimal circRNA expression construct. With *LPAR1* minigene the question was followed up, if the upstream BP adenosine is necessary for circRNA biogenesis. Only by mutating all adenosines in the upstream intron, the production of WT circRNAs was abolished (Starke et al, 2015). This shows that BP selection is flexible as known from linear splicing (Corvelo et al, 2010). Additional evidence for spliceosomal processing of circRNAs was provided by its inhibition via isoginkgetin, which inhibits canonical splicing via blocking of U4/U5/U6 tri-snRNP assembly with the spliceosome (Starke et al, 2015; O'Brien et al, 2008). Moreover, components of the snRNPs, as well as of the exon junction complex were found to be associated with circRNAs (Chen et al, 2017).

3.1.2 Regulation of circRNA expression by RCR elements

These experiments provide the answer for the question if circRNAs are generated by the spliceosome. But, linear mRNAs and circRNAs are often co-expressed, and the question what determines if an exon is circularized or linearly spliced remained open. Therefore the role of intronic base-pairing, across the circularizing exon was investigated. The data presented in **Figure 17**, lead to the conclusion that RCR elements enhance circularization efficiency. But they are not necessary to produce a circRNA from RCR-CL Delta minigene. The same was observed for circSRY in *in vitro* splicing assays using HeLa nuclear extracts (Pasman et al, 1996). Moreover, competing interactions of RCR elements influence the circularization efficiency and production of different circRNA isoforms (Zhang et al, 2016a; Liang & Wilusz, 2014).

Due to the fact that circRNAs are differentially expressed between cell types and tissues, the involvement of additional protein factors is likely, even for those candidates where circularization is promoted by RCR elements. One factor which antagonizes circRNA biogenesis is ADAR-1. Base-pairing of RCR elements is weakened by ADAR-1 mediated A-I conversions in the hybridized regions (Ivanov et al, 2015; Rybak-Wolf et al, 2015). Whereas NF90/NF110 promote circRNA production, probably by stabilizing the interaction of RCR elements (Li et al, 2017).

3.1.3 Proteins involved in circRNA biogenesis

The fact that not all circularizing exons contain RCR regions in their flanking introns, is indicative for the existence of more than one biogenesis pathway. Thus, additional *trans*-acting factors must

be involved to facilitate discrimination between exons which are linearly spliced or circularized. Such mode of recognition is known from alternative spliced exons, where splicing activators or repressors bind to regulatory sequence elements (Matlin et al, 2005). Therefore the influence of ESEs in circularization was tested.

Two ESE motifs from a set of bioinformatically predicted and experimentally validated sequence elements with enhancer activity were chosen, and were inserted into the circularizing exon of *LPAR1* minigene (Fairbrother et al, 2002). This specific minigene was used on the one hand because no circRNA flanking RCR elements were identified; on the other hand to compare the influence of ESEs on linear and circular splicing, as well as competition between both splicing modes. In HeLa cells no effects on circularization, or linear splicing were observed (**Figure 18**). One possibility is, that the selected ESEs recruit proteins, which do not influence circRNA biogenesis. Another scenario is that recruited proteins are not expressed in the adequate amount, or they are not expressed in the right proportion with other e.g. antagonizing regulators in HeLa cells. ESE and ESS elements in combination with overexpression of splicing factors were shown to influence the ratio between circRNAs and their linear counterparts (Wang & Wang, 2015). However, it was not clearly shown if linear splicing or circularization was affected.

There is evidence that, besides the RCR-mediated circRNA formation, a related protein-mediated mechanism exists. Instead of RNA-RNA interactions across the circularizing exon, protein-protein interactions (e.g. dimerization) could bring the splice sites of the circularizing exon in close proximity. The RBPs MBL, Rbm20 and QKI have been implicated to influence circRNA biogenesis in such a manner. These factors bind in circRNA flanking introns and positively affect circRNA levels (Ashwal-Fluss et al, 2014; Conn et al, 2015; Khan et al, 2016). For MBL, which regulates formation of a circRNA originating from its own mRNA in *Drosophila*, a negative feedback loop mechanism was suggested. The *MBL* circRNA has not only several MBL binding sites in the flanking introns, but there are also interaction sites located within the circularized exon. By RNA immunoprecipitation experiments MBL was shown to physically interact with the circRNA (Ashwal-Fluss et al, 2014). Nevertheless, it still needs to be shown if these proteins influence circRNA biogenesis by mere binding or if a physical interaction of the proteins is required.

In the RCR-CL B minigene most of the natural exon sequence was replaced by 384 nt of *HNRNP L* intron 6, which contains several hnRNP L binding sites. This sequence element is an ISE, which is responsible for feedback-loop inhibition of hnRNP L expression by activating a cryptic poison exon in its own pre-mRNA (Rossbach et al, 2009). Moreover, binding of hnRNP L globally modulates alternative splicing in a position–dependent manner (Rossbach et al, 2014). Interaction of hnRNP L in upstream introns close to the PPT leads to repression of the exon. Whereas binding

in exons, can lead either to activation of the exon by recruiting U1, or even repression by masking the 5'ss (Rossbach et al, 2014). In order to prevent interference of hnRNP L and to guarantee unbiased results, the sequence with hnRNP L binding sites was substituted by an unspecific vector sequence in the RCR-CL Delta construct. By comparing RCR-CL B WT and RCR-CL Delta WT, differences in circRNA expression levels are not very pronounced. But mutations, which decrease 5'ss strength, show more drastic effects in the RCR-CL B minigene (**Figure 16** and Appendix **Figure A1**). This indicates that hnRNP L might have a regulatory role in circRNA biogenesis. It would be interesting to investigate if hnRNP L has repressive effects on circularization of exons with weak 5'ss. Interestingly, hnRNP L was found among the candidates, which affect circRNA expression in siRNA library screens (Li et al, 2017).

3.1.4 Conclusion

In summary, the results from the mutational analysis of RCR-CL Delta and RCR-CL B clearly show the participation of the spliceosome in formation of circRNAs. There are two broadly accepted models how circRNAs are generated: I) Direct backsplicing, mediated by protein-protein interactions, but it is assumed that circularization is influenced mainly by RCR elements in the flanking introns. II) Backsplicing subsequent to exon skipping, from the exon-containing lariat (Ebbesen et al, 2016). Nevertheless, these models do not explain why circRNAs are differentially expressed between cell types. The regulatory mechanism which drives exon circularization is still unclear. Considering the complex network of proteins involved in alternative splicing, the regulation of circRNA biogenesis might also be dependent on such elaborated protein networks. With tools like crosslinking immunoprecipitation (CLIP) in combination with RNA-seq, the interaction sites of RBPs can be mapped genome-wide (Ule et al, 2005; König et al, 2010). Utilization of such methods will help to clarify regulation of backsplicing in general. Besides regulation by RBPs, it was already shown that the transcription rate can modulate backsplicing efficiency (Zhang et al, 2016b). The analysis of relations between chromatin modifications, transcription rate and circRNA biogenesis might also provide novel insights into regulation of circRNA production.

3.2 Synthesis and expression of circRNAs

3.2.1 circRNA expression via the RCR-minimal expression construct

In the second part of my work I developed artificial circRNAs for miRNA inhibition. Initially, it was planned to substitute the unspecific sequence of RCR-CL Delta with several miRNA binding sites to express circRNA sponges in cells. These attempts failed. The expression level was either very low, or it was not possible to confirm circularity via northern blot, although RT-PCR products were detectable (data not shown). It might have been the case that the detected PCR products have originated from *trans*-spliced instead of circularized exons. The repetitive nature of the tandem arranged miRNA binding sites was problematic in all tested circularization methods. This was the main reason why development of a method to highly express or efficiently synthesize circRNAs was particularly challenging. One attempt to overcome this problem was to randomize the high-affinity miR-122 binding sites. For this purpose, several endogenous and experimentally validated miR-122 target sites were chosen and manually diversified to obtain a non-repetitive *CDR1as*/*ciRS-7*-like sequence. In pulldown and pmirGLO Dual-Luciferase reporter assays these *CDR1as*/*ciRS 7*-like sequence did not show the desired effects, due to reduced affinity for miR-122 (data not shown). But such sponge sequences might be suitable to repress miRNAs that are not as abundant as miR-122, or to fine-tune the miRNA accessibility for their targets. This could be a way to modulate their regulatory function on gene expression in cells.

3.2.2 PIE-generated circRNAs

In order to establish a method to generate artificial circRNAs, the heterologous expression of circRNAs via PIE self-splicing in *E.coli* and its subsequent purification was tested. Umekage and colleagues were able to purify 190 µg of circRNA from 1 L *E.coli* culture by using this method (Umekage & Kikuchi, 2009). To establish the procedure, the original construct with the streptavidin aptamer sequence between the splice sites was used (**Figure 25**). Expression of circRNAs in *E.coli* via PIE, did not produced reliable evidence for expression of a RNA with circular configuration. RT-PCR analysis indicated production of a circRNA (**Figure 26**), nevertheless, detection of circRNAs purified from *E.coli* via northern blot failed (**Figure 28**). Possibly, low abundance of the PIE-generated circRNAs in the analyzed samples might be causative for detection problems. The circRNAs expressed in *E.coli* were first enriched via anion exchange chromatography and should be subsequently purified by antisense selection with biotinylated oligos. The project was not continued, and the PIE circRNA expression system was not further optimized for miRNA sponge expression, because I) Northern blot detection and antisense

selection are based on the same hybridizing region. II) Due to lack of a solid evidence for the circular configuration of the expressed RNAs. III) It became apparent, that repetitive miR-122 binding sites are problematic in circRNA expression. The self-splicing mechanism relies on characteristic folding with a catalytic core of approximately 100 nt (Ahsen & Schroeder, 1993). Assuming that multiple miR-122 binding sites form disadvantageous secondary structures, insertion of highly structured sequences would most probably interfere with the self-splicing mechanism. But this method might be a suitable way to circularize sequences, which are less repetitive and relatively short. In a study recently published by Chen et al. (2017), PIE self-splicing constructs were used for *in vitro* circRNA synthesis. After purification these circRNAs were transfected into cells. However, circularity was confirmed by RNase R treatment and RNA analysis via Bioanalyzer and not with northern blots (Chen et al, 2017).

3.2.3 *In vitro* circRNA synthesis by ligation

The problem to circularize multiple miRNA binding sites was solved by optimizing a method where *in vitro* transcribed RNAs were ligated by T4 RNA ligase (Pan, 2000). Compared to the miRNA sponges (*bulge* and *perfect*), the unspecific, non-repetitive sequence (*shuffle*) circularized more efficiently with this method (**Figure 29 B**). The circRNAs were separated from unprocessed substrates and linear dimers by gel-purification. Only limited amounts of circRNA sponges could be generated via *in vitro* synthesis and subsequent gel-purification. But it was possible to clearly show the circular configuration of the ligated RNAs by aberrant running behavior in PAA gels and by RNase R treatment (**Figure 29 C and D**). Additional evidence for circularity were obtained by sequence analysis of the junction-spanning PCR product and by analysis of circRNA migration in denaturing PAA gels with different PAA percentage (data not shown) (Tabak et al, 1988).

3.2.4 Circularization strategies

For functional characterization of circRNAs, it is important to establish methods to on the one hand over-express circRNAs, or on the other hand synthesize and deliver them to cells. Several circRNA expression vectors, which produce circRNAs through spliceosomal processing have been constructed (Hansen et al, 2013b; Liang & Wilusz, 2014; Starke et al, 2015). In contrast to overexpression systems for proteins, the circRNA expression constructs do not always reliably yield circRNAs in all cell lines. Substitution of the exonic sequence by a sequence of interest might abolish circRNA expression or strongly reduce circRNA levels (Liang & Wilusz, 2014). But there are clearly advantages of endogenously and spliceosome-generated circRNAs. Firstly, such

circRNAs undergo most probably their natural nuclear export pathway; and secondly they are complexed with their original interaction partners, which are thought to associate during biogenesis (Chen et al, 2017).

An alternative strategy to circularize a sequence of interest, is tRNA splicing. In archaea and some eukaryotes tRNA genes contain introns, which are removed during tRNA maturation (Yoshihisa, 2014). The tRNA introns are removed and circularized in archaea by endonucleases and enzymatic ligation (Salgia, 2003). By creating genetically engineered *Drosophila* tRNA genes, where the native intron was exchanged by an aptamer sequences, circularized aptamers (*Spinach2* and *Broccoli*) were expressed in human cells (Lu et al, 2015b).

Taking into account, that circRNAs have also been found in yeast, it might be possible to produce circRNAs via an expression vector optimized for the yeast splicing machinery (Wang et al, 2014; Barrett et al, 2015). By using yeast cultures, it would be possible to produce circRNAs processed by the spliceosome in large culture volumes. The circRNAs expressed in yeast could be purified in similar manner as the PIE-generated circRNAs from *E.coli* (Umekage & Kikuchi, 2009). Splicing events in yeast are less complex and therefore easier to influence, compared to splicing in humans (Will & Lührmann, 2011). Moreover, as one of the major model organisms for investigations of the splicing mechanism, the tools to genetically manipulate splicing events in yeast are well developed (Hossain & Johnson, 2014).

3.2.5 Conclusion

The appropriate method for circularization seems to be strongly sequence-dependent and has to be adjusted to the experimental setup and biological question. The knowledge about determinants and constraints of circRNA biogenesis are still very limited. Thus, circRNA expression systems and *in vitro* synthesis methods are not yet fully developed. But with a growing interest in this field these problems will be overcome soon. *In vitro* synthesis by ligation is, as shown in this study definitively a proper method to produce circRNAs. It is particularly suitable for sequences which are problematic in other circularization methods. A vector-driven expression of circRNAs within the cell is of course less time consuming, compared to synthesis or heterologous expression and subsequent purification. But for some applications (e.g. potential future circRNA therapeutics) delivery of purified circRNAs might be more adequate.

3.3 Characterization of artificial circRNA sponges

3.3.1 Subcellular localization and stability of artificial circRNAs

Besides specificity and affinity, localization and half-life are important characteristics of miRNA inhibitor. Thus, the *in vitro* synthesized circRNAs and their linear counterparts were examined with regard to these characteristics. Mature miRNAs and HCV replication are located in the cytoplasm. Therefore it is important for the miRNA sponges to be localized in the cytoplasm as well. The artificial circRNAs were transfected with Lipofectamine 2000, and biochemical fractionation of nuclear and cytoplasmic compartments was performed. Then, RNAs were isolated and the transfected RNAs were detected by northern blot. Both linear RNAs and circRNAs were equally distributed between nucleus and cytoplasm (**Figure 30**).

The exact mechanism how transfected nucleic acids enter the nucleus is not clear. Even for transfection of DNA, which has been a standard method for many years, supporting studies are scarce. If plasmid DNA is transfected into cells, expression can only take place, when the plasmid had entered the nucleus. There are many speculations about how plasmid DNA reaches the nucleus upon transfection: I) In dividing cells, nucleic acids enter the nucleus during mitosis. II) The promoter regions of the plasmids bind proteins with nuclear localization signals, which aid import into the nucleus (Vaughan et al, 2006). III) Plasmids are actively transported to the nucleus by microtubule, associated dynein (Vaughan et al, 2006).

For circRNAs an active export mechanism is assumed, because most circRNAs are found in the cytoplasm (Salzman et al, 2012; Jeck et al, 2013; Guo et al, 2014). Moreover, export factors like DDX93B, THOC4 and XPO5 were found to co-precipitate with circRNAs (Chen et al, 2017). The import of circRNAs into the nucleus has not been studied in detail, yet. But recent studies, which implicate circRNAs in transportation of their interaction partners, draw attention to this topic. For example a circRNA derived from *AMOTL1* mRNA (circ-Amotl1) was shown to be involved in translocation of Stat3 and the oncogenic protein c-myc to the nucleus (Yang et al, 2017a; Yang et al, 2017c). Besides active transportation, molecules smaller than 40 kilo Dalton (kDa) can enter the nucleus by passive diffusion (Knockenhauer & Schwartz, 2016). The RNAs examined in this study have a molecular weight of approximately 100 kDa. For this reason it is not very likely that the RNAs have entered the nucleus passively. There is either an active import mechanism, or the RNAs were incorporated into the nucleus after mitosis, as it is assumed for plasmid DNA.

The half-life of the artificial circRNAs, which were produced by ligation was measured in comparison to the corresponding linear counterpart (**Figure 31**). The *in vitro* synthesized circRNAs had half-life times between 7 h to 9 h. The half-life of the linear RNAs was measured between 5 h

to 8 h, which is much longer than expected (**Table 2**). A non-polyadenylated RNA without cap would usually be quickly degraded (Houseley & Tollervey, 2009). Only the circRNA with the *bulge* binding sites was significantly more stable compared to its linear equivalent (**Table 2**). The LNA-modified or GalNAC-conjugated miR-122 antagomiRs miravirsen ($t_{1/2}$=30 days) and RG-101 ($t_{1/2}$= 14 days) offer exceptional high stability (van der Ree et al, 2014; van der Ree et al, 2017). Due to different experimental setups the values from this work are not comparable to half-life times of miravirsen and RG-101. By directly comparing stability of antisense oligos with or without modifications in cell culture medium with 10% FBS, the LNA-modified oligo had a half-life of approximately 40 h. This was certainly much more stable compared to the 2'O-Methyl (2'OMe)-modified oligo ($t_{1/2}$= 5 h) and the naked siRNA ($t_{1/2}$= 2 h) (Grünweller et al, 2003). For better evaluation of circRNA stability in comparison to other oligos, further experiments are required. The half-life times of endogenous circRNAs were determined to be up to 48 h, depending on the experimental setup (Cocquerelle et al, 1993; Jeck et al, 2013; Memczak et al, 2013; Liang & Wilusz, 2014). The observed discrepancy between the half-life of endogenous circRNAs and the artificial circRNAs can be explained, by the fact that bound proteins most probably protect endogenous circRNAs from being degraded.

The RNAs were transfected via lipofection. This is not the optimal way to efficiently deliver RNAs into cells. It had been reported, that RNAs are incompletely released from liposome particles, making them inaccessible to decay (Barreau et al, 2006). The more unbiased way to deliver the RNAs would have been electroporation. But preparation of artificial circRNA sponges, especially those containing multiple miRNA binding sites, was too inefficient to produce the required RNA amounts for electroporation.

The long half-life of the linear RNAs could be explained by a stabilizing effect of miR-122 binding. Since miR-122 binding is thought to prevent HCV RNA from degradation, the transfected linear RNAs might also be protected (Sedano & Sarnow, 2014; Li et al, 2015). Nonetheless, this would not explain the half-life of the linear *shuffle* control RNA, which did not have any apparent miRNA binding sites. In fact, the transfected linear RNAs with miR-122 binding sites might be less stable than measured with this experimental procedure. Due to their configuration circRNAs migrate slower through PAA gels, thus they are retained in the gel matrix (Tabak et al, 1988). Upon cleavage or maybe to some extent also shearing, the circRNAs are linearized and migrate then, at their expected size (see **Figure 31**, *shuffle*). Interestingly, the signals in northern blots for stability analysis indicate that the linearized products of the circRNA sponges *bulge* and *perfect* were rapidly degraded (**Figure 31**). Under the assumption that linear RNAs and linearized circRNAs are degraded in the same manner, the transfected linear RNAs might be less stable

than measured. It could be possible that the linear RNAs are very short-lived and the detected signals corresponded to RNAs, which had not been released from the liposome particles, yet. Although same amounts of linear and circular RNAs were transfected, the signal at the 4 h time point for linear RNAs was much lower compared to the signal of circRNAs (see **Figure 31**).

Both circular miR-122 sponges (*bulge and perfect*) were not significantly less stable compared to the *shuffle* circRNA. *CDR1as*/*ciRS-7* can be cleaved by AGO-2 due to its nearly perfectly complementary miR-671 binding site (Hansen et al, 2011). For this reason cleavage of the circRNA with *perfect* binding sites was expected. Unexpectedly, a destabilizing effect of the *perfect* binding sites was not observed in the stability assays. However, it is also known that perfectly complementary target sites support release of the miRNA from AGO-2 (De et al, 2013). The terminal nucleotides of miRNAs are typically engaged in AGO binding (Schirle et al, 2014). But if the 5' and 3'ends of miRNAs hybridize with the target, the miRNAs dissociate from AGO-2 (De et al, 2013). The miR-122 binding sites used here, were designed to interact with the terminal ends of miR-122 (**Figure 20**). Whereas interaction of miR-671 lacks complementarity to *CDR1as*/*ciRS-7* at its 5' and 3' ends (Piwecka et al, 2017). The disassembly of miR-122 form AGO-2 could explain, why circRNAs with *perfect* binding sites were not or not efficiently cleaved, as it was expected. In contrast to that, the pmirGLO reporter RNAs which contained *bulge* and *perfect* binding sites were clearly destabilized (**Figure 22**). This is in line with the proposed mechanism of target gene silencing by miRNAs (Bartel, 2009; Jonas & Izaurralde, 2015). It implies, that circRNAs are differently affected by RISC compared to mRNAs, which have a 5'cap and poly(A)-tail.

3.3.2 Artificial circRNA sponges specifically sequester miR-122 from HCV RNA

The functional inhibition of miR-122 by artificial circRNA sponges was demonstrated with different HCV reporter systems. The exact mechanism how miR-122 promotes HCV infection is not completely solved. Anyway, the role of miR-122 in HCV infection has led to the development of antagomiRs for therapeutic use (Janssen et al, 2013; van der Ree et al, 2017). Proof for miR-122 interaction with the binding sites used here was provided by biochemical, and molecular biological methods (**Figure 22** and **Figure 23**). The transfected artificial miR-122 sponges were characterized with respect to stability and their subcellular distribution (**Figure 30** and **Figure 31**). Finally, the inhibition of HVC by miR-122 circRNA sponges was studied in well-established HCV model systems (Hussain et al, 2012; Lohmann & Bartenschlager, 2014). The results provide evidence that artificial circRNAs with miR-122 binding sites were able to compete with the HCV RNA for miR-122 binding. The adverse effects on HCV were significant and specific for circRNAs

with miR-122 binding sites (**Figure 32**, **Figure 35** and **Figure 36**). This leads to the conclusion that miR-122 was functionally sequestered by artificial circRNAs with designed high-affinity miR-122 binding sites. Interestingly, the bovine viral diarrhea virus (BVDV), a *Pestivirus,* which is a genera of the *Flaviviridae* is dependent on miR-17 and let-7 families. Additionally, BVDV was shown to act as a potent miRNA decoy (Scheel et al, 2016). This raises the question, if miRNA sequestration is a general viral mechanism to alter gene expression, and to create a favorable environment for virus propagation. Besides HCV and BVDV, poliovirus was recently implicated to be dependent on miR-134 (Orr-Burks et al, 2017).

For comprehensive analysis, the effects of circRNA sponges on HCV were compared to the effects of their linear counterparts, as well as to miravirsen. Miravirsen is a LNA-modified oligo, which binds miR-122 and inhibits its function. It has been developed for HCV treatment and was the first antagomiR tested in humans (van der Ree et al, 2014). The effects of circRNA sponges on HCV were comparable to miravirsen in HCV infected cells and the HCV-FL reporter system (**Figure 36** and **Figure 32**). But performance of circRNAs in experiments with Huh-luc/neo NS3-3'ET cells was superior to miravirsen (**Figure 35**). This is interesting, because the experiments in the replicon cell line Huh-luc/neo NS3-3'ET resembles the situation of a persistent HCV infection (Lohmann, 1999). In experiments with full-length JC1 HCV in cell culture, miR-122 sponges and HCV RNA were co-transfected. Strictly speaking, these experiments show that miR-122 sponges inhibit development of a persistent infection by miR-122 sequestration (**Figure 36**). But the results from experiments with Huh-luc/neoNS3-3'ET cells indicate that miRNA sponges will successfully decrease JC1 HCV levels in cells, which have developed a persistent HCV infection. The linear and circular miR-122 sponges had in HCV-FL experiments and in HCV infected cells equal efficacy. This is not astonishing, because the linear sponges have exactly the same sequence as the circRNA sponges, and linear RNAs were much more stable than expected.

3.3.3 Artificial circRNAs as miRNA inhibitors

The idea of creating artificial circRNA sponges to functionally inhibit miRNAs arouse from the hypothesis that *CDR1as*/*ciRS-7* and circSRY function as endogenous miRNA sponges. Nevertheless, new results in *CDR1as*/*ciRS-7* KD mice do not clearly promote the assumption. The data indicate that *CDR1as*/*ciRS-7* might function as miR-7 vehicle or reservoir, involved in stabilization and transportation of miR-7 (Piwecka et al, 2017). Furthermore, a set of circRNAs seems to regulate cellular distribution of the proteins NF90/NF110 in response to viral infection.

These proteins interact with circRNAs under normal conditions and are mainly nuclear. In the nucleus NF90/110 promote circRNA biogenesis. By mimicking a viral infection, NF90/NF110 levels are reduced in the nucleus and circRNA biogenesis decreases. Instead, NF90/NF110 interact with viral RNAs and their levels in the cytoplasm increase (Li et al, 2017). The underlying mechanism, how NF90/NF110 are released upon infection, or if the circRNAs serves as competitor, is not clear. Additionally, circ-Amotl1 is also implicated in translocation of bound proteins (c-myc and Stat3) to the nucleus (Yang et al, 2017a; Yang et al, 2017c).

Nevertheless, the hypothesis of miRNA sponges, also known as competing endogenous RNA (ceRNA) hypothesis is not new (Denzler et al, 2014; Salmena et al, 2011; Ebert & Sharp, 2010). Several coding and non-coding RNAs act as miRNA sponges to regulate gene expression in *trans* (Kartha & Subramanian, 2014). Among the identified ceRNAs are mainly pseudogenes and long non-coding RNAs (lncRNAs) (Poliseno et al, 2010; Cesana et al, 2011).

Moreover, several approaches have been studied in the last years to inhibit miRNA function by using antisense oligos. LNA-, but also 2'OMe-modified or peptide nucleic acid (PNA)-conjugated oligos are commonly used to advance efficacy or duration. LNA-modified oligos have increased target affinity, by forcing the ribose into the 3'-endo conformation. Additionally, this modification mediates resistance to endo- and exonucleases (Ishida & Selaru, 2013). Miravirsen, which targets miR-122 for HCV inhibition was the first LNA-modified antisense oligo tested in humans (Janssen et al, 2013). But several other LNA-modified drugs are currently in clinical trials (van Rooij & Kauppinen, 2014). However, LNA–modified drugs have been linked to hepatotoxic effects, which cannot be explained by downregulation of the target. The hepatotoxic effects occur due to the LNA-modification itself (Swayze et al, 2007). For miravirsen no such toxic effects were identified, but long-term studies are not completed, yet (van der Ree et al, 2014). RG-101, which is the second miR-122 inhibitor in clinical trials, is a GalNAC-conjugated antagomiR (van der Ree et al, 2017). The GalNAC-moiety mediates very efficient delivery to hepatocytes by recognition of the asialoglycoprotein receptor (Huang, 2017). There is a wide range of chemical conjugates and nucleotide modifications, which have advantages and disadvantages. In the future, circRNAs could extend the variety of RNA therapeutics.

Besides *CDR1as/ciRS-7*, some other circRNAs were recently implicated in inhibition of miRNAs (Zheng et al, 2016; He et al, 2017; Yu et al, 2017; Han et al, 2017). The concept of a natural circRNA sponge has been controversially discussed. It is assumed that circRNA abundance in general is too low to compete for miRNA binding with target mRNAs (Denzler et al, 2014). But what if a single circRNA could, despite of being lowly expressed or having only few miRNA binding sites, affect many miRNA molecules? Depending on the architecture of the miRNA interaction with

its target mRNA, stability of the bound miRNA is enhanced or decreased (Katoh et al, 2009; Buck et al, 2010). Target sites with high complementarity can induce tailing of miRNAs, which leads to miRNA decay (trimming) (Ameres et al, 2010; La Mata et al, 2015). A characteristic ladder of the detected miRNA appears in high resolution PAA northern blots (Marcinowski et al, 2012; Ameres et al, 2010). However, miR-122 is post-transcriptionally mono-adenylated in Huh7 cells, which is the parental cell line of Huh7.5. The mono-adenylation, which is mediated by the non-canonical cytoplasmic poly(A) polymerase GLD-2 stabilizes miR-122 (Katoh et al, 2009). It might be the case that mono-adenylation protects miRNAs from being tailed and prevents hence decay. Interestingly, HCV core protein inhibits GLD-2, which leads to destabilization of miR-122 (Kim et al, 2016). The characteristic miRNA ladders were not observed in miRNA northern blots after 5 days of co-transfection with full-length JC1 HCV in Huh7.5 cells (data not shown). If circRNAs could induce tailing and trimming, one would expect to observe the miRNA ladder, because GLD-2 is inhibited by the HCV core protein in the experiments with full-length HCV. As apparent from western blots, translation of the core protein is abolished by the linear and circular miR-122 sponges (*bulge* and *perfect*) (**Figure 36**). For this reason no conclusion can be drawn. Nevertheless, the data currently available do not exclude the possibility that circRNAs could induce tailing and trimming of miRNAs (Zheng et al, 2016; Piwecka et al, 2017; He et al, 2017; Yu et al, 2017; Han et al, 2017). For this reason it would definitely be interesting to study the reciprocal influence of miRNAs and circRNAs. What if circRNAs could induce tailing and trimming of miRNAs, or if they would disassemble bound miRNAs from the effector complex? If the disassembly of a miRNA from the effector-complex could be achieved, it would probably even be possible to reprogram the AGO-bound miRNome. In these cases, a single circRNA could affect many miRNA molecules. Endogenous circRNAs would be much more potent than expected and artificial circRNAs would be able to surpass any antagomiR, which inhibits miRNA function by mere binding.

3.3.4 circRNAs and their potential as therapeutics

miRNAs are important regulators in gene expression, and their deregulation is linked to several diseases (Sayed & Abdellatif, 2011). For example miR-122 downregulation is related to development of HCC. Miravirsen was shown to upregulate cellular miR-122 targets, but HCV itself acts as miR-122 decoy and causes deregulation of miR-122 target genes (Luna et al, 2015). Therefore, sequestration of miR-122 by miravirsen or by circRNA sponges from its cellular targets is in the case of HCV infection negligible. For many other diseases, sequestration of miRNAs and the upregulation of cellular targets could be a desirable effect. The potential applications are

endless. To give one example, many miRNAs are aberrantly expressed in cancers. There are two categories of miRNAs which would be suitable targets for anti-cancer circRNA sponges: I) miRNAs, which play a crucial role in cancer development or propagation (oncomiRs) II) miRNAs, which are involved in cancer metastasis (metastamiRs) (Piva et al, 2013). In mice mammary tumor models, the inhibition of a metastamiR (miR-10b) by chemically modified antagomiRs was tested. A drastic reduction in lung metastases was achieved by blocking miR-10b (Ma et al, 2010).

Alternatively, it is conceivable that circRNAs can be used to sequester disease-relevant RBPs. It would even be possible to bind proteins, which do not have RNA binding domains by developing specific aptamers (Tuerk & Gold, 1990; Darmostuk et al, 2015). For the purpose of sequestration of proteins, circRNAs might be particular suitable, because circularity could be beneficial in terms of structure constraints (Lasda & Parker, 2014). The structure of an aptamer is the key for its functionality in binding the interaction partner. Most probably the structure of a circRNA is more stable compared to a linear RNA, simply because the RNA has less possibilities to adopt alternative structures. The HVC model system could even be used to test the functional capability of designed circRNAs for protein sequestration. Besides miR-122, HCV requires several cellular RBPs for its propagation. A set of RBPs including hnRNP L, hnRNP D, La protein, Imp-1, PTB and PCBP2 promote IRES-dependent translation (reviewed in Niepmann, 2013). A 18 amino acid N-terminal La peptide sequesters PTP and PCBP2 and thereby inhibits HCV translation (Fontanes et al, 2009). Although research on host targeting agents for HCV treatment is pursued, inhibitors for cellular RBPs seem to play a minor role in drug development (Zeisel et al, 2015). Nevertheless circRNAs, which sequester HCV host factors, could help to understand the role of these host factors in the HCV life cycle.

The therapeutic application of circRNAs, mainly exogenously delivered might bear the risk of immunogenicity. Recent reports link exogenously produced and transfected circRNAs to the activation of innate immune response (Chen et al, 2017; Li et al, 2017). For exogenous circRNAs, the RIG-I pathway is activated, which appears to be due to lack of proteins, which would assemble during the natural biogenesis pathway (Chen et al, 2017). In the experiments performed in this work, no circRNA-specific but miR-122-unspecific effects were observed. The *shuffle* circRNA did neither have adverse effects on HCV, nor on cell viability (**Figure 35** and **Figure 36**). This might be attributed to the fact that RIG-I is inactive in Huh7.5 cells, because of a HCV-adaptive mutation (Sumpter et al, 2005). Besides that, HCV has evolved multiple strategies to inhibit RIG-I signaling (Breiman et al, 2005; Otsuka et al, 2005; Eksioglu et al, 2011; Kaukinen et al, 2013; Nitta et al, 2013). Thus, the RIG-I pathway would not interfere with the application of circRNAs in HCV infection. The role of natural, as well as artificial circRNAs in innate immunity needs further

investigation. It is not clear, which interaction partner of the circRNA triggers RIG-I signaling, since RIG-I was not found among the bound proteins (Chen et al, 2017). In other systems, where RIG-I pathway or other RNA-recognizing mechanisms of the cell (TLR-3 or MDA-5) are active, exogenously delivered circRNAs could be masked. The use of pseudouridine or other nucleotide modifications, could circumvent the detection of artificial circRNAs in the cell to anticipate undesired immune responses (Karikó et al, 2005; Durbin et al, 2016).

3.3.5 Conclusion

The data presented in the second part of my work, clearly show HCV-adverse effects of circular and linear miR-122 sponges in different HCV reporter systems. The specific inhibition of HCV by sponges containing miR-122 binding sites provides strong evidence for a functional sequestration of miR-122 from HCV RNA. Further experiments could be, the analysis of AGO immunoprecipitation in combination with sequencing of miRNA:target chimeras, which is termed cross-linking ligation and sequencing of hybrids (CLASH) (Helwak & Tollervey, 2014). Thereby sequestration of miR-122 by circRNA sponges could be further validated and even be quantitated (Luna et al, 2015).

miR-122 was selected as target for designed circRNA sponges because of its exceptional high abundance in liver cells, and its role as HCV host factor. It was not the intention of this work to design circRNAs for HCV treatment. Expertise, experimental model systems and equipment in our laboratory is not adapted for development of HCV remedies. Additionally, HCV DAADs with a cure rate of almost 100 % have become available in 2013. The scope of this work was to show that circRNAs can be designed for therapeutic applications in general, using HCV as a model system. This has been successful within the available possibilities. The circRNAs designed in this work have comparable efficacy to miravirsen, in cell culture systems. This makes them valuable agents to extend the spectrum of the growing field of RNA-therapeutics. Beyond that, several studies aimed to find disease-related changes in circRNA expression patterns to identify new drug targets and biomarkers (Boeckel et al, 2015; Zhang et al, 2017; Maass et al, 2017). Thousands of circRNAs were reliably detected in blood samples, and identification of circRNA biomarkers would provide the opportunity to non-invasive screen for disease marker (Memczak et al, 2015).

3.4 Future perspectives

The central dogma postulates a division of powers between DNA, RNA and protein. For several decades cell biology was very protein-centered, because of the conception that mainly proteins execute the important functions in the cell. The exploration of transcriptomes has changed this protein-centered view. More RNAs than expected have important structural, catalytic or regulatory functions. Many classes of non-coding RNAs, such as miRNAs, long non-coding RNAs (lncRNAs), small nucleolar RNAs (snoRNAs), small Cajal-body associated RNAs (scaRNAs), and many more have been identified. The most prominent example is the discovery of the miRNA/siRNA pathway, which illustrates that gene expression is much more complex than assumed, and not exclusively protein-governed. The impact of these findings becomes obvious by saying that siRNAs have become widely-used tools in molecular biology and miRNAs have emerged as biomarkers or even therapeutic targets.

Being investigated more extensively only during the last five years, the global impact of circRNAs is not clear, yet. There are many open questions: I) What factors determine whether an exon is circularized or linearly spliced? II) How do circRNAs influence their interaction partners (eg. miRNAs or proteins)? III) What is their role in immunity, brain function, disease, development or differentiation? IV) What are future fields of application for synthetic or artificial circRNAs? The new class of circRNAs has the potential to impact or even revolutionize scientific field like immunology, cancer biology, neurobiology, biotechnology, and most probably many more.

4 MATERIAL AND METHODS

4.1 Material

4.1.1 Chemicals

10X Phosphate Buffered Saline (PBS)	Gibcon
Agarose	Roth
Ammonium persulfate (APS)	BioRad
Ampicillin	Roth
Blocking Reagent	Roche
Boric acid	Roth
Bovine Serum Albumin (BSA)	Roche
Bromphenol blue	Merck
Calcium chloride ($CaCL_2$)	Merck
CDP-Star Chemiluminescent Substrate	Sigma-Aldrich
Chemiluminescent detection films	GE Healthcare
Chloroform	Roth
Desoxy-Ribonucleotides (dNTPs)	Peqlab
Digoxygenine (DIG) RNA labeling mix	Roche
Dimethyl pyrocarbonate (DMPC)	Sigma-Aldrich
Dimethylformamide (DMF)	Roth
Dithothreitol (DTT)	Sigma-Aldrich
DMEM	Gibcon
Ethanol (EtOH)	Roth
Ethidium bromide	Roth
Ethylene glycol tetraacetic acid (EGTA)	Sigma-Aldrich
Ethylenediaminetetraacetic acid (EDTA)	Roth
Fetale Bovine Serum (FBS)	Gibcon
Formaldehyde	Roth
Formamide	Roth

Glycerol	Roth
Glycine	Roth
Glycogen	Peqlab
Isopropanol	Roth
Potassium chloride (KCl)	Roth
Lumi-Light Western Blotting Substrate	Roche
Magnesium chloride ($MgCl_2$)	Merck
Maleic acid	Roth
Methanol	Roth
Milk powder (fat-free)	Roth
NorthernMax hybridization buffer	Ambion
N-Lauroylsarcosin	Sigma-Aldrich
Phenol (water-saturated)	Roth
Phenol/chloroform/isoamylalcohol (25:42:1)	Roth
Radioactively labelled Nucleotides	Hartmann Analytics
Roti-Nylon plus	Roth
Rotiphorese gel 30% (37.5:1)	Roth
Rotiphorese gel 40% (19:1)	Roth
Sodium acetate (NaOAc)	Merck
Sodium chloride (NaCl)	Roth
Sodium hydroxide (NaOH)	Roth
Sodium-Dodecyl-Sulfat (SDS)	Roth
Tetramethylethylenediamine (TEMED)	BioRad
Tris(hydroxymethyl)aminomethane (Tris)	Roth
Trizol Reagent	Thermo Fisher Scientific
Tween 20	Sigma-Aldrich
Urea	Roth

Xylene cyanol	Flucka
Yeast tRNA	Roche
β-mercaptoethanol	Sigma-Aldrich

4.1.2 Laboratory equipment

ÄKTApurifier	Amersham Biosciences
Bioanalyzer 2100	Agilent
Centro LB Lunimometer	Berthold
Excella Eco-170	New Brunswick Scientific
G:Box Gel Documentation	Syngene
GeneAmp PCR Sysgtem 9700	Applied Biosystems
Gene Pulser Cuvette (0.2 cm)	BioRad
HB-1000 Hybridizer	UVP
Heraeus Multifuge X1R	Thermo Scientific
Mini PROTEAN Electrophoresis System	BioRad
NanoDrop 1000 Spectrophotometer	Thermo Scientific
Thermomixer Thriller	Peqlab
Thermo Scientific Safe 2020	Thermo Scientific
Trans-Blot Semi-Dry Transfer Cell	BioRad
Trans-Blot Turbo	BioRad
Typhoon FLA 9500	GE Healthcare
Veriti Thermal Cycler	Applied Biosystems
Vortex-Genie2	Bender & Hobein AG

4.1.3 Commercial kits

Beetle Juice Kit	pjk
DIG-detection system	Roche
Digoxigenin-LNA-probes	Exiqon
HiScribe T7 High Yield RNA Synthesis Kit	NEB
MinElute Gel Extraction Kit	QIAGEN
NE-PER Nuclear and Cytoplasmic Extraction Kit	Thermo Fisher Scientific
NeutrAvidin agarose beads	Thermo Fisher Scientific
Plasmid Maxi Kit	QIAGEN
QIAprep Spin Miniprep Kit	QIAGEN
QIAquick Gel Extraction Kit	QIAGEN
qScript cDNA Synthesis Kit	Quantabio
qScript flex cDNA kit	Quantabio
Quick Spin RNA Columns	Roche
Renilla Juice Kit	pjk
RNeasy Mini Kit	QIAGEN
TOPO TA Cloning Kit	Thermo Fisher Scientific

4.1.4 Eukaryotic cell lines and bacterial strains

HeLa (human cervix carcinoma cells)	Leibniz-Institut DSMZ *(Deutsche Sammlung von Mikroorganismen und Zellkulturen)*
Huh7, Huh7.5 (human hepatocellular carcinoma cells)	kindly provided by Michael Niepmann *(Universität Giessen, Deutschland)*
Huh-luc/neoNS3-3'ET	kindly provided by Volker Lohmann *(Universitätsklinikum Heidelberg, Deutschland)*
KRX *E.coli* Competent cells	Promega
One Shot TOP10 Competent *E.coli*	Thermo Fischer Scientific

4.1.5 Media, supplements and transfection reagents

DMEM	Gibco
Fetal bovine Serum (FBS)	Gibco
G418 Geneticin 50 mg/ml	Gibco
GlutaMAX	Gibco
Lipofectaminee 2000 transfection reagent	Thermo Fisher Scientific
non-essential Amino Acids	Sigma-Aldrich
OptiMEM	Gibco
Trypsine EDTA solution	Gibco
TurboFect *in vitro* transfection reagent	Thermo Fisher Scientific

4.1.6 Plasmids

pcDNA3	Invitrogen
pcDNA3-CNTROB Long	This study
pcDNA3-CNTROB Short	This study
pcDNA3-PIE-streptavidin aptamer	This study
pcDNA3-RCR-CL B WT	This study
pcDNA3-RCR-CL Delta WT (RCR-CNTROB) and mutants	This study
pciRS-7	kindly provided by Jørgen Kjems *(University Aarhus, Denmark*)
pciRS-7-CL B	kindly provided by Silke Schreiner
pCR2.1-TOPO	Invitrogen
pCR2.1-bulge	kindly provided by Oliver Rossbach *(Universität Giessen, Deutschland*)
pCR2.1-perfect	"
pCR2.1-shuffle	"
peGFP	kindly provided by Rainer Renkawitz *(Universität Giessen, Deutschland*)
pFK-JFH1-J6 C-846_dg	kindly provided by Ralf Bartenschlager *(Universitätsklinikum Heidelberg, Deutschland)*
pHCV-FL	kindly provided by Michael Niepmann *(Universität Giessen, Deutschland*)
pmirGLO Dual-Luciferase miRNA Target Expression Vector (empty vector)	Promega
pmirGLO-4xbulge mut	kindly provided by Oliver Rossbach *(Universität Giessen, Deutschland*)
pmirGLO-4xbulge WT	"
pmirGLO-4xIGF1R mut	"
pmirGLO-4xIGF1R WT	"
pmirGLO-4xperfect mut	"
pmirGLO-4xperfect WT	"

pmirGLO-HNRNPK	"
pmirGLO-KPNB1	"
pmirGLO-LAPTM4A	"

4.1.7 Enzymes and inhibitors

*Apa*I	New England Biolabs (NEB)
*Bam*HI-HF	NEB
*Eco*RI-HF	NEB
*Hind*III-HF	NEB
*Mlu*I	NEB
*Nhe*I-HF	NEB
Phusion High-Fidelity DNA polymerase	NEB
RNase R	Epicentre
RNaseOUT	Thermo Fisher Scientific
RQ1 DNase	Promega
*Sac*I	NEB
T4 DNA ligase	NEB
T4 PNK	NEB
T4 RNA ligase 1	NEB
T7 RNA polymerase	Thermo Fisher Scientific
Taq polymerase	Purified by S. Schreiner and C. Preusser
*Xba*I-HF	NEB

4.1.8 Antibodies

Anti-Dioxigenine-AP Fab Fragments	Roche
GAPDH monoclonal antibody 71.1	Sigma-Aldrich
HCV core monoclonal antibody C7-50	Thermo Fisher Scientific
HCV NS3 monoclonal antibody 8G-2	Abcam
hnRNP A1 monoclonal antibodiy 4B10	Santa Cruz Biotechnology
hnRNP L monoclonal antibody 4D11	Sigma-Aldrich

4.2 Methods

4.2.1 Bacterial and eukaryotic cell culture techniques

Eukaryotic cells or bacterial strains were manipulated and cultivated under sterile conditions, using a biological safety cabinet or a Bunsen burner, respectively. Solutions, media and laboratory plastic ware were either bought certified as sterile or were autoclaved at 120 ℃ for 20 min and 2 bar. The laboratory glassware was sterilized by incubation for 2 h at 180℃.

4.2.1.1 Bacterial growth conditions

E.coli were grown in LB medium (1% tryptone, 0.5 % yeast extract, 0.5% NaCl all (w/v)) or on LB agar (Roth) plates at 37℃ using Ampicillin (100 µg /ml) as selection marker. *E.coli* were harvested by centrifugation for 5-10 min at 2,000 xg and 4℃, followed by washing with 1x PBS (1:10 dilution of 10x PBS Gibco) and centrifugation as before.

4.2.1.2 Transformation of *E.coli*

Transformation of *E.coli* was performed with chemically competent cells, which were thawed on ice. Then 50 µl of *E.coli* suspension was mixed with 1-50 ng of plasmid DNA or with 5 µl of the ligation reaction, followed by incubation for 10 min on ice. The mixture was incubated for 30 s at 42℃ and placed on ice for 1 min. 300 µl LB medium was added and cells were shaked 60 min at 37℃ in a Thermomixer (Eppendorf). Then, 100 µl of the mixture was distributed on a LB agar plate with 100 µg/ml ampicillin. The plates were incubated overnight (ON) at 37℃. The next day, clones were analyzed by PCR. For plasmid preparation 3 ml LB medium were inoculated with clones from the plate (**4.2.1.1**).

4.2.1.3 Eukaryotic cell culture

HeLa cells were maintained in Dulbecco's Modified Eagle's Medium (DMEM) supplemented with 10% fetal bovine serum (FBS). Media for Huh7.5 and Huh-luc/neoNS3-3'ET cells were additionally supplemented with GlutaMAX (Gibco) and non-essential amino acids (Sigma-Aldrich). G418 (100 µg/ml) selection marker was used to maintain Huh-luc/neoNS3-3'ET cells, but was not added under experimental conditions. Cells were passaged 1:10 or 1:20 two to three times a week in 10 cm dishes and incubated at 37℃ and 5% CO_2 in an Excella Eco-170 incubator. At approximately 80% of confluency, cells were washed with pre-warmed 1x PBS and incubated 1 min with Trypsin EDTA at 37℃. Cells were suspended in pre-warmed culture medium and seeded in 10 cm dishes.

4.2.2 General preparative methods for nucleic acid

For handling RNA, RNase-free plastic ware was used. Experiments were performed wearing gloves and using RNase-free buffers. For inactivation of RNases, double-distilled (dd) water (H_2O) was treated with 1% (v/v) Dimthyl dicarbonate (DMPC) stirring constantly for 1 h. Afterwards the DMPC-treated H_2O was autoclaved two times at 120℃ for 20 min.

4.2.2.1 Phenol/chloroform extraction

Nucleic acids were purified from reaction mixtures or extracts by adding one volume of phenol/chloroform, followed by thorough mixing using a vortex mixer (Bender & Hobein AG). The samples were centrifuged for 10 min at 25,000 xg and 4℃. The upper aqueous phase was transferred to a new reaction tube and nucleic acids were precipitated.

4.2.2.2 Precipitation of nucleic acids

For precipitation, nucleic acids were mixed with 2.5 volumes of 100% ethanol (EtOH) and 0.1 volumes of 3 M sodium acetate (NaOAc) (pH 5.2), or 0.5-0.7 volumes of isopropanol. For precipitation of low amounts of nucleic acids 10 µg glycogen were added. The samples were incubated on ice or at -20℃ for a minimum of 20 mi n. Precipitated nucleic acids were pelleted by centrifugation for 20 min at 25,000 xg and 4℃. The pellet was washed with 75% EtOH, and centrifugation was performed for 5 min as before. When precipitating DNA, the pellet was dissolved in ddH_2O. Whereas RNA pellets were dissolved in RNase-free (DMPC-treated) ddH_2O.

4.2.2.3 Photometric measurement of nucleic acid concentrations

The concentrations of total RNA in solution were measured using 1-1.5 µl for spectrophotometry with a NanoDrop 1000 (Thermo Scientific). Concentrations of DNA solutions were measured via BioPhotometer (Eppendorf) and a quartz glass cuvette. Therefore nucleic acids 1 µl of the sample was diluted 1:100 in ddH_2O.

4.2.2.4 Plasmid preparation

For molecular cloning purposes, plasmid DNA was purified from 3 ml *E.coli* cultures via QIAprep Spin Miniprep Kit (Qiagen). Plasmid Maxi Kit (Qiagen) was used for preparation of plasmid DNA from 50-100 ml *E.coli* culture. Plasmid preparations were performed according to the protocols provided by the manufacturer. Plasmid DNA, which would be used for transfections was washed two-times with endotoxin removal buffer, precipitated with isopropanol and dissolved in sterile H_2O using the biological safety cabinet.

4.2.2.5 Isolation of genomic DNA

HEK-293 genomic DNA (gDNA) was isolated using DNAzol (Thermo Fisher Scientific) following the manufacturer's instructions. Isolated gDNA was used for cloning purposes (CNTROB Long, CNTROB Short, RCR-CLB, RCR-CLB)

4.2.2.6 RNA extraction

RNA was isolated from extracts or enzymatic reactions by phenol/chloroform extraction and ethanol (EtOH) precipitation (**4.2.2.2**). When isolating RNA from cells, Trizol reagent (Thermo Fischer Scientific) was used as described in the manufacturer's instructions.

4.2.2.7 T7 *in vitro* transcription

RNAs were *in vitro* synthesized via T7 RNA polymerase from transcription templates containing a T7 promoter. The reaction mixture as described in **Table 3** was incubated between 1-3 h at 37℃. Then, 4 µl 10x RQ1 DNase buffer and 4 µl RQ1 DNase (Promega), as well as 12 µl ddH_2O were added and incubated for 20 minutes at 37℃.

Table 3 T7 *in vitro* transcription reaction mixture.

volume (µl)	component
5	Template (max 1 µg final concentration)
4	5x transcription Buffer
2	ATP (100 mM)
2	GTP (100 mM)
2	UTP (100 mM)
2	CTP (100 mM)
0.5	RNaseOUT
2	T7 polymerase (50 u/µl)
4	H_2O
20	total volume

The *in vitro* transcripts were purified by phenol/chloroform extraction and EtOH precipitated. For *in vitro* transcripts, RNA concentrations were measured by comparing band densities on an agarose gel. Therefore a standard, which was prepared by dilution series of yeast tRNA was co-analyzed with the sample of interest. Alternatively, *in vitro* transcripts were quantified via Bioanalyzer 2100 (Agilent) run using the RNA 6000 nano kit (Agilent), following the manufacturer's instructions.

4.2.3 General analytical methods for nucleic acids

4.2.3.1 Standard PCR

PCR reactions were performed with *Taq* polymerase (expressed and purified by Silke Schreiner and Christian Preusser) under standard PCR conditions as described below (**Table 4**). For preparative PCR reactions the reaction mixture was scaled up to 50 µl or 100 µl reaction volume. For molecular cloning and HCV-FL template preparation Phusion High-Fidelity polymerase (NEB) was used as described in the manual.

Table 4 *Taq* PCR reaction mixture.

volume (µl)	component
2	DNA/cDNA
1	forward primer (10 µM)
1	reverse primer (10 µM)
2.5	10x *Taq* PCR buffer
1	dNTPs (10 µM)
0.5	$MgCl_2$ (25 mM)
0.5	*Taq* polymerase
16.5	H_2O
25	total volume

The PCR reactions were performed, using the GeneAmp PCR System 9700 Cycler, or Veriti Thermal Cycler (Applied Biosystems). The PCR program used for amplification is depicted below (**Table 5**).

Table 5 Standard *Taq* polymerase PCR program.

step	duration	temperature	cycles
initial denaturation	2 min	95℃	
denaturation	10 s	95℃	x25-35
annealing	15 s	56-60℃	
elongation	20-120 s	72℃	
final elongation	7 min	72℃	
storage	infinite	4℃	

4.2.3.2 RT-PCR

For RT-PCR analysis, RNA was reverse transcribed using the qScript cDNA synthesis kit or the qScript flex cDNA kit (Quantabio), following the manufacturer's instructions. cDNA was diluted 1:2 and 2-4 µl were used for PCR reaction (**Table 4**). Then PCR products were analyzed by agarose gel electrophoresis (**4.2.3.3**).

4.2.3.3 Agarose gel electrophoresis

Plasmid DNA, PCR products or DNA fragments were analyzed by agarose gel electrophoresis. 0.8-2% (w/v) agarose was melted in 1x TBE buffer (89 mM Tris, 89 mM boric acid, 2 mM EDTA) by microwave heating. When the agarose had cooled to 50℃, EtBr (0.5 µg/ml) was added. Gels were cast and after having solidified, the samples were mixed 1:6 with 6x DNA loading dye (60% glycerol, 6x TBE, 0.2% xylene cyanol and 0.2% orange G) and loaded onto the agarose gel. The gel run was performed using 1x TBE running buffer and 120 V for 20-60 min. Nucleic acids were visualized by EtBr staining and irradiation with UV light. The gels were documented using G:Box Gel documentation (Syngene).

4.2.3.4 Denaturing agarose gel electrophoresis

1.2% agarose was dissolved in 90 ml ddH_2O and 10 ml 10x FA gel buffer (200 mM MOPS, 50 mM NaOAc, 10 mM EDTA; pH 7.0) and melted using a microwave oven. When the agarose had cooled to 50℃, 1.8 ml 37% formaldehyde and EtBr (0.5 µg/ml) were added. RNA samples were mixed 1:5 with 5x FA RNA loading dye (50% (v/v) formamide, 2.7 M formaldehyde, 1x FA gel buffer, 0.2% bromophenol blue, 0.2% xylene cyanol), followed by heat denaturing for 5 min at 65℃. The denatured samples were store on ice until loaded. The gel run was performed in 1x FA running buffer (20 mM MOPS, 5 mM NaOAc, 1mM EDTA, 2.7 M formaldehyde), at 100 V for 1.5 h. RNAs were visualized by irradiation with UV light or nucleic acids were transferred to a nylon membrane by vacuum blotting and subsequently detected by northern blot (**4.2.3.7**).

4.2.3.5 Denaturing PAA gel electrophoresis

Denaturing PAA gels were cast using the Mini PROTEAN Electrophoresis System (Biorad) or custom gel system. The gel was prepared by mixing the acrylamide gel solution (20% acrylamide 40%; 19:1 acrylamide/bisacrylamide, 50% (w/v) urea, 1x TBE buffer) with (1x TBE, 50% (w/v) urea). The mixing ratio was dependent on the desired PAA percentage of the gel. For example, a 10% PAA gel was obtained by mixing both solutions in a 1:1 ratio. To induce polymerization 100 µl of 10% (w/v) ammonium persulfate (APS) and 10 µl of Tetramethylethylenediamine (TEMED) were added per 10 ml of the gel mixture. The gels were pre-run for 20 minutes at 200 V. The samples were dissolved in RNA loading buffer (90% formamide, 1x TBE, 0.25% bromphenol blue, 0.25% xylene cyanol), denatured for 2 min at 95℃, cooled at least for 1 minute on ice. RNAs were electrophoresed using Mini PROTEAN electrophoresis chambers (Biorad), 1x TBE running buffer and 200 V for 30-90 min. Gels were stained with EtBr for 10 min in 1x TBE EtBr solution (50 µg/ml) on a shaker, or RNAs were detected by northern blot (**4.2.3.6** or **4.2.3.7**).

4.2.3.6 PAA northern blot

Samples were separated by denaturing PAA gel electrophoresis on small gels using the Mini PROTEAN Electrophoresis System (**4.2.3.5**). For better resolution, large PAA gels (20 cm x 40 cm) were cast and the gel run was performed using 23 W for 45-90 min. RNAs were transferred via semi-dry electroblotting to a nylon membrane, using 15 V and 3 mA/cm^2 for 1 h. Then, RNAs were crosslinked to the membrane with 254 nm UV light and 120 mJ/cm^2 using BLX-254 UV-Crosslinker (Bio-Link). Afterwards, the membrane was transferred to a hybridization tube, which was placed into a HB-1000 Hybridizer (UVP). Pre-hybridization was performed at 65℃ for at least 1 h. DIG-labelled RNA probes were diluted between 10-50 ng/ml in hybridization buffer and hybridized at 65℃ ON. Either NorthernMax hybridiza tion buffer (Ambion) or Church buffer (7% SDS, 50% formamide, 5x SSC, 2% blocking reagent (Roche), 50 mM Na^2PO^4; pH7.0, 0.1% (v/v) N-lauroylsarcosin) were used. The next day, the membrane was washed two times with 2x northern washing buffer (2x SSC, 0.01% SDS), followed by two washing steps with 0.5x northern washing buffer (0.5x SSC, 0.01% SDS). Then the membrane was transferred to a tray and was incubated in 2% blocking reagent (Roche) dissolved in Maleic acid buffer (100 mM maleic acid, 150 mM NaCl; pH 7.5) for 1 h at room temperature (RT). Anti-DIG-AP Fab fragments (Roche) were added 1:1,000 (v/v) to the blocking solution. The membrane was incubated for 1 h, followed by three washing steps each 30 min with DIG washing buffer (0.3% (v/v) Tween 20 in Maleic acid buffer). For detection the membrane was incubated 5 min with 0.1% CPD Star (Sigma-Aldrich) in DIG Detection buffer (100 mM Tris/HCl pH 9.5; 100 mM NaCl) and the luminescence signals were detected by exposure to chemiluminescent detection films (GE Healthcare). When using ^{32}P labelled probes, Phosphor Screens (GE Healthcare) were exposed between 12 h and 5 days. Then, signals were detected by phosphor imaging using Typhoon FLA 9500 and quantified by ImageQuant TL (both GE Healthcare).

4.2.3.7 Agarose vacuum northern blot

RNAs were separated by 1.2% denaturing agarose gel-electrophoresis (**4.2.3.4**). The gel was incubated for 15 min in 20x SSC (3 M NaCl, 300 mM sodiumcitrat; pH 7.0). For assembly of the blot, the bottom plate of the vacuum blotter, a nylon membrane, a transparency film, the agarose gel and the cover plate of the vacuum blotter were stacked bottom to top. Then the vacuum blotter was connected to the vacuum pump and vacuum was adjusted to 50 mbar. Transfer by vacuum blotting was performed for 2 h. Every 15 min the gel surface was moistened with 20x SSC. Afterwards, samples were cross-linked to the membrane by UV light as described above. The membrane was washed three times with ddH_2O. Pre-hybridization, hybridization and detection were performed as described (**4.2.3.6**).

4.2.3.8 Synthesis of DIG-labelled RNA probes

DIG-labelled RNA probes were synthesized via T7 *in vitro* transcription using PCR-generated transcription templates. The T7 promotor for transcription was attached via reverse primer in a preparative 50 µl standard *Taq* PCR reaction. The fragments were separated by agarose gel electrophoresis, cut from the gel and were extracted from the gel matrix using Qiagen gel extraction kit min elute (Qiagen) following the manufacturer's instructions. The *in vitro* transcription was performed using T7 RNA polymerase (Thermo Fisher Scientific) and DIG RNA labelling Mix (Roche) as described in **Table 6** for 3 h at 37°C. The DNA template was digested by adding 4 µl 10x RQ1 reaction buffer, 12 µl RNase-free ddH_2O and 4 µl RQ1 DNase (Promega). The reaction was incubated for 30 min at 37°C. RNA probes were purified by using mini Quick Spin RNA columns (Roche), followed by phenol/chloroform extraction and EtOH precipitation. DIG-labelled RNA probes were heat denatured at 85°C for 5 min, then placed on ice for 5 min and diluted at 10-50 ng/ml in Church buffer or NorthernMax hybridization buffer (Ambion).

Table 6 DIG-labelling of RNA probes.

volume (µl)	component
5	PCR template (100-500 ng)
4	5xTranscription buffer
2	10 x DIG RNA labeling Mix
2	T7 RNA polymerase (50 u/µl)
0.5	RNaseOUT
6.5	H_2O
20	total volume

4.2.3.9 Radioactive 5'end labelling of DNA northern probes

Antisense oligos for northern blot detection were designed with a 5' terminal A to enhance labelling efficiency of T4 Polynucleotide Kinase (PNK) (NEB). The reaction mixture (see **Table 7**) was incubated for 1 h at 37°C, followed by incubation at 95°C for 2 min. The DNA oligos were purified by using mini Quick Spin Oligo columns (Roche). Approximately 1/3 of the purified oligos were mixed with NorthernMax hybridization buffer (Ambion).

Table 7 Radioactive 5'end labelling reaction mixture.

volume (µl)	component
5	10× PNK buffer
2	T4 PNK enzyme
36.5	H_2O
2.5	add DNA probe (20 µM)
4	add [γ-^{32}P]-ATP (SCP-801)
50	total volume

4.2.3.10 Synthesis of internally radioactively labelled northern probes

For synthesis of internally labelled northern probes T7 *in vitro* transcription was performed using [α-^{32}P]-UTP. The reaction mixture (see **Table 8**) was incubated for 2 h at 37℃. Radioactively labelled transcripts were purified by gel-filtration using mini Quick Spin RNA columns (Roche). 1 µl of input was saved for liquid scintillation counting to determine labelling efficiency. RNA integrity was controlled by denaturing PAA gel electrophoresis (**4.2.3.5**).

Table 8 T7 *in vitro* transcription using α^{32}P-UTP for radioactive labelling.

volume (µl)	component
10	5x Transcription buffer
5	DTT (100 mM)
2.5	ATP (10 mM)
1	UTP (2 mM)
2.5	CTP (10 mM)
2.5	GTP (10 mM)
2	DNA template
1	RNaseOUT
2	T7 RNA polymerase
2	[α-^{32}P]-UTP (SCP-210)
19.5	H_2O
50	total volume

4.2.4 General analytical methods for proteins

4.2.4.1 Western Blot

Extracts were diluted 1:1 in Laemmli loading dye (1.5% SDS and 10% glycerol, 62.5 mM Tris -HCl; pH 6.8, 0.0025% Bromophenol blue, 2% β-mercaptoethanol), and were boiled for 10 min in a water bath. Proteins were separated by SDS-polyacrylamide gel electrophoresis (SDS-PAGE) (Laemmli, 1970). The gel, nitrocellulose membrane and blotting paper were equilibrated for 2 min in Transfer buffer (25 mM Tris, 190 mM glycine, 20% methanol). Transfer onto the nitrocellulose membrane was performed with 25 V, 1.3 A for 30 min using Trans-Blot Turbo Transfer System (Biorad). Then, the membrane was washed twice, 10 min for each washing-step with PBS-T (1x

PBS, 0.1% Tween 20). After 30 min of blocking with 5% milk powder in 1x PBS, the primary antibody (for dilution see **Table 9**) was added for 1 h, followed by 3-times of washing with PBS-T. The secondary antibody (HRP-conjugated goat anti-mouse) was diluted 1:10,000 in the blocking solution, and was incubated with the membrane for 45 min, followed by 3-times washing with PBS-T. The signal was developed by adding 2 ml LumiLight Western Blotting Substrate (Roche) and the membrane was exposed to chemiluminescent detection films (GE Healthcare).

Table 9 Dilution of primary antibodies.

Antibody	Dilution
hnRNP L monoclonal antibody 4D11	1:10,000
GAPDH monoclonal antibody 71.1	1:10,000
hnRNP A1 monoclonal antibodiy 4B10	1:500
HCV core monoclonal antibody C7-50	1:1,000
HCV NS3 monoclonal antibody 8G-2	1:1,000

4.2.5 Molecular cloning

Methods for molecular cloning were performed as described in (Sambrook & Russell, 2001). Restriction enzymes were purchased from *New England Biolabs* (NEB) and digests were performed using the recommended buffer systems. All plasmid constructed in this study were confirmed by Sanger sequencing (Seqlab).

4.2.5.1 Cloning of minigene and circRNA expression constructs

All constructed minigenes were cloned into pcDNA3 vector backbone (Invitrogen).

Table 10 Cloning strategy of RCR-CL B and RCR-CL Delta mini gene construct.

Mutant	Forward (fw) primer / reverse (rv) primer (5'-3')	Restriction Enzymes	Vector backbone	Cloning Strategy
3'ss M1	CTGAAAGCTTCTTCCTTCCTCAGCTTCCTG / ACATGGATCCCAGGAGGAGCCCGACCAGGA	*Hind*III/ *Bam*HI	RCR-CL B	mutation introduced via rv primer
3'ss M2	CTGAAAGCTTCTTCCTTCCTCAGCTTCCTG / ACATGGATCCCAGGAGGAACCTGACCAGGA	*Hind*III/ *Bam*HI	RCR-CL B	mutation introduced via rv primer
3'ss M3	CTGAAAGCTTCTTCCTTCCTCAGCTTCCTG / ACATGGATCCCAGGAGGATGCTGACCAGGA	*Hind*III/ *Bam*HI	RCR-CL Delta	mutation introduced via rv primer
5'ss M1	GGCTCACTTCATCCACAGTTAACTGGGGGCAGAA GTCAG / AATTCTGACTTCTGCCCCCAGTTAACTGTGGATG AAGTGAGCCGC	*Sac*II/ *Eco*RI	RCR-CL B	insertion of annealed synthetic oligos

Mutant	fw primer / rv primer (5'-3')	Restriction Enzymes	Vector backbone	Cloning Strategy
5'ss M2	GGCTCACTTCATCCACATGTAACTGGGGGCAGAA GTCAG / AATTCTGACTTCTGCCCCCAGTTACATGTGGATG AAGTGAGCCGC	*Sac*II/ *Eco*RI	RCR-CL B	insertion of annealed synthetic oligos
5'ss M3	GGCTCACTTCATCCACAGGTCACTGGGGGCAGAA GTCAG / AATTCTGACTTCTGCCCCCAGTGACCTGTGGATG AAGTGAGCCGC	*Sac*II/ *Eco*RI	RCR-CL Delta	insertion of annealed synthetic oligos
PPT M1	CTGAAAGCTTCTTCCTTCCTCAGCTTCCTG / AATGGAATGGGGCCAGTCTGAGTCAAAGCACAGT AGGTTTAAAGA GACCTGGCCCCATTCCATTGGGCAGGCTCCTCCT GGGATCC / CATCCGCGGAGATCAGCACACTGGAGACG	*Hind*III/ *Sac*II	RCR-CL B	two step PCR with overlapping primers
PPT M2	CTGAAAGCTTCTTCCTTCCTCAGCTTCCTG / CAATTTTTGGCCCTTTCCCTCAGTCAAAGCACAG TAGGTTTAAAGA AGGGAAAGGGCCAAAAATTGAGCAGGCTCCTCCT GGGATCC / CATCCGCGGAGATCAGCACACTGGAGACG	*Hind*III/ *Sac*II	RCR-CL B	two step PCR with overlapping primers
∆ BP	CTGAAAGCTTCTTCCTTCCTCAGCTTCCTG / GCAGAAAGAAGGGCCAAAGCACA TGTGCTTTGGCCCTTCTTTCTGC / CATCCGCGGAGATCAGCACACTGGAGACG	*Hind*III/ *Sac*II	RCR-CL B	two step PCR with overlapping primers
∆ Repeat	TAGCGAATTCAGCTCACTCAAAGGCGGTAA / TGCGGCCGCCGCCTGGTATCTTTATAGTCC	*Eco*RI/ *Not*I	RCR-CL B	insert CLB or CL Delta sequence into cloning intermediate
3' sub. Repeat	TAGCGAATTCAGCTCACTCAAAGGCGGTAA / TGCGGCCGCCGCCTGGTATCTTTATAGTCC	*Eco*RI/ *Not*I	RCR-CL Delat ∆ Repeat	insertion cloned from pBR322
5' sub Repeat	ACCCAAGCTTTGGTATCTTTATAGTCCTGTCGGG TTTCGCCACCTCTGACTTGAGCGTCGATTTTTGT GATGCTCGTCAGGGGGGCGGAGCCTATGGAAAAA CGCCAGCAACGCGGCCTTTTTACGGTTCCTGGCC TTTTGCTGGCCTTTTGCTCACATGTTCTTTCCTG CGTTATCCCCTGATTCTGTGGATAACCGTATTAC CGCCTTTGAGTGAGCTAATTTGGATGACACGAAA CTGGCTTCTTTCTGCCTCTCTCCTGGTCAGGCTC CTCCTGGGATCCTAGAAAGCCAGTCCGCAGAAAC GGTGCTGACCCCGGATGAATGTCAGCTACTGGGC TATCTGGACAAGGGAAAACGCAAGCGCAAAGAGA AAGCAGGTAGCTTGCAGTGGGCTTACATGGCGAT AGCTAGACTGGGCGGTTTTATGGACAGCAAGCGA ACCGGAATTGCCAGCTGGGGCGCCCTCTGGTAAG GTTGGGAAGCCCTGCAAAGTAAACTGGATGGCTT TCTTGCCGCCAAGGATCTGATGGCGCAGGGGATC AAGATCTGATCAAGAGACAGGATGAGGATCGTTT CGCCGCGGTCT	*Hind*III/ *Sac*I	RCR-CL Delat ∆ Repeat	Insert synthetic oligo (GeneArt Strings)

The splice signals (5'ss, 3'ss, PPT, BP) of *CNTROB* exon 13 were predicted by browser-based sequence analysis tool Human Splicing Finder (Desmet et al, 2009). The influence of the mutations on splice site strength was also predicted by Human Splicing Finder. Secondary structure of the minigenes were modelled with RNAfold (Lorenz et al, 2011).

For cloning of ESE elements into *LPAR1* minigene, synthetic oligos (**Table 11**) were annealed and introduced via restriction enzymes *Nhe*I/*Sac*II into the plasmid *LPAR1* WT (Starke et al, 2015). The insertions were adapted from (Fairbrother et al, 2002).

Table 11 Cloning strategy for insertion of ESEs into *LPAR1* minigene.

Mutant	fw primer sequence (5'-3')	rv primer sequence (5'-3')
ESE 1	CTAGCATTGGGATCTTCACACAGCGTCGAGTCTGATCCGC	GTAACCCTAGAAGTGTGTCGCAGCTCAGACTAGG
ESE M1	CTAGCATTGGGATATTCACACAGCGTCGAGTCTGATCCGC	GTAACCCTATAAGTGTGTCGCAGCTCAGACTAGG
ESE 2	CTAGCGCCTGTGAAGAATTCTGGTGTCGAGTCTGATCCGC	GCGGACACTTCTTAAGACCACAGCTCAGACTAGG
ESE M2	CTAGCGCCTGTGAATAATTCTGGTGTCGAGTCTGATCCGC	GCGGACACTTATTAAGACCACAGCTCAGACTAGG
N	CTAGCCCTGGCCGCTGAGCTGGCCGTCGAGTCTGATCCGC	GGGACCGGCGACTCGACCGGCAGCTCAGACTAGG

For cloning of the PIE circRNA expression construct (pcDNA3-PIE-streptavidin aptamer), a synthetic DNA fragment (GeneArt Strings), was inserted into vector backbone pcDNA3 using restriction enzymes *Hind*III and *Apa*I. The expression cassette was adapted from (Umekage & Kikuchi, 2012).

Table 12 Synthetic DNA fragment for cloning of pcDNA3-PIE streptavidin aptamer.

synthetic DNA fragment	sequence (5'-3')
PIE streptavidin aptamer	ACATAAGCTTGGTTCTACATAAATGCCTAACGACTATCCCTTTGGGGAGTAGGGTCAAGTGACTCGAAACG ATAGACAACTTGCTTTAACAAGTTGGAGATATAGTCTGCTCTGCATGGTGACATGCAGCTGGATATAATTC CGGGGTAAGATTAACGACCTTATCTGAACATAATGCTACCGTTTAATATTGCTAGCCCGACCAGAATCATG CAAGTGCGTAAGATAGTCGCGGGCCGGTCTAGATGTTTTCTTGGGTTAATTGAGGCCTGAGTATAAGGTGA CTTATACTTGTAATCTATCTAAACGGGGAACCTCTCTAGTAGACCAATCCCGTGCTAAATTGTAGGACTA TGCATATCCTTAGCGAAAGCTAAGGATTTTTTTTGGGCCCTCAAG

4.2.6 circRNA biogenesis

4.2.6.1 Transfection of minigene constructs

HeLa cells were transfected using TurboFect reagent (Thermo Fisher Scientific). The transfection mixture (**Table 13**) was distributed at the bottom of a 6 cm dish. The reaction mixture was incubate for 15 min at RT, before seeding 5x10^5 cells per dish in 5 ml medium. After 4 h, fresh medium was applied and cells were incubated for between 14-16 h. The next day, cells were harvested in 1 ml

PBS using cell scrapers. After pelleting the cells by centrifugation for 5 min at 2,000 xg and 4℃, 1 ml Trizol was added, followed by RNA isolation using Trizol reagent (Thermo Fisher Scientific) and RNeasy mini kit (Qiagen). To eliminate residual plasmid DNA, the samples were treated with 5 units (u) RQ1 DNase (Promega) in a 50 µl volume for 30 min at 37℃. The RNA was either analyzed by RT-PCR (**4.2.3.2**) or northern blot (**4.2.3.6** or **4.2.3.7**).

Table 13 TurboFect transfection mixture.

volume (µl)	component
6	Plasmid DNA (1µg/µl)
12	TurobFect
600	OptiMEM
618	total volume

4.2.6.2 Analysis of minigene processing products by RT-PCR

HeLa cells were transfected with minigene constructs, and RNA was isolated as described in (**4.2.2.6**). cDNA synthesis was performed using 500 ng of total RNA, random hexamers and the qScript flex kit (Quantabio), following the manufacturer's instructions. Then 2-4 µl of the 1:1 diluted cDNA was subjected to PCR analysis (**4.2.3.1**). The PCR products were analyzed by 2% agarose gel electrophoresis (**4.2.3.3**).

Table 14 Primers for RT-PCR analysis of minigene processing products.

Gene/target	fw primer sequence (5'-3')	rv primer sequence (5'-3')
E13 total	AAGGAGGAGAGGAGGGTCTG	GATCTGAGGAGGAACTGCAAAG
E13 circ	CCAGACCTCACTTCATCCAC	GATCTGAGGAGGAACTGCAAAG
E12-13	AGCTGCTCAGCACCACTCTC	GATCTGAGGAGGAACTGCAAAG
E13-14	CCAGACCTCACTTCATCCAC	CAGGTCCAGGATCTTCCTCA
CNTROB Long/ Short circ	CCAGACCTCACTTCATCCAC	TCTGCAGAATTCCAGCACAC
CNTROB Long/ Short total	GTGTGCTGGAATTCTGCAGA	GATCTGAGGAGGAACTGCAAAG
RCR-CL Delta circ	TAGACTGGGCGGTTTTATGG	GCGGACTGGCTTTCTAGGAT
RCR-CL Delta total	TAGAAAGCCAGTCCGCAGAA	TTCGCTTGCTGTCCATAAAA
RCR-CL B circular	ATGGAGGGACACTACCCACT	TGTGCGTGTCTCCTGGTATG
RCR CLB linear	ATGGAGGGACACTACCCACT	CTGATCAGCGAGCTCTAGCA
LPAR1 circular	GTACCCGCGGATCAGACTC	TGGCTGCCATCTCTACTTCC
LPAR1 linear upstream	TAGTTCTGGGGCGTGTTCA	GTACCCGCGGATCAGACTC
LPAR1 linear downstream	TAGAAGGCACAGTCGAGG	GAAGGCAATGGACTCGTTGT
LPAR1 skipping/ inclusion	TAGTTCTGGGGCGTGTTCA	GAAGGCAATGGACTCGTTGT
β-actin	CGGAATGCTGGCATTTCTTA	TGGACTTCGAGCAAGAGATG

4.2.6.3 Topo TA cloning

PCR products from RCR-CL Delta-derived circRNAs were analyzed by TOPO-TA cloning, followed by Sanger sequencing. The PCR products were cut from a 2% agarose gel and were purified using the Qiagen MinElute Gel Extraction Kit. Then, the purified PCR products were ligated and transformed in a single reaction into *E.coli* TOP10 competent cells via TOPO-TA cloning kit (Thermo Fisher Scientific), as described in the manual. After blue/white selection, positive clones were inoculated into 3 ml LB medium. These cultures were used to isolate plasmid DNA, which then was sequenced. Sequences were analyzed by alignment to the sequence of the parental plasmids using ClustalOmega (Sievers et al, 2011).

4.2.6.4 Verification of circularity by agarose and PAA northern blot analysis

HeLa cells were transfected with RCR-CL B and ciRS-7-CL B (**4.2.6.1**), and RNA was isolated after 16 h of expression. 5 µg of total RNA were loaded onto a (20 x 40 cm) denaturing 6% PAA gel, or a denaturing 1.2% agarose gel. RNAs were subjected to gel electrophoresis as described in (**4.2.3.4** and **4.2.3.5**), and analyzed by northern blot as described in **4.2.3.6** and **4.2.3.7**. For northern blot analysis of processing products of RCR-CL Delta WT and mutant derivatives, 0.4 µg of HeLa total RNA was loaded onto a 6% denaturing PAA gel, and analyzed as described in **4.2.3.6**. Primers for generation of transcription templates for synthesis of DIG-labelled RNA probes are listed below (**Table 15**)

Table 15 Primers for generation of transcription templates to synthesize DIG-labelled RNA probes.

Gene/target	fw primer sequence (5'-3')	rv primer sequence (5'-3')
RCR-CL B junction probe	CAATCCATGTCTTCCGGACT	TAATACGACTCACTATAGGGGCGGAGATCAGCACAC TGGAGACG
RCR-CL B exon probe	AAACCAAAACAGACCTAAAACCA	TAATACGACTCACTATAGGGTCTCCAGTTGGTGCAGATTATG
RCR-CL Delta total probe	TAGAAAGCCAGTCCGCAGAA	TAATACGACTCACTATAGGGGCGAAACGATCCTCATCCT

4.2.6.5 RNase R digest of HeLa total RNA

1 µg of HeLa total RNA was treated with or without 2.5 u RNase R at 37℃ for 3 h. RNAs were purified via phenol/chloroform extraction and EtOH precipitation. Samples were dissolved in equal volumes and analyzed by RT-PCR using random hexamers and qScript flex kit (Quantabio) for cDNA synthesis.

4.2.7 circRNA synthesis and characterization of *in vitro* generated circRNAs

4.2.7.1 PIE *in vitro* self-splicing

First, the circRNA expression plasmid pcDNA3-PIE-streptavidin aptamer (kindly provided by So Umekage) was linearized for run-off transcription. The plasmid was digested with *Apa*I ON and purified by phenol/chloroform extraction and EtOH precipitation. *In vitro* transcripts were generated using T7 HiScribe RNA transcription kit (NEB), the template was digested with RQ1 DNase as described before. *In vitro* transcripts were purified by phenol/chloroform extraction and EtOH precipitation. In order to disrupt the secondary structure of the PIE ribozyme, transcripts were incubated for 2 min at 85°C and were cooled immediately on ice. Then, 10 µg of transcript was refolded in self-splicing buffer (40 mM Tris; pH 7.4, 20 mM $MgCl_2$, 5 mM DTT) in a volume of 40 µl for 10 min at RT. Self-splicing was induced by adding either 4 mM, 8 mM or 100 mM GTP (Sigma-Aldrich) and incubation at 42°C. After 1 h and 3 h aliquots of 20 µl were taken from each reaction. The self-splicing reaction was terminated by disruption of secondary structure via heat denaturation at 85°C for 2 min and immediate cooling of the sample on ice. Self-splicing products were analyzed by agarose or denaturing PAA gel electrophoresis (see **4.2.3.3** and **4.2.3.4**).

4.2.7.2 RNase R treatment of PIE-generated circRNAs

PIE-generated *in vitro* self-splicing products were phenol/chloroform purified, EtOH precipitated and were digested with 1.25 u RNase R for analytical purposes. RNAs were purified as before and 20% of the recovered RNAs were analyzed on a 10% denaturing PAA gel.

4.2.7.3 circRNA expression in *E.coli*

E.coli KRX were transformed with pcDNA3-PIE streptavidin aptamer, clones were singularized on LB agar plates and analyzed by RT-PCR (**4.2.1.2** and **4.2.3.2**). Positive clones were used to inoculate LB medium and T7 RNA polymerase was induced by adding 0.1% (1:200 dilution of 20% rhamnose) at OD_{600} of 0.7. After induction the culture was grown at 30°C for 2 h. *E.coli* were harvested by centrifugation for 10 min at 15,000 xg and 4°C, washed 2 times with 1x PBS. Bacterial pellets were frozen in liquid nitrogen and stored at 80°C.

4.2.7.4 circRNA expression in Huh7

Huh7 cells were seeded at $5x10^5$ cells in a 6 cm dish the day before transfection. The next day 6 µg of pcDNA3-PIE-streptavidin aptamer or eGFP as control were transfected using Lipofectamine 2000 (Thermo Fisher Scientific), following the manufacturer's instructions (**Table 16**). After 4 h the medium was replaced with fresh medium and cells were grown ON. The cells were harvested by using a cell scraper in 1 ml 1x PBS and pelleted by centrifugation for 2 min at

2,000 xg and 4℃. Afterwards RNA was isolated and 2 00 ng of RNA were reverse transcribed and analyzed by RT-PCR using 30 cycles.

Table 16 Lipofectamine 2000 transfection mixture.

volume (µl)	component
6	Plasmid DNA (1µg/µl)
18	Lipofectamine 2000
600	OptiMEM
624	total volume

4.2.7.5 RT-PCR analysis (PIE)

RNAs isolated from PIE circRNA expressions in *E.coli* cultures or in Huh7 cells were reverse transcribed using qScript cDNA synthesis kit (Quantabio). cDNA, which corresponded to 20 ng of RNA and primers indicated below (**Table 17**) were used in RT-PCR analysis with 30 PCR cycles and standard PCR conditions (**Table 5**). PCR products were resolved by 2% agarose gel electrophoresis.

Table 17 Primers for RT-PCR analysis.

Gene/target	fw primer sequence 5'-3'	rv primer sequence 5'-3'
PIE circular	GGGCCGGTCTAGATGTTTTC	GCACTTGCATGATTCTGGTC
PIE precursor	TTCCGGGGTAAGATTAACGA	CAGGCCTCAATTAACCCAAG
U6	CTCGCTTCGGCAGCACATA	GCTTCACGAATTTGCGTGTCA

4.2.7.6 Large scale RNA isolation from *E.coli* culture

Two 500 ml Erlenmeyer flasks with 200 ml LB medium were inoculated with pre-cultures from *E.coli* transformed with pcDNA3-streptavidin aptamer. When the cultures had reached an OD_{600} of 0.7 the expression was induced by.1% of a 1:200 dilution of 20% rhamnose. The temperature was shifted from 37℃ to 30 ℃ and after 2 h of exp ression *E.coli* was harvested using two 500 ml centrifugation tubes and centrifugation for 10 min at 15,000 xg at 4℃. The medium was discarded and bacterial pellets were suspended in 10 ml resuspension buffer (300 mM saccharose, 10 mM NaOAc pH 4.5). Then, 10 ml of Lysis buffer (2% SDS, 10 mM NaOAc pH 4.5) was added and the solutions were mixed by inverting. The lysed bacteria were transferred to 50 ml falcon tubes and incubated for 90 s in a 65℃ water bath. Afterwards , 1 volume of pre-warmed 65℃ water-saturated phenol was added and incubated for another 3 min. The tubes were frozen in liquid nitrogen and thawed at RT for a few minutes, followed by centrifugation for 10 min at 16,000 xg at RT. The aqueous phase was transferred to a fresh 50 ml falcon. Phenolization of the samples followed by centrifugation was repeated two times. Then 20 ml of chloroform/isoamylalcohol 24:1 was added,

mixed by vortexing and the tubes were centrifuged for 3 min at 16,000 xg at RT. The upper aqueous phase was transferred to a new tube and the chloroform/isoamylalcohol washing-step was repeated 2 times. The RNAs were precipitated by adding 2.5 volumes 100% EtOH and 0.1 volumes 3M NaOAc pH 4.5 for 1 h at 20℃. The RN As were pelleted by centrifugation for 20 min at 16,000 xg and 4℃, washed two times with 75% EtOH and were resuspended in 1ml RNase-free ddH_2O. Residual DNA was digested by 100 u RQ1 DNase (Promega) in 1x RQ1 DNase buffer (Promega) in a volume of 2 ml at 37℃ for 30 min. RNAs were recovered by standard phenol/chloroform extraction and EtOH precipitation. The quality of *E.coli* total RNA isolated via large scale isolation was confirmed by 1.2 % denaturing agarose gel electrophoresis (**4.2.3.4**).

4.2.7.7 Anion exchange chromatography

For enrichment of PIE-generated circRNAs anion exchange chromatography was performed using ÄKTApurifier (Amersham Biosciences), a 5 ml HiTrap Q FF column (GE Healthcare) and a linear NaCl gradient from 200-800 mM in Elution buffer (20 mM Tris; pH 7.6, 0.1 mM EDTA, and 8 mM $MgCl_2$) (Umekage & Kikuchi, 2009). For the test purification 1.6 µg of *E.coli* total RNA from uninduced cultures was mixed with 0.9 µg of RNA isolated from the *in vitro* self-splicing reaction were loaded onto the HiTrap Q FF column. For purification of PIE-generated circRNAs expressed in *E.coli*, 100 µg of total RNA were loaded onto the column. RNAs were precipitated from 700 µl fractions by adding 0.7 volumes isopropanol and centrifugation for 20 min at 25,000 xg and 4℃. 60% of the recovered RNAs per fraction were analyzed by RT-PCR using every second fraction (**4.2.3.2**).

4.2.7.8 Northern blot analysis of PIE-generated circRNA

In order to confirm the expression of PIE-generated circRNAs in *E.coli* northern blot analysis was performed. Therefore RNAs were separated by denaturing PAA gel electrophoresis (**4.2.3.5**) and transferred by semi-dry electroblotting to a nylon membrane (**4.2.3.6**). RNAs were detected by using 5'end ^{32}P labelled DNA oligos detecting the junction of the circRNA or by using a total probe, which hybridized to the streptavidin aptamer sequence (see **Table 18**). The probes were heat denatured for 2 min at 85℃ and mixed with Northern Max hybridization buffer (Ambion). The membranes were pre-hybridized and hybridized at 30°C. After washing two times with 2x northern washing buffer (2x SSC, 0.01% SDS), and two additional washing-steps with 0.5x northern washing buffer (0.5x SSC, 0.01% SDS) at RT, the signals were detected by phosphor imaging as described in (**4.2.3.6**).

Table 18 Northern probes for analysis of PIE-generated circRNAs.

Northern probe	Sequence 5'-3'
PIE junction probe	ATAAACGGTAAACCCAAGAAAAC
PIE total probe	ACACTTGCATGATTCTGGTCG

4.2.7.9 *In vitro* circRNA preparation by ligation

For *in vitro* circularization via ligation, transcription templates were generated by cleavage of the plasmids pCR2.1-bulge, pcR2.1-perfect, pCR2.1-shuffle (kindly provided by Oliver Rossbach) using *Eco*RI. The transcription templates were gel-purified by agarose gel electrophoresis and recovery via MinElute Gel Extraction Kit (Qiagen). Then 200 ng of template DNA was *in vitro* transcribed using 4-fold molar excess, which corresponds to 40 mM of GMP (Sigam) and HiScribe T7 RNA synthesis kit (NEB). Transcription was performed for 2 h at 37℃, followed by RQ1 treatment using 2 u RQ1 DNase (Promega) for 30 min at 37℃. RNAs were purified using mini Quick Spin RNA Columns (Roche). Then, the transcripts were denatured at 85℃ in the presence of 50 mM NaCl, and renatured, decreasing the temperature 1℃ every 10 s until RT was reached. Next, T4 RNA ligase buffer and RNaseOUT (Thermo Fisher Scientific) were added and incubated for 10 min at 37℃. Afterwards 200 nM ATP, 15% (v/v) DMSO and 50 u T4 RNA ligase 1 (NEB) were added, and the reaction was incubated in a volume of 250 µl at 16℃ ON. The ligation products were purified and analyzed by denaturing PAA gel electrophoresis (see **4.2.3.4**).

4.2.7.10 Gel purification of circRNAs

The circularized and linear monomers were purified from a preparative 7% denaturing PAA gel. Fragments were visualized by UV-shadowing and excised from the gel. The gel was disintegrated by centrifugation into a fresh 1.5 ml reaction tube, through a 0.2 ml reaction tube with a small hole introduced by a heated syringe needle. The smashed gel was incubated in 700 µl PK-buffer (100 mM Tris; pH7.5, 150 mM NaCl, 1% SDS, 12.5 mM EDTA) for 1 h at 50℃. The solution was centrifuged through a Costar SpinX column at 9,000 xg for 2 min at RT. RNAs were purified using phenol/chloroform extraction and EtOH precipitation.

4.2.7.11 RNase R digest of *in vitro* synthesized circRNAs

100 ng of the gel-purified RNAs were incubated in presence or absence of 1.5 u RNase R (Epicentre) in a reaction volume of 10 µl for 30 min at 37℃. 50% of the reaction were mixed with 1 volume of 2x RNA loading dye, denatured at 85℃ for 2 min and loaded on a 7% denaturing PAA gel.

4.2.7.12 Subcellular fractionation

The day before transfection, Huh7.5 cells were seeded on 6 cm dishes using 5x 10^5 cells per dish. The next day, 3 µg of circular or linear RNA were transfected using 9 µl Lipofectamine 2000 (Thermo Fisher Scientific). After approximately 16 h, cells were harvested and adjusted to the cell count. Subcellular fractionation was performed using the NE-PER Nuclear and Cytoplasmic Extraction kit (Thermo Fisher Scientific). RNAs were isolated from 75% of each sample and were subjected to denaturing PAA gel-electrophoresis and northern blot analysis (**4.2.3.6**). The transfected RNAs (*bulge*, *perfect*, *shuffle*) were detected by internally ^{32}P labelled RNA probes targeting the region, which is identical between the three constructs. Additionally, U1 snRNA was detected by internally ^{32}P labelled RNA probes. The remaining lysates were subjected to western blotting, detecting hnRNP A1 and cytoplasmic GAPDH (**4.2.4.1**).

4.2.7.13 circRNA stability assays

For RNA stability assays, 2x10^5 Huh7.5 cells were seeded in 6-well dishes the day before transfection. The next day, 100 ng/well of circular or linear RNA was transfected using 0.5 µl Lipofectamine 2000 (Thermo Fisher Scientific) per transfection mixture. After 4 h cells were washed with 1x PBS and the medium was changed. Cells were harvested by adding Trizol reagent (Thermo Fisher Scientific) at time points 4 h, 8 h, 14 h, 24 h and 32 h. RNAs were isolated and 20% of each sample was subjected to denaturing PAA gel electrophoresis and northern blot analysis using internally ^{32}P labelled RNA probes for U1 snRNA and the transfected RNAs (as described above).

Table 19 ^{32}P internally labelled RNA probes for northern blot detection.

Northern probe	sequence 5'-3'
constant region	AACUCGAUUGUGCCCUUGGACGAGACUGAACGCUAGCAGUUAGCCGAACAUACAAAUAAGCUUACCGCCC
U1 snRNA	AGGGGAAAGCGCGAACGCAGUCCCCCACUACCACAAAUUAUGCAGUCGAGUUUCCCACAUUUGGGGAAAUCG CAGGGGUCAGCACAUCCGGAGUGCAAUGGAUAAGCCUCGCCCUGGGAAAACCACCUUCGUGAUCAUGGUAUC UCCCCUGCCAGGUAAGUAU

Northern blot signals were quantified using ImageQuant TL (GE Helathcare), values were normalized to 4 h time point and fraction means of two biological replicates were plotted and fitted to *Equation 1* in order to determine τ. The half-life was calculated using Equation 2. Data and statistical analysis for half-life time measurement were performed using OriginPro 8 (OriginLab).

Equation 1: $y = A1 * exp(-x/\tau)+y0$

Equation 2: $t_{1/2} = \tau * \ln(2)$

4.2.8 Characterization of miR-122 binding sites

4.2.8.1 pmirGLO Dual-Luciferase assay

Luciferase reporter assays were performed using the pmirGLO Dual-Luciferase miRNA Target Expression Vector (Promega). Four copies the miRNA-122 binding sites *bulge*, *perfect*, *IGF1R* and corresponding seed mutants were ordered as synthesized ssDNA oligos, annealed, and cloned into the 3'UTR of the Firefly luciferase. For controls, fragments of unrelated 3'-UTRs (*KPNB1*, *HNRNPK*, and *LAPTM4A*) were cloned into the Firefly luciferase 3'UTR. $0.8x10^5$ Huh7.5 cells were seeded per 12-well the day before the transfection. The following day, 0.5 µg of plasmid DNA were transfected using 1.5 µl Lipofectamine 2000 (Thermo Fisher Scientific) per transfection mixture. The transfected cells were grown ON and analyzed in technical triplicates using beetle juice and Renilla juice (PJK) and a Centro LB 960 Microplate Luminometer (Berthold). The Firefly luciferase activity was normalized to Renilla luciferase activity and adjusted to *LAPTM4A* negative control. The transfections were performed in triplicates and means as well as standard deviations were determined.

4.2.8.2 RT-PCR analysis of pmirGLO reporter RNAs

For RT-PCR, $5x10^5$ Huh7.5 cells were seeded on 6 cm dishes and transfected with 5 µg of the reporter plasmids using 15 µl Lipofectamine 2000 (Thermo Fisher Scientific). Cells were harvested 2 days post transfection, total RNA was isolated using Trizol reagent (Thermo Fisher Scientific) and the RNeasy kit (Qiagen). To eliminate plasmid DNA contaminations, samples were additionally treated with 3 u RQ1 DNase (Promega) for 30 min at 37℃. The samples were analyzed by RT-PCR, using 0.5 µg of total RNA for cDNA synthesis via qScript cDNA Synthesis Kit (Quantabio). PCR was performed with 23 PCR cycles and PCR products were analyzed by 2% agarose gel electrophoresis.

Table 20 Primers for RT-PCR analysis.

Gene/target	fw primer sequence 5'-3'	rv primer sequence 5'-3'
FF	CCAAGAAGGGCGGCAAGAT	GCCAACTCAGCTTCCTTTCG
RN	AACTGGAGCCTGAGGAGTTC	TAGCTCCCTCGACAATAGCG
GAPDH	TGCACCACCAACTGCTTAGC	GGCATGGACTGTGGTCATGAG

4.2.8.3 *In vitro* pulldown

In vitro transcripts were generated using the HiScribe T7 RNA Synthesis Kit (NEB) and 3'end biotinylation was performed as described in (Hartmann et al, 2014). 800 fmol of 3'end biotinylated *in vitro* transcripts were bound to ON with tRNA, BSA and glycogen pre-blocked NeutrAvidin agarose beads (Thermo Fisher Scientific). The immobilized *in vitro* transcripts were mixed with extracts generated by RIPA buffer (25 mM Tris-HCl; pH 7.6, 150 mM NaCl, 1% NP-40, 1% sodium deoxycholate, 0.1% SDS) lysis of Huh7 cells. Beads and extracts were incubated for 1 h at 37℃ on a wheel. After 4 washing steps with Pulldown washing buffer (600 mM KCl, 20 mM HEPES; pH7.5), and one time with a similar washing buffer containing only 150 mM NaCl, the bound RNAs were isolated using Trizol (Thermo Fisher Scientific). Recovered RNAs were analyzed by denaturing PAA gel electrophoresis and northern blot using 1-ethyl-3-(3-dimethylaminopropyl)carbodiimide hydrochloride (EDC) crosslinking and ^{32}P-labeled DNA oligo (aCAAACACCATTGTCACACTCCA) to visualize bound miRNA-122 via autoradiography (Kim et al, 2010).

4.2.9 Sequestration of miR-122 by circRNA sponges

4.2.9.1 Synthesis of HCV-FL Reporter RNAs

Transcription templates were generated via preparative PCR in a volume of 50 µl volume using Phusion polymerase, specific primers (see **Table 21**) and pHCV-FL (Henke et al, 2008). Transcription templates were gel-purified via 1% agarose gel electrophoresis and MinElute Gel Extraction Kit (Qiagen). HCV-FL reporter RNAs were generated by *in vitro* transcription using 1 µg of gel-purified template and HiScribe T7 RNA Synthesis Kit (NEB) in a 50 µl volume for 1.5 h at 37℃. The transcription template was digested us ing RQ1 DNase (Promega) and purified using mini Quick Spin RNA Columns (Roche), followed by phenol/chloroform extraction and EtOH precipitation. For quality control, HCV-FL reporter RNAs were analyzed by 1.2% denaturing agarose gel electrophoresis (**4.2.3.4**).

Table 21 Primers for generation of HCV-FL transcription templates.

Gene/target	fw primer sequence 5'-3'	rv primer sequence 5'-3'
HCV-FL transcription template	AATTAATACGACTCACTATAGCCAG	ACATGATCTGCAGAGAGGCC

4.2.9.2 HCV-FL Luciferase assay

The day before the first transfection, $0.8x10^5$ Huh7.5 cells per 12-well were seeded, and gel-purified linear or circular RNAs (bulge, perfect, shuffle), as well as miravirsen were transfected using 0.5 µl Lipofectamine 2000 (Thermo Fisher Scientific) per transfection mixture. Cells were incubated ON and medium was changed 1 h prior to the second transfection. 150 ng/well of HCV-FL reporter RNA were transfected using 0.5 µl Lipofectamine 2000 (Thermo Fisher Scientific) per transfection mixture. After transfection, cells were incubated for 4 h, followed by lysis and measurement of Firefly luciferase activity as described above. Three wells per condition were transfected to determine the mean luciferase activity and standard deviations. A one sided t-test for unequal variances was performed to determine the level of significance compared to mock transfection.

4.2.9.3 RT-PCR analysis of HCV-FL reporter RNAs

Huh7.5 cells were transfected as described above, total RNA was isolated and RT-PCR was performed using 20 ng RNA for cDNA synthesis. PCR reactions were performed using specific primers (see **Table 22**) and 23 cycles (**4.2.3.2**).

Table 22 Primers used for RT-PCR analysis of HCV-FL reporter RNAs.

Gene/target	fw primer sequence 5'-3'	rv primer sequence 5'-3'
HCV-FL	TGAGCACGAATCCTAAACCTC	TGAGCACGAATCCTAAACCTC
GAPDH	TGCACCACCAACTGCTTAGC	GGCATGGACTGTGGTCATGAG

4.2.9.4 Huh-luc/neoNS3-3'ET luciferase assay

One day prior transfection, $1x10^5$ Huh-luc/neoNS3-3'ET cells were seeded per 12-well (Lohmann, 1999). The next day, linear and circular RNAs (*bulge*, *perfect* and *shuffle*) as well as miravirsen were transfected using 0.5 µl Lipofectamine 2000 (Thermo Fisher Scientific) per transfection mixture. After incubation for 4 h the medium was changed, and cells were lysed at time points 4 h, 12 h, 24 h, and 48 h. Luciferase activity was measured as described before. Three transfections were performed per condition, to determine means and standard deviations.

4.2.9.5 HCV infective cell culture system

HCV FL-J6/JFH-1 genomes were generated by *in vitro* transcription using T7 RNA Polymerase (NEB) from *Mlu*I-cut plasmid pFK-JFH1-J6 C-846_dg (JC1). Huh7.5 cells were seeded 2 x10^5 cells per 6-well the day before transfection. The next day 200 ng of circular RNAs, linear RNAs (*bulge*, *perfect*, *shuffle*) or miravirsen were co-transfected with 955 ng HCV FL-J6/JFH-1 using Lipofectamine 2000 (Thermo Fisher Scientific). For controls mock transfection and HCV FL-J6/JFH 1 infection only was performed. 5 days after transfection cell lysates were analyzed by western blot detecting HCV core and NS3 proteins, along with the cellular hnRNP L and GAPDH (**4.2.4.1**).

5 REFERENCES

Ahsen U von & Schroeder R (1993) RNA as a catalyst: Natural and designed ribozymes. *BioEssays* **15:** 299–307

Ambros V (2003) A uniform system for microRNA annotation. *RNA* **9:** 277–279

Ameres SL, Horwich MD, Hung J-H, Xu J, Ghildiyal M, Weng Z & Zamore PD (2010) Target RNA-directed trimming and tailing of small silencing RNAs. *Science* **328:** 1534–1539

Ashwal-Fluss R, Meyer M, Pamudurti NR, Ivanov A, Bartok O, Hanan M, Evantal N, Memczak S, Rajewsky N & Kadener S (2014) circRNA biogenesis competes with pre-mRNA splicing. *Molecular cell* **56:** 55–66

Ast G (2004) How did alternative splicing evolve? *Nature reviews. Genetics* **5:** 773–782

Azuma-Mukai A, Oguri H, Mituyama T, Qian ZR, Asai K, Siomi H & Siomi MC (2008) Characterization of endogenous human Argonautes and their miRNA partners in RNA silencing. *Proceedings of the National Academy of Sciences of the United States of America* **105:** 7964–7969

Bai S, Nasser MW, Wang B, Hsu S-H, Datta J, Kutay H, Yadav A, Nuovo G, Kumar P & Ghoshal K (2009) MicroRNA-122 inhibits tumorigenic properties of hepatocellular carcinoma cells and sensitizes these cells to sorafenib. *The Journal of biological chemistry* **284:** 32015–32027

Barreau C, Dutertre S, Paillard L & Osborne HB (2006) Liposome-mediated RNA transfection should be used with caution. *RNA* **12:** 1790–1793

Barrett SP, Wang PL & Salzman J (2015) Circular RNA biogenesis can proceed through an exon-containing lariat precursor. *eLife* **4:** e07540

Bartel DP (2004) MicroRNAs: Genomics, biogenesis, mechanism, and function. *Cell* **116:** 281–297

Bartel DP (2009) MicroRNAs: Target recognition and regulatory functions. *Cell* **136:** 215–233

Bartenschlager R, Penin F, Lohmann V & André P (2011) Assembly of infectious hepatitis C virus particles. *Trends in microbiology* **19:** 95–103

Behrens SE, Tomei L & Francesco R de (1996) Identification and properties of the RNA-dependent RNA polymerase of hepatitis C virus. *The EMBO journal* **15:** 12–22

Bentley DL (2014) Coupling mRNA processing with transcription in time and space. *Nature reviews. Genetics* **15:** 163–175

Berezhna SY, Supekova L, Sever MJ, Schultz PG & Deniz AA (2011) Dual regulation of hepatitis C viral RNA by cellular RNAi requires partitioning of Ago2 to lipid droplets and P-bodies. *RNA* **17:** 1831–1845

Boeckel J-N, Jaé N, Heumüller AW, Chen W, Boon RA, Stellos K, Zeiher AM, John D, Uchida S & Dimmeler S (2015) Identification and Characterization of Hypoxia-Regulated Endothelial Circular RNA. *Circulation research* **117:** 884–890

Braun S, Domdey H & Wiebauer K (1996) Inverse splicing of a discontinuous pre-mRNA intron generates a circular exon in a HeLa cell nuclear extract. *Nucleic acids research* **24:** 4152–4157

Breiman A, Grandvaux N, Lin R, Ottone C, Akira S, Yoneyama M, Fujita T, Hiscott J & Meurs EF (2005) Inhibition of RIG-I-dependent signaling to the interferon pathway during hepatitis C virus expression and restoration of signaling by IKKepsilon. *Journal of virology* **79:** 3969–3978

Buck AH, Perot J, Chisholm MA, Kumar DS, Tuddenham L, Cognat V, Marcinowski L, Dölken L & Pfeffer S (2010) Post-transcriptional regulation of miR-27 in murine cytomegalovirus infection. *RNA* **16:** 307–315

Burd CE, Jeck WR, Liu Y, Sanoff HK, Wang Z & Sharpless NE (2010) Expression of linear and novel circular forms of an INK4/ARF-associated non-coding RNA correlates with atherosclerosis risk. *PLoS genetics* **6:** e1001233

Burroughs AM, Ando Y, Hoon MJL de, Tomaru Y, Nishibu T, Ukekawa R, Funakoshi T, Kurokawa T, Suzuki H, Hayashizaki Y & Daub CO (2010) A comprehensive survey of 3' animal miRNA modification events and a possible role for 3' adenylation in modulating miRNA targeting effectiveness. *Genome research* **20:** 1398–1410

Burstow NJ, Mohamed Z, Gomaa AI, Sonderup MW, Cook NA, Waked I, Spearman CW & Taylor-Robinson SD (2017) Hepatitis C treatment: Where are we now? *International journal of general medicine* **10:** 39–52

Capel B, Swain A, Nicolis S, Hacker A, Walter M, Koopman P, Goodfellow P & Lovell-Badge R (1993) Circular transcripts of the testis-determining gene Sry in adult mouse testis. *Cell* **73:** 1019–1030

Cesana M, Cacchiarelli D, Legnini I, Santini T, Sthandier O, Chinappi M, Tramontano A & Bozzoni I (2011) A long noncoding RNA controls muscle differentiation by functioning as a competing endogenous RNA. *Cell* **147:** 358–369

Chen L-L & Yang L (2015) Regulation of circRNA biogenesis. *RNA biology* **12:** 381–388

Chen YG, Kim MV, Chen X, Batista PJ, Aoyama S, Wilusz JE, Iwasaki A & Chang HY (2017) Sensing Self and Foreign Circular RNAs by Intron Identity. *Molecular cell* **67:** 228-238.e5

Chi SW, Zang JB, Mele A & Darnell RB (2009) Argonaute HITS-CLIP decodes microRNA-mRNA interaction maps. *Nature* **460:** 479–486

Chou CH, Chang NW, Shrestha S, Hsu SD, Lin YL, Lee WH, Yang CD, Hong HC, Wei TY, Tu SJ, Tsai TR, Ho SY, Jian TY, Wu HY, Chen PR, Lin NC, Huang HT, Yang TL, Pai CY & Tai CS (2016) miRTarBase 2016: Updates to the experimentally validated miRNA-target interactions database. *Nucleic acids research* **44:** D239-47

Cocquerelle C, Daubersies P, Majérus MA, Kerckaert JP & Bailleul B (1992) Splicing with inverted order of exons occurs proximal to large introns. *The EMBO journal* **11:** 1095–1098

Cocquerelle C, Mascrez B, Hétuin D & Bailleul B (1993) Mis-splicing yields circular RNA molecules. *FASEB journal* **7:** 155–160

Conn SJ, Pillman KA, Toubia J, Conn VM, Salmanidis M, Phillips CA, Roslan S, Schreiber AW, Gregory PA & Goodall GJ (2015) The RNA binding protein quaking regulates formation of circRNAs. *Cell* **160:** 1125–1134

Conrad KD, Giering F, Erfurth C, Neumann A, Fehr C, Meister G & Niepmann M (2013) MicroRNA-122 dependent binding of Ago2 protein to hepatitis C virus RNA is associated with enhanced RNA stability and translation stimulation. *PloS one* **8:** e56272

Conrad KD & Niepmann M (2014) The role of microRNAs in hepatitis C virus RNA replication. *Archives of virology* **159:** 849–862

Corvelo A, Hallegger M, Smith CWJ & Eyras E (2010) Genome-wide association between branch point properties and alternative splicing. *PLoS computational biology* **6:** e1001016

Crick F (1970) Central dogma of molecular biology. *Nature* **227:** 561–563

Daguenet E, Dujardin G & Valcárcel J (2015) The pathogenicity of splicing defects: Mechanistic insights into pre-mRNA processing inform novel therapeutic approaches. *EMBO reports* **16:** 1640–1655

Darmostuk M, Rimpelova S, Gbelcova H & Ruml T (2015) Current approaches in SELEX: An update to aptamer selection technology. *Biotechnology advances* **33:** 1141–1161

Daugaard I & Hansen TB (2017) Biogenesis and Function of Ago-Associated RNAs. *Trends in genetics* **33:** 208–219

De N, Young L, Lau P-W, Meisner N-C, Morrissey DV & MacRae IJ (2013) Highly complementary target RNAs promote release of guide RNAs from human Argonaute2. *Molecular cell* **50:** 344–355

Denzler R, Agarwal V, Stefano J, Bartel DP & Stoffel M (2014) Assessing the ceRNA hypothesis with quantitative measurements of miRNA and target abundance. *Molecular cell* **54:** 766–776

Desmet F-O, Hamroun D, Lalande M, Collod-Béroud G, Claustres M & Béroud C (2009) Human Splicing Finder: An online bioinformatics tool to predict splicing signals. *Nucleic acids research* **37:** e67

Díaz-Toledano R, Ariza-Mateos A, Birk A, Martínez-García B & Gómez J (2009) In vitro characterization of a miR-122-sensitive double-helical switch element in the 5' region of hepatitis C virus RNA. *Nucleic acids research* **37:** 5498–5510

Dubuisson J & Cosset F-L (2014) Virology and cell biology of the hepatitis C virus life cycle: An update. *Journal of hepatology* **61:** 3-13

Durbin AF, Wang C, Marcotrigiano J & Gehrke L (2016) RNAs Containing Modified Nucleotides Fail To Trigger RIG-I Conformational Changes for Innate Immune Signaling. *mBio* **7**

Ebbesen KK, Hansen TB & Kjems J (2016) Insights into circular RNA biology. *RNA biology:* 1–11

Ebert MS & Sharp PA (2010) Emerging roles for natural microRNA sponges. *Current biology* **20:** R858-61

Egger D, Wolk B, Gosert R, Bianchi L, Blum HE, Moradpour D & Bienz K (2002) Expression of Hepatitis C Virus Proteins Induces Distinct Membrane Alterations Including a Candidate Viral Replication Complex. *Journal of virology* **76:** 5974–5984

Eksioglu EA, Zhu H, Bayouth L, Bess J, Liu H-Y, Nelson DR & Liu C (2011) Characterization of HCV interactions with Toll-like receptors and RIG-I in liver cells. *PloS one* **6:** e21186

Fairbrother WG, Yeh R-F, Sharp PA & Burge CB (2002) Predictive identification of exonic splicing enhancers in human genes. *Science* **297:** 1007–1013

Fica SM, Mefford MA, Piccirilli JA & Staley JP (2014) Evidence for a group II intron-like catalytic triplex in the spliceosome. *Nature structural & molecular biology* **21:** 464–471

Fica SM, Tuttle N, Novak T, Li N-S, Lu J, Koodathingal P, Dai Q, Staley JP & Piccirilli JA (2013) RNA catalyses nuclear pre-mRNA splicing. *Nature* **503:** 229–234

Fontanes V, Raychaudhuri S & Dasgupta A (2009) A cell-permeable peptide inhibits hepatitis C virus replication by sequestering IRES transacting factors. *Virology* **394:** 82–90

Ford E & Ares M (1994) Synthesis of circular RNA in bacteria and yeast using RNA cyclase ribozymes derived from a group I intron of phage T4. *Proceedings of the National Academy of Sciences of the United States of America* **91:** 3117–3121

Fu X-D & Ares M (2014) Context-dependent control of alternative splicing by RNA-binding proteins. *Nature reviews. Genetics* **15:** 689–701

Gebert LFR, Rebhan MAE, Crivelli SEM, Denzler R, Stoffel M & Hall J (2014) Miravirsen (SPC3649) can inhibit the biogenesis of miR-122. *Nucleic acids research* **42:** 609–621

Gerresheim GK, Dünnes N, Nieder-Röhrmann A, Shalamova LA, Fricke M, Hofacker I, Höner Zu Siederdissen C, Marz M & Niepmann M (2017) microRNA-122 target sites in the hepatitis C virus RNA NS5B coding region and 3' untranslated region: Function in replication and influence of RNA secondary structure. *Cellular and molecular life sciences* **74:** 747–760

Glažar P, Papavasileiou P & Rajewsky N (2014) circBase: A database for circular RNAs. *RNA* **20:** 1666–1670

Gruner H, Cortés-López M, Cooper DA, Bauer M & Miura P (2016) CircRNA accumulation in the aging mouse brain. *Scientific reports* **6:** 38907

Grünweller A, Wyszko E, Bieber B, Jahnel R, Erdmann VA & Kurreck J (2003) Comparison of different antisense strategies in mammalian cells using locked nucleic acids, 2'-O-methyl RNA, phosphorothioates and small interfering RNA. *Nucleic acids research* **31:** 3185–3193

Guo JU, Agarwal V, Guo H & Bartel DP (2014) Expanded identification and characterization of mammalian circular RNAs. *Genome biology* **15:** 409

Ha M & Kim VN (2014) Regulation of microRNA biogenesis. *Nature reviews. Molecular cell biology* **15:** 509–524

Han D, Li J, Wang H, Su X, Hou J, Gu Y, Qian C, Lin Y, Liu X, Huang M, Li N, Zhou W, Yu Y & Cao X (2017) Circular RNA circMTO1 acts as the sponge of microRNA-9 to suppress hepatocellular carcinoma progression. *Hepatology* **66:** 1151–1164

Hansen TB, Jensen TI, Clausen BH, Bramsen JB, Finsen B, Damgaard CK & Kjems J (2013a) Natural RNA circles function as efficient microRNA sponges. *Nature* **495:** 384–388

Hansen TB, Kjems J & Damgaard CK (2013b) Circular RNA and miR-7 in cancer. *Cancer research* **73:** 5609–5612

Hansen TB, Wiklund ED, Bramsen JB, Villadsen SB, Statham AL, Clark SJ & Kjems J (2011) miRNA-dependent gene silencing involving Ago2-mediated cleavage of a circular antisense RNA. *The EMBO journal* **30:** 4414–4422

Hartmann RK, Bindereif A, Schön A & Westhof E (2014) *Handbook of RNA Biochemistry.* Wiley-VCH Verlag GmbH & Co. KGaA, Weinheim, Germany

He R, Liu P, Xie X, Zhou Y, Liao Q, Xiong W, Li X, Li G, Zeng Z & Tang H (2017) circGFRA1 and GFRA1 act as ceRNAs in triple negative breast cancer by regulating miR-34a. *Journal of experimental & clinical cancer research* **36:** 145

Helwak A & Tollervey D (2014) Mapping the miRNA interactome by cross-linking ligation and sequencing of hybrids (CLASH). *Nature protocols* **9:** 711–728

Henke JI, Goergen D, Zheng J, Song Y, Schüttler CG, Fehr C, Jünemann C & Niepmann M (2008) microRNA-122 stimulates translation of hepatitis C virus RNA. *The EMBO journal* **27:** 3300–3310

Hentze MW & Preiss T (2013) Circular RNAs: Splicing's enigma variations. *The EMBO journal* **32:** 923–925

Hossain MA & Johnson TL (2014) Using yeast genetics to study splicing mechanisms. *Methods in molecular biology* **1126:** 285–298

Houseley J & Tollervey D (2009) The many pathways of RNA degradation. *Cell* **136:** 763–776

Hsu S-H, Wang B, Kota J, Yu J, Costinean S, Kutay H, Yu L, Bai S, La Perle K, Chivukula RR, Mao H, Wei M, Clark KR, Mendell JR, Caligiuri MA, Jacob ST, Mendell JT & Ghoshal K (2012) Essential metabolic, anti-inflammatory, and anti-tumorigenic functions of miR-122 in liver. *The Journal of clinical investigation* **122:** 2871–2883

Huang Y (2017) Preclinical and Clinical Advances of GalNAc-Decorated Nucleic Acid Therapeutics. *Molecular therapy. Nucleic acids* **6:** 116–132

Hussain S, Barretto N & Uprichard SL (2012) New hepatitis C virus drug discovery strategies and model systems. *Expert opinion on drug discovery* **7:** 849–859

Ishida M & Selaru FM (2013) miRNA-Based Therapeutic Strategies. *Current anesthesiology reports* **1:** 63–70

Ivanov A, Memczak S, Wyler E, Torti F, Porath HT, Orejuela MR, Piechotta M, Levanon EY, Landthaler M, Dieterich C & Rajewsky N (2015) Analysis of intron sequences reveals hallmarks of circular RNA biogenesis in animals. *Cell reports* **10:** 170–177

Janssen HLA, Reesink HW, Lawitz EJ, Zeuzem S, Rodriguez-Torres M, Patel K, van der Meer AJ, Patick AK, Chen A, Zhou Y, Persson R, King BD, Kauppinen S, Levin AA & Hodges MR (2013) Treatment of HCV infection by targeting microRNA. *The New England journal of medicine* **368:** 1685–1694

Jeck WR & Sharpless NE (2014) Detecting and characterizing circular RNAs. *Nature biotechnology* **32:** 453–461

Jeck WR, Sorrentino JA, Wang K, Slevin MK, Burd CE, Liu J, Marzluff WF & Sharpless NE (2013) Circular RNAs are abundant, conserved, and associated with ALU repeats. *RNA* **19:** 141–157

Jinek M & Doudna JA (2009) A three-dimensional view of the molecular machinery of RNA interference. *Nature* **457:** 405–412

Jonas S & Izaurralde E (2015) Towards a molecular understanding of microRNA-mediated gene silencing. *Nature reviews. Genetics* **16:** 421–433

Jopling CL, Norman KL & Sarnow P (2006) Positive and negative modulation of viral and cellular mRNAs by liver-specific microRNA miR-122. *Cold Spring Harbor symposia on quantitative biology* **71:** 369–376

Jopling CL, Schütz S & Sarnow P (2008) Position-dependent function for a tandem microRNA miR-122-binding site located in the hepatitis C virus RNA genome. *Cell host & microbe* **4:** 77–85

Jopling CL, Yi M, Lancaster AM, Lemon SM & Sarnow P (2005) Modulation of hepatitis C virus RNA abundance by a liver-specific MicroRNA. *Science* **309:** 1577–1581

Jurica MS & Moore MJ (2003) Pre-mRNA splicing: Awash in a sea of proteins. *Molecular cell* **12:** 5–14

Kambach C, Walke S, Young R, Avis JM, La Fortelle E de, Raker VA, Lührmann R, Li J & Nagai K (1999) Crystal structures of two Sm protein complexes and their implications for the assembly of the spliceosomal snRNPs. *Cell* **96:** 375–387

Karikó K, Buckstein M, Ni H & Weissman D (2005) Suppression of RNA recognition by Toll-like receptors: The impact of nucleoside modification and the evolutionary origin of RNA. *Immunity* **23:** 165–175

Kartha RV & Subramanian S (2014) Competing endogenous RNAs (ceRNAs): New entrants to the intricacies of gene regulation. *Frontiers in genetics* **5:** 8

Katoh T, Sakaguchi Y, Miyauchi K, Suzuki T, Kashiwabara S-I, Baba T & Suzuki T (2009) Selective stabilization of mammalian microRNAs by 3' adenylation mediated by the cytoplasmic poly(A) polymerase GLD-2. *Genes & development* **23:** 433–438

Kaukinen P, Sillanpää M, Nousiainen L, Melén K & Julkunen I (2013) Hepatitis C virus NS2 protease inhibits host cell antiviral response by inhibiting IKKε and TBK1 functions. *Journal of medical virology* **85:** 71–82

Khan MAF, Reckman YJ, Aufiero S, van den Hoogenhof MMG, van der Made I, Beqqali A, Koolbergen DR, Rasmussen TB, van der Velden J, Creemers EE & Pinto YM (2016) RBM20 Regulates Circular RNA Production From the Titin Gene. *Circulation research* **119:** 996–1003

Kim G-W, Lee S-H, Cho H, Kim M, Shin E-C & Oh J-W (2016) Hepatitis C Virus Core Protein Promotes miR-122 Destabilization by Inhibiting GLD-2. *PLoS pathogens* **12:** e1005714

Kim SW, Li Z, Moore PS, Monaghan AP, Chang Y, Nichols M & John B (2010) A sensitive non-radioactive northern blot method to detect small RNAs. *Nucleic acids research* **38:** e98

Knockenhauer KE & Schwartz TU (2016) The Nuclear Pore Complex as a Flexible and Dynamic Gate. *Cell* **164:** 1162–1171

König J, Zarnack K, Rot G, Curk T, Kayikci M, Zupan B, Turner DJ, Luscombe NM & Ule J (2010) iCLIP reveals the function of hnRNP particles in splicing at individual nucleotide resolution. *Nature structural & molecular biology* **17:** 909–915

Kramer MC, Liang D, Tatomer DC, Gold B, March ZM, Cherry S & Wilusz JE (2015) Combinatorial control of Drosophila circular RNA expression by intronic repeats, hnRNPs, and SR proteins. *Genes & development* **29:** 2168–2182

La Mata M de, Alonso CR, Kadener S, Fededa JP, Blaustein M, Pelisch F, Cramer P, Bentley D & Kornblihtt AR (2003) A slow RNA polymerase II affects alternative splicing in vivo. *Molecular cell* **12:** 525–532

La Mata M de, Gaidatzis D, Vitanescu M, Stadler MB, Wentzel C, Scheiffele P, Filipowicz W & Großhans H (2015) Potent degradation of neuronal miRNAs induced by highly complementary targets. *EMBO reports* **16:** 500–511

Laemmli UK (1970) Cleavage of structural proteins during the assembly of the head of bacteriophage T4. *Nature* **227:** 680–685

Lanford RE, Hildebrandt-Eriksen ES, Petri A, Persson R, Lindow M, Munk ME, Kauppinen S & Ørum H (2010) Therapeutic silencing of microRNA-122 in primates with chronic hepatitis C virus infection. *Science* **327:** 198–201

Lasda E & Parker R (2014) Circular RNAs: Diversity of form and function. *RNA* **20:** 1829–1842

Legnini I, Di Timoteo G, Rossi F, Morlando M, Briganti F, Sthandier O, Fatica A, Santini T, Andronache A, Wade M, Laneve P, Rajewsky N & Bozzoni I (2017) Circ-ZNF609 Is a Circular RNA that Can Be Translated and Functions in Myogenesis. *Molecular cell* **66:** 22-37.e9

Leisegang MS, Martin R, Ramírez AS & Bohnsack MT (2012) Exportin t and Exportin 5: TRNA and miRNA biogenesis - and beyond. *Biological chemistry* **393:** 599–604

Li X, Liu C-X, Xue W, Zhang Y, Jiang S, Yin Q-F, Wei J, Yao R-W, Yang L & Chen L-L (2017) Coordinated circRNA Biogenesis and Function with NF90/NF110 in Viral Infection. *Molecular cell* **67:** 214-227.e7

Li Y, Yamane D & Lemon SM (2015) Dissecting the roles of the 5' exoribonucleases Xrn1 and Xrn2 in restricting hepatitis C virus replication. *Journal of virology* **89:** 4857–4865

Liang D & Wilusz JE (2014) Short intronic repeat sequences facilitate circular RNA production. *Genes & development* **28:** 2233–2247

Lim LP & Burge CB (2001) A computational analysis of sequence features involved in recognition of short introns. *Proceedings of the National Academy of Sciences of the United States of America* **98:** 11193–11198

Lohmann V (1999) Replication of Subgenomic Hepatitis C Virus RNAs in a Hepatoma Cell Line. *Science* **285:** 110–113

Lohmann V & Bartenschlager R (2014) On the history of hepatitis C virus cell culture systems. *Journal of medicinal chemistry* **57:** 1627–1642

Lohmann V, Körner F, Herian U & Bartenschlager R (1997) Biochemical properties of hepatitis C virus NS5B RNA-dependent RNA polymerase and identification of amino acid sequence motifs essential for enzymatic activity. *Journal of virology* **71:** 8416–8428

Lorenz R, Bernhart SH, Höner Zu Siederdissen C, Tafer H, Flamm C, Stadler PF & Hofacker IL (2011) ViennaRNA Package 2.0. *Algorithms for molecular biology* **6:** 26

Lu T, Cui L, Zhou Y, Zhu C, Fan D, Gong H, Zhao Q, Zhou C, Zhao Y, Lu D, Luo J, Wang Y, Tian Q, Feng Q, Huang T & Han B (2015a) Transcriptome-wide investigation of circular RNAs in rice. *RNA* **21:** 2076–2087

Lu Z, Filonov GS, Noto JJ, Schmidt CA, Hatkevich TL, Wen Y, Jaffrey SR & Matera AG (2015b) Metazoan tRNA introns generate stable circular RNAs in vivo. *RNA* **21:** 1554–1565

Luedde T & Schwabe RF (2011) NF-κB in the liver--linking injury, fibrosis and hepatocellular carcinoma. *Nature reviews. Gastroenterology & hepatology* **8:** 108–118

Luna JM, Barajas JM, Teng K-Y, Sun H-L, Moore MJ, Rice CM, Darnell RB & Ghoshal K (2017) Argonaute CLIP Defines a Deregulated miR-122-Bound Transcriptome that Correlates with Patient Survival in Human Liver Cancer. *Molecular cell* **67:** 400-410.e7

Luna JM, Scheel TKH, Danino T, Shaw KS, Mele A, Fak JJ, Nishiuchi E, Takacs CN, Catanese MT, Jong YP de, Jacobson IM, Rice CM & Darnell RB (2015) Hepatitis C virus RNA functionally sequesters miR-122. *Cell* **160:** 1099–1110

Ma L, Reinhardt F, Pan E, Soutschek J, Bhat B, Marcusson EG, Teruya-Feldstein J, Bell GW & Weinberg RA (2010) Therapeutic silencing of miR-10b inhibits metastasis in a mouse mammary tumor model. *Nature biotechnology* **28:** 341–347

Maass PG, Glažar P, Memczak S, Dittmar G, Hollfinger I, Schreyer L, Sauer AV, Toka O, Aiuti A, Luft FC & Rajewsky N (2017) A map of human circular RNAs in clinically relevant tissues. *Journal of molecular medicine* **11**:1179-1189

Marcinowski L, Tanguy M, Krmpotic A, Rädle B, Lisnić VJ, Tuddenham L, Chane-Woon-Ming B, Ruzsics Z, Erhard F, Benkartek C, Babic M, Zimmer R, Trgovcich J, Koszinowski UH, Jonjic S, Pfeffer S & Dölken L (2012) Degradation of cellular mir-27 by a novel, highly abundant viral transcript is important for efficient virus replication in vivo. *PLoS pathogens* **8:** e1002510

Matlin AJ, Clark F & Smith CWJ (2005) Understanding alternative splicing: Towards a cellular code. *Nature reviews. Molecular cell biology* **6:** 386–398

Memczak S, Jens M, Elefsinioti A, Torti F, Krueger J, Rybak A, Maier L, Mackowiak SD, Gregersen LH, Munschauer M, Loewer A, Ziebold U, Landthaler M, Kocks C, Le Noble F & Rajewsky N (2013) Circular RNAs are a large class of animal RNAs with regulatory potency. *Nature* **495:** 333–338

Memczak S, Papavasileiou P, Peters O & Rajewsky N (2015) Identification and Characterization of Circular RNAs As a New Class of Putative Biomarkers in Human Blood. *PloS one* **10:** e0141214

Moore MJ & Proudfoot NJ (2009) Pre-mRNA processing reaches back to transcription and ahead to translation. *Cell* **136:** 688–700

Moore MJ, Scheel TKH, Luna JM, Park CY, Fak JJ, Nishiuchi E, Rice CM & Darnell RB (2015) miRNA-target chimeras reveal miRNA 3'-end pairing as a major determinant of Argonaute target specificity. *Nature communications* **6:** 8864

Moore MJ & Sharp PA (1993) Evidence for two active sites in the spliceosome provided by stereochemistry of pre-mRNA splicing. *Nature* **365:** 364–368

Mortimer SA & Doudna JA (2013) Unconventional miR-122 binding stabilizes the HCV genome by forming a trimolecular RNA structure. *Nucleic acids research* **41:** 4230–4240

Nguyen THD, Galej WP, Fica SM, Lin P-C, Newman AJ & Nagai K (2016) CryoEM structures of two spliceosomal complexes: Starter and dessert at the spliceosome feast. *Current opinion in structural biology* **36:** 48–57

Nieder-Röhrmann A, Dünnes N, Gerresheim GK, Shalamova LA, Herchenröther A & Niepmann M (2017) Cooperative enhancement of translation by two adjacent microRNA-122/Argonaute 2 complexes binding to the 5' untranslated region of hepatitis C virus RNA. *The Journal of general virology* **98:** 212–224

Niepmann M (2013) Hepatitis C virus RNA translation. *Current topics in microbiology and immunology* **369:** 143–166

Nigro JM, Cho KR, Fearon ER, Kern SE, Ruppert JM, Oliner JD, Kinzler KW & Vogelstein B (1991) Scrambled exons. *Cell* **64:** 607–613

Nitta S, Sakamoto N, Nakagawa M, Kakinuma S, Mishima K, Kusano-Kitazume A, Kiyohashi K, Murakawa M, Nishimura-Sakurai Y, Azuma S, Tasaka-Fujita M, Asahina Y, Yoneyama M, Fujita T & Watanabe M (2013) Hepatitis C virus NS4B protein targets STING and abrogates RIG-I-mediated type I interferon-dependent innate immunity. *Hepatology* **57:** 46–58

O'Brien K, Matlin AJ, Lowell AM & Moore MJ (2008) The biflavonoid isoginkgetin is a general inhibitor of Pre-mRNA splicing. *The Journal of biological chemistry* **283:** 33147–33154

Orr-Burks NL, Shim B-S, Wu W, Bakre AA, Karpilow J & Tripp RA (2017) MicroRNA screening identifies miR-134 as a regulator of poliovirus and enterovirus 71 infection. *Scientific data* **4:** 170023

Otsuka M, Kato N, Moriyama M, Taniguchi H, Wang Y, Dharel N, Kawabe T & Omata M (2005) Interaction between the HCV NS3 protein and the host TBK1 protein leads to inhibition of cellular antiviral responses. *Hepatology* **41:** 1004–1012

Pamudurti NR, Bartok O, Jens M, Ashwal-Fluss R, Stottmeister C, Ruhe L, Hanan M, Wyler E, Perez-Hernandez D, Ramberger E, Shenzis S, Samson M, Dittmar G, Landthaler M, Chekulaeva M, Rajewsky N & Kadener S (2017) Translation of CircRNAs. *Molecular cell* **66:** 9-21.e7

Pan T (2000) Probing RNA structure and function, by circular permutation. *Methods in enzymology* **317:** 313–330

Pasman Z, Been MD & Garcia-Blanco MA (1996) Exon circularization in mammalian nuclear extracts. *RNA* **2:** 603–610

Pasquinelli AE (2012) MicroRNAs and their targets: Recognition, regulation and an emerging reciprocal relationship. *Nature reviews. Genetics* **13:** 271–282

Patel AA & Steitz JA (2003) Splicing double: Insights from the second spliceosome. *Nature reviews. Molecular cell biology* **4:** 960–970

Paul D, Madan V & Bartenschlager R (2014) Hepatitis C virus RNA replication and assembly: Living on the fat of the land. *Cell host & microbe* **16:** 569–579

Perron MP & Provost P (2008) Protein interactions and complexes in human microRNA biogenesis and function. *Frontiers in bioscience* **13:** 2537–2547

Petkovic S & Müller S (2015) RNA circularization strategies in vivo and in vitro. *Nucleic acids research* **43:** 2454–2465

Piva R, Spandidos DA & Gambari R (2013) From microRNA functions to microRNA therapeutics: Novel targets and novel drugs in breast cancer research and treatment (Review). *International journal of oncology* **43:** 985–994

Piwecka M, Glažar P, Hernandez-Miranda LR, Memczak S, Wolf SA, Rybak-Wolf A, Filipchyk A, Klironomos F, Cerda Jara CA, Fenske P, Trimbuch T, Zywitza V, Plass M, Schreyer L, Ayoub S, Kocks C, Kühn R, Rosenmund C, Birchmeier C & Rajewsky N (2017) Loss of a mammalian circular RNA locus causes miRNA deregulation and affects brain function. *Science* **357:** 6357-6368

Poliseno L, Salmena L, Zhang J, Carver B, Haveman WJ & Pandolfi PP (2010) A coding-independent function of gene and pseudogene mRNAs regulates tumour biology. *Nature* **465:** 1033–1038

Popescu C-I, Riva L, Vlaicu O, Farhat R, Rouillé Y & Dubuisson J (2014) Hepatitis C virus life cycle and lipid metabolism. *Biology* **3:** 892–921

Popescu C-I, Rouillé Y & Dubuisson J (2011) Hepatitis C virus assembly imaging. *Viruses* **3:** 2238–2254

Puttaraju M & Been MD (1992) Group I permuted intron-exon (PIE) sequences self-splice to produce circular exons. *Nucleic acids research* **20:** 5357–5364

Roberts APE, Lewis AP & Jopling CL (2011) miR-122 activates hepatitis C virus translation by a specialized mechanism requiring particular RNA components. *Nucleic acids research* **39:** 7716–7729

Romero-Brey I, Merz A, Chiramel A, Lee J-Y, Chlanda P, Haselman U, Santarella-Mellwig R, Habermann A, Hoppe S, Kallis S, Walther P, Antony C, Krijnse-Locker J & Bartenschlager R (2012) Three-dimensional architecture and biogenesis of membrane structures associated with hepatitis C virus replication. *PLoS pathogens* **8:** e1003056

Rossbach O, Hung L-H, Khrameeva E, Schreiner S, König J, Curk T, Zupan B, Ule J, Gelfand MS & Bindereif A (2014) Crosslinking-immunoprecipitation (iCLIP) analysis reveals global regulatory roles of hnRNP L. *RNA biology* **11:** 146–155

Rossbach O, Hung L-H, Schreiner S, Grishina I, Heiner M, Hui J & Bindereif A (2009) Auto- and cross-regulation of the hnRNP L proteins by alternative splicing. *Molecular and cellular biology* **29:** 1442–1451

Rybak-Wolf A, Stottmeister C, Glažar P, Jens M, Pino N, Giusti S, Hanan M, Behm M, Bartok O, Ashwal-Fluss R, Herzog M, Schreyer L, Papavasileiou P, Ivanov A, Öhman M, Refojo D, Kadener S & Rajewsky N (2015) Circular RNAs in the Mammalian Brain Are Highly Abundant, Conserved, and Dynamically Expressed. *Molecular cell* **58:** 870–885

Salgia SR (2003) Two reactions of Haloferax volcanii RNA splicing enzymes: Joining of exons and circularization of introns. *RNA* **9:** 319–330

Salmena L, Poliseno L, Tay Y, Kats L & Pandolfi PP (2011) A ceRNA hypothesis: The Rosetta Stone of a hidden RNA language? *Cell* **146:** 353–358

Salzman J, Chen RE, Olsen MN, Wang PL & Brown PO (2013) Cell-type specific features of circular RNA expression. *PLoS genetics* **9:** e1003777

Salzman J, Gawad C, Wang PL, Lacayo N & Brown PO (2012) Circular RNAs are the predominant transcript isoform from hundreds of human genes in diverse cell types. *PloS one* **7:** e30733

Sambrook J & Russell DW (2001) *Molecular cloning: A laboratory manual.* Cold Spring Harbor Laboratory Press, Cold Spring Harbor, N.Y

Sanger HL, Klotz G, Riesner D, Gross HJ & Kleinschmidt AK (1976) Viroids are single-stranded covalently closed circular RNA molecules existing as highly base-paired rod-like structures. *Proceedings of the National Academy of Sciences of the United States of America* **73:** 3852–3856

Sarnow P & Sagan SM (2016) Unraveling the Mysterious Interactions Between Hepatitis C Virus RNA and Liver-Specific MicroRNA-122. *Annual review of virology* **3:** 309–332

Sayed D & Abdellatif M (2011) MicroRNAs in development and disease. *Physiological reviews* **91:** 827–887

Scheel TKH, Luna JM, Liniger M, Nishiuchi E, Rozen-Gagnon K, Shlomai A, Auray G, Gerber M, Fak J, Keller I, Bruggmann R, Darnell RB, Ruggli N & Rice CM (2016) A Broad RNA Virus Survey Reveals Both miRNA Dependence and Functional Sequestration. *Cell host & microbe* **19:** 409–423

Scheel TKH & Rice CM (2013) Understanding the hepatitis C virus life cycle paves the way for highly effective therapies. *Nature medicine* **19:** 837–849

Schirle NT, Sheu-Gruttadauria J & MacRae IJ (2014) Structural basis for microRNA targeting. *Science* **346:** 608–613

Schmidt CA, Noto JJ, Filonov GS & Matera AG (2016) A Method for Expressing and Imaging Abundant, Stable, Circular RNAs In Vivo Using tRNA Splicing. *Methods in enzymology* **572:** 215–236

Schneider T, Hung L-H, Schreiner S, Starke S, Eckhof H, Rossbach O, Reich S, Medenbach J & Bindereif A (2016) CircRNA-protein complexes: IMP3 protein component defines subfamily of circRNPs. *Scientific reports* **6:** 31313

Sedano CD & Sarnow P (2014) Hepatitis C virus subverts liver-specific miR-122 to protect the viral genome from exoribonuclease Xrn2. *Cell host & microbe* **16:** 257–264

Selbach M, Schwanhäusser B, Thierfelder N, Fang Z, Khanin R & Rajewsky N (2008) Widespread changes in protein synthesis induced by microRNAs. *Nature* **455:** 58–63

Sharp PA (1994) Split genes and RNA splicing. *Cell* **77:** 805–815

Shimakami T, Yamane D, Jangra RK, Kempf BJ, Spaniel C, Barton DJ & Lemon SM (2012a) Stabilization of hepatitis C virus RNA by an Ago2-miR-122 complex. *Proceedings of the National Academy of Sciences of the United States of America* **109:** 941–946

Shimakami T, Yamane D, Welsch C, Hensley L, Jangra RK & Lemon SM (2012b) Base pairing between hepatitis C virus RNA and microRNA 122 3' of its seed sequence is essential for genome stabilization and production of infectious virus. *Journal of virology* **86:** 7372–7383

Shirley BC, Mucaki EJ, Whitehead T, Costea PI, Akan P & Rogan PK (2013) Interpretation, stratification and evidence for sequence variants affecting mRNA splicing in complete human genome sequences. *Genomics, proteomics & bioinformatics* **11:** 77–85

Sievers F, Wilm A, Dineen D, Gibson TJ, Karplus K, Li W, Lopez R, McWilliam H, Remmert M, Söding J, Thompson JD & Higgins DG (2011) Fast, scalable generation of high-quality protein multiple sequence alignments using Clustal Omega. *Molecular systems biology* **7:** 539

Spingola M, Grate L, Haussler D & Ares M (1999) Genome-wide bioinformatic and molecular analysis of introns in Saccharomyces cerevisiae. *RNA* **5:** 221–234

Starke S, Jost I, Rossbach O, Schneider T, Schreiner S, Hung L-H & Bindereif A (2015) Exon circularization requires canonical splice signals. *Cell reports* **10:** 103–111

Sumpter R, Loo Y-M, Foy E, Li K, Yoneyama M, Fujita T, Lemon SM & Gale M (2005) Regulating intracellular antiviral defense and permissiveness to hepatitis C virus RNA replication through a cellular RNA helicase, RIG-I. *Journal of virology* **79:** 2689–2699

Swayze EE, Siwkowski AM, Wancewicz EV, Migawa MT, Wyrzykiewicz TK, Hung G, Monia BP & Bennett CF (2007) Antisense oligonucleotides containing locked nucleic acid improve potency but cause significant hepatotoxicity in animals. *Nucleic acids research* **35:** 687–700

Szabo L, Morey R, Palpant NJ, Wang PL, Afari N, Jiang C, Parast MM, Murry CE, Laurent LC & Salzman J (2015) Statistically based splicing detection reveals neural enrichment and tissue-specific induction of circular RNA during human fetal development. *Genome biology* **16:** 126

Tabak HF, van der Horst G, Smit J, Winter AJ, Mul Y & Groot Koerkamp MJ (1988) Discrimination between RNA circles, interlocked RNA circles and lariats using two-dimensional polyacrylamide gel electrophoresis. *Nucleic acids research* **16:** 6597–6605

Tarr AW, Khera T, Hueging K, Sheldon J, Steinmann E, Pietschmann T & Brown RJP (2015) Genetic Diversity Underlying the Envelope Glycoproteins of Hepatitis C Virus: Structural and Functional Consequences and the Implications for Vaccine Design. *Viruses* **7:** 3995–4046

Thibault PA, Huys A, Amador-Cañizares Y, Gailius JE, Pinel DE & Wilson JA (2015) Regulation of Hepatitis C Virus Genome Replication by Xrn1 and MicroRNA-122 Binding to Individual Sites in the 5' Untranslated Region. *Journal of virology* **89:** 6294–6311

Tsai W-C, Hsu S-D, Hsu C-S, Lai T-C, Chen S-J, Shen R, Huang Y, Chen H-C, Lee C-H, Tsai T-F, Hsu M-T, Wu J-C, Huang H-D, Shiao M-S, Hsiao M & Tsou A-P (2012) MicroRNA-122 plays a critical role in liver homeostasis and hepatocarcinogenesis. *The Journal of clinical investigation* **122:** 2884–2897

Tuerk C & Gold L (1990) Systematic evolution of ligands by exponential enrichment: RNA ligands to bacteriophage T4 DNA polymerase. *Science* **249:** 505–510

Ule J, Jensen K, Mele A & Darnell RB (2005) CLIP: A method for identifying protein-RNA interaction sites in living cells. *Methods* **37:** 376–386

Umekage S & Kikuchi Y (2007) Production of circular streptavidin RNA aptamer in vivo. *Nucleic acids symposium series (2004):* 391–392

Umekage S & Kikuchi Y (2009) In vitro and in vivo production and purification of circular RNA aptamer. *Journal of biotechnology* **139:** 265–272

Umekage S & Kikuchi Y (2012) In Vivo Circular RNA Expression by the Permuted Intron-Exon Method. In *Innovations in Biotechnology* **4:** 76–90

van der Ree MH, van der Meer AJ, Bruijne J de, Maan R, van Vliet A, Welzel TM, Zeuzem S, Lawitz EJ, Rodriguez-Torres M, Kupcova V, Wiercinska-Drapalo A, Hodges MR, Janssen HLA & Reesink HW (2014) Long-term safety and efficacy of microRNA-targeted therapy in chronic hepatitis C patients. *Antiviral research* **111:** 53–59

van der Ree MH, Vree JM de, Stelma F, Willemse S, van der Valk M, Rietdijk S, Molenkamp R, Schinkel J, van Nuenen AC, Beuers U, Hadi S, Harbers M, van der Veer E, Liu K, Grundy J, Patick AK, Pavlicek A, Blem J, Huang M & Grint P et al (2017) Safety, tolerability, and antiviral effect of RG-101 in patients with chronic hepatitis C: A phase 1B, double-blind, randomised controlled trial. *The Lancet* **389:** 709–717

van Rooij E & Kauppinen S (2014) Development of microRNA therapeutics is coming of age. *EMBO molecular medicine* **6:** 851–864

Vaughan EE, DeGiulio JV & Dean DA (2006) Intracellular trafficking of plasmids for gene therapy: Mechanisms of cytoplasmic movement and nuclear import. *Current gene therapy* **6:** 671–681

Venø MT, Hansen TB, Venø ST, Clausen BH, Grebing M, Finsen B, Holm IE & Kjems J (2015) Spatio-temporal regulation of circular RNA expression during porcine embryonic brain development. *Genome biology* **16:** 245

Wahl MC, Will CL & Lührmann R (2009) The spliceosome: Design principles of a dynamic RNP machine. *Cell* **136:** 701–718

Wang PL, Bao Y, Yee M-C, Barrett SP, Hogan GJ, Olsen MN, Dinneny JR, Brown PO & Salzman J (2014) Circular RNA is expressed across the eukaryotic tree of life. *PloS one* **9:** e90859

Wang Y & Wang Z (2015) Efficient backsplicing produces translatable circular mRNAs. *RNA* **21:** 172–179

Wee LM, Flores-Jasso CF, Salomon WE & Zamore PD (2012) Argonaute divides its RNA guide into domains with distinct functions and RNA-binding properties. *Cell* **151:** 1055–1067

Westholm JO, Miura P, Olson S, Shenker S, Joseph B, Sanfilippo P, Celniker SE, Graveley BR & Lai EC (2014) Genome-wide analysis of drosophila circular RNAs reveals their structural and sequence properties and age-dependent neural accumulation. *Cell reports* **9:** 1966–1980

Will CL & Lührmann R (2011) Spliceosome structure and function. *Cold Spring Harbor perspectives in biology* **3:** a003707

Wyman SK, Knouf EC, Parkin RK, Fritz BR, Lin DW, Dennis LM, Krouse MA, Webster PJ & Tewari M (2011) Post-transcriptional generation of miRNA variants by multiple nucleotidyl transferases contributes to miRNA transcriptome complexity. *Genome research* **21:** 1450–1461

Xu H, Guo S, Li W & Yu P (2015) The circular RNA Cdr1as, via miR-7 and its targets, regulates insulin transcription and secretion in islet cells. *Scientific reports* **5:** 12453

Yang Q, Du WW, Wu N, Yang W, Awan FM, Fang L, Ma J, Li X, Zeng Y, Yang Z, Dong J, Khorshidi A & Yang BB (2017a) A circular RNA promotes tumorigenesis by inducing c-myc nuclear translocation. *Cell death and differentiation* **24:** 1609–1620

Yang Y, Fan X, Mao M, Song X, Wu P, Zhang Y, Jin Y, Yang Y, Chen L-L, Wang Y, Wong CC, Xiao X & Wang Z (2017b) Extensive translation of circular RNAs driven by N(6)-methyladenosine. *Cell research* **27:** 626–641

Yang Z-G, Awan FM, Du WW, Zeng Y, Lyu J, Wu D, Gupta S, Yang W & Yang BB (2017c) The Circular RNA Interacts with STAT3, Increasing Its Nuclear Translocation and Wound Repair by Modulating Dnmt3a and miR-17 Function. *Molecular therapy* **9:** 2062-2074.

Yeo G & Burge CB (2004) Maximum entropy modeling of short sequence motifs with applications to RNA splicing signals. *Journal of computational biology* **11:** 377–394

Yoshihisa T (2014) Handling tRNA introns, archaeal way and eukaryotic way. *Frontiers in genetics* **5:** 213

You X, Vlatkovic I, Babic A, Will T, Epstein I, Tushev G, Akbalik G, Wang M, Glock C, Quedenau C, Wang X, Hou J, Liu H, Sun W, Sambandan S, Chen T, Schuman EM & Chen W (2015) Neural circular RNAs are derived from synaptic genes and regulated by development and plasticity. *Nature neuroscience* **18:** 603–610

Yu CY, Li TC, Wu YY, Yeh CH, Chiang W, Chuang CY & Kuo HC (2017) The circular RNA circBIRC6 participates in the molecular circuitry controlling human pluripotency. *Nature communications* **8:** 1149

Zaphiropoulos PG (1996) Circular RNAs from transcripts of the rat cytochrome P450 2C24 gene: Correlation with exon skipping. *Proceedings of the National Academy of Sciences of the United States of America* **93:** 6536–6541

Zeisel MB, Crouchet E, Baumert TF & Schuster C (2015) Host-Targeting Agents to Prevent and Cure Hepatitis C Virus Infection. *Viruses* **7:** 5659–5685

Zhang S, Zhu D, Li H, Li H, Feng C & Zhang W (2017) Characterization of circRNA-Associated-ceRNA Networks in a Senescence-Accelerated Mouse Prone 8 Brain. *Molecular therapy* **9:** 2053-2061

Zhang X-O, Dong R, Zhang Y, Zhang J-L, Luo Z, Zhang J, Chen L-L & Yang L (2016a) Diverse alternative back-splicing and alternative splicing landscape of circular RNAs. *Genome research* **26:** 1277–1287

Zhang X-O, Wang H-B, Zhang Y, Lu X, Chen L-L & Yang L (2014) Complementary sequence-mediated exon circularization. *Cell* **159:** 134–147

Zhang Y, Xue W, Li X, Zhang J, Chen S, Zhang J-L, Yang L & Chen L-L (2016b) The Biogenesis of Nascent Circular RNAs. *Cell reports* **15:** 611–624

Zhao Y, Alexandrov PN, Jaber V & Lukiw WJ (2016) Deficiency in the Ubiquitin Conjugating Enzyme UBE2A in Alzheimer's Disease (AD) is Linked to Deficits in a Natural Circular miRNA-7 Sponge (circRNA; ciRS-7). *Genes* **7:** e116

Zheng Q, Bao C, Guo W, Li S, Chen J, Chen B, Luo Y, Lyu D, Li Y, Shi G, Liang L, Gu J, He X & Huang S (2016) Circular RNA profiling reveals an abundant circHIPK3 that regulates cell growth by sponging multiple miRNAs. *Nature communications* **7:** 11215

6 APPENDIX

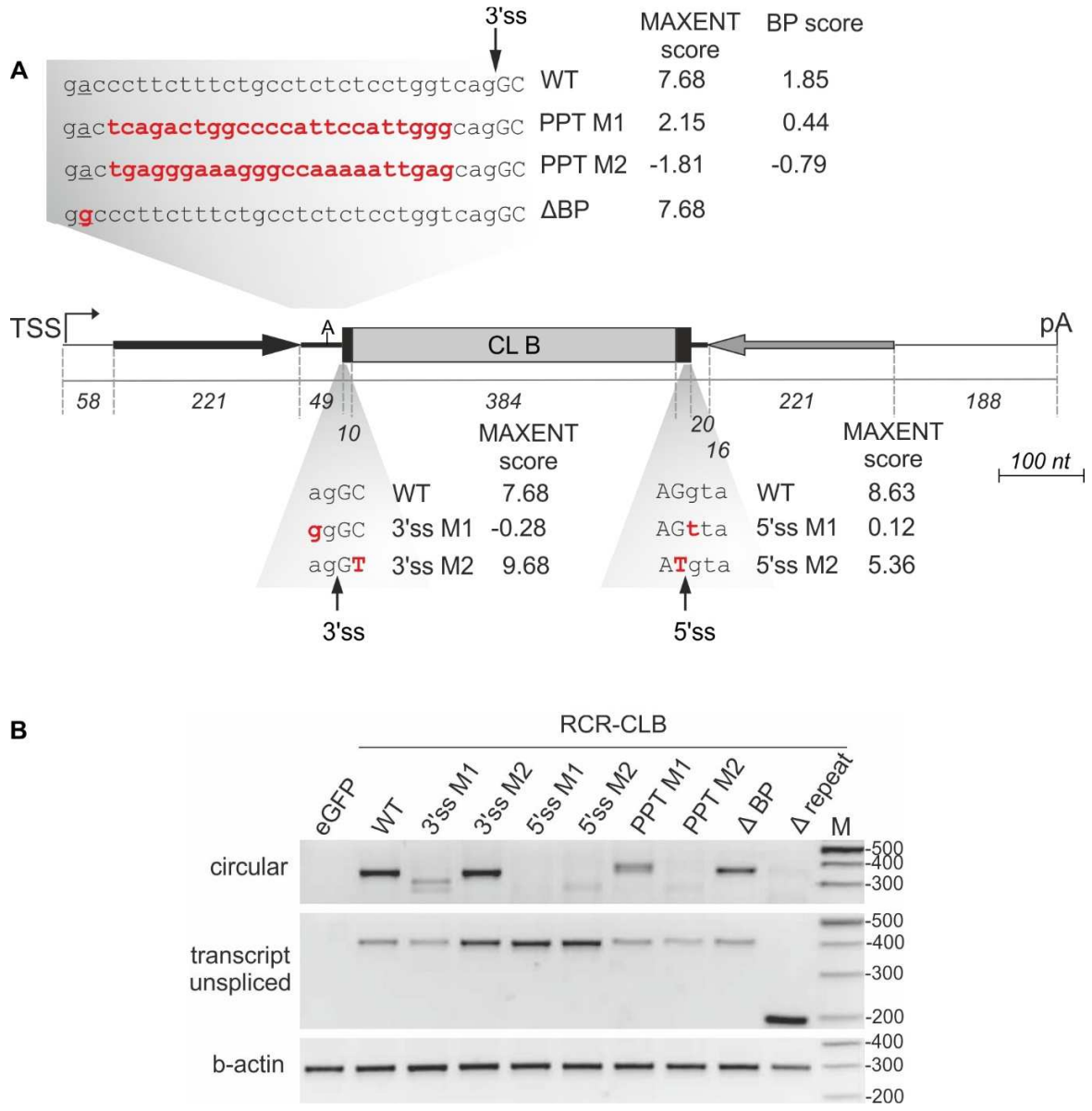

Figure A1 Mutational analysis of RCR-CLB minimal circRNA expression construct.
Schematic representation of the RCR-CL B mini-gene and the introduced mutations (M).The basal splice signals, such as the polypyrimidine tract (PPT) , the branch point (BP), 3'ss and 5'ss were mutated and altered nucleotides are highlighted in red. The influence of particular mutations on the splice site strength was predicted using MAXENT score, or on the branch point using BP score (**A**).
RCR-CL B mini-gene mutant derivatives shown in (A) and a deletion mutant for the repeat region (Δ repeat) were transfected into HeLa cells. The changes in the splicing pattern of the mutant derivatives were analyzed by using semi-quantitative RT-PCR. The circular isoform was detected with divergent primers in the circularizing exon, whereas the unspliced transcript was detected using convergent primers in the exon and near the polyadenylation signal (**B**). For controls eGFP was transfected and β-actin (b-actin) served as loading control.

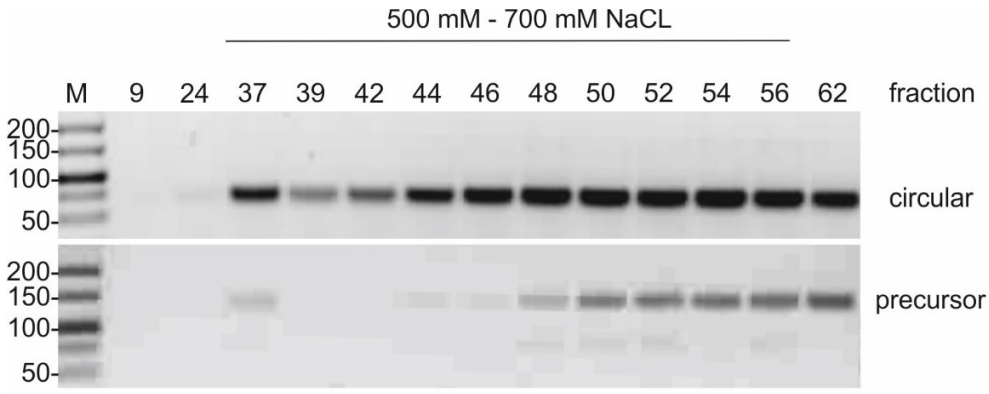

Figure A2 Test-purification of *in vitro* PIE ribozyme-generated circRNAs from *E.coli* total RNA.
1.6 µg *E.coli* RNA purified from uninduced culture were mixed with 0.9 µg of the *in vitro* PIE self-splicing reaction and subjected to anion exchange chromatography. Nucleic acids were eluted using a linear gradient from 500 mM to 800 mM NaCl. The RNA was isolated and fractions indicated were analyzed by RT-PCR detecting the circRNA or the unprocessed precursor of the PIE ribozyme.

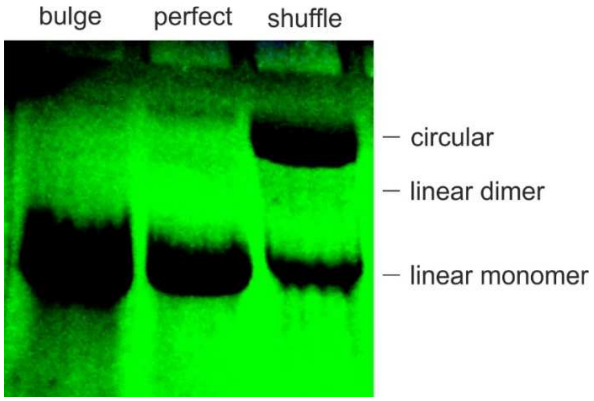

Figure A3 UV shadowing of *in vitro* synthesized circRNAs for gel-purification.
In vitro synthesized circRNAs were separated from linear dimers and monomers by preparative 7% PAA-gel electrophoresis. After the run, the gel was placed on a thin-layer chromatography plate and was irradiated with 254 nm UV light. Upon irradiation the plate emits green fluorescence, which is quenched by the nucleic acids. These appear as shadow bands.

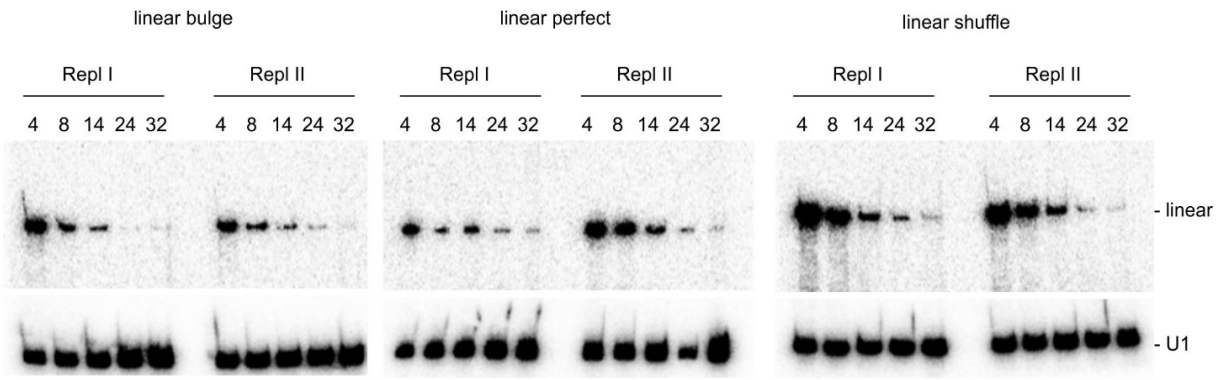

Figure A4 Stability analysis of transfected linear RNAs
The gel-purified linear RNAs (*bulge*, *perfect* and *shuffle*) were transfected into Huh7.5 cells. Total RNA was isolated from two replicates (Repl I, Repl II) at time points 4, 8, 14, 24 and 32 h. 30% of each sample was loaded and the transfected linear RNAs plus U1 snRNA were detected using ^{32}P internally labelled RNA probes (as described before). The lower panel showing U1 snRNA is displayed by a shorter exposure.

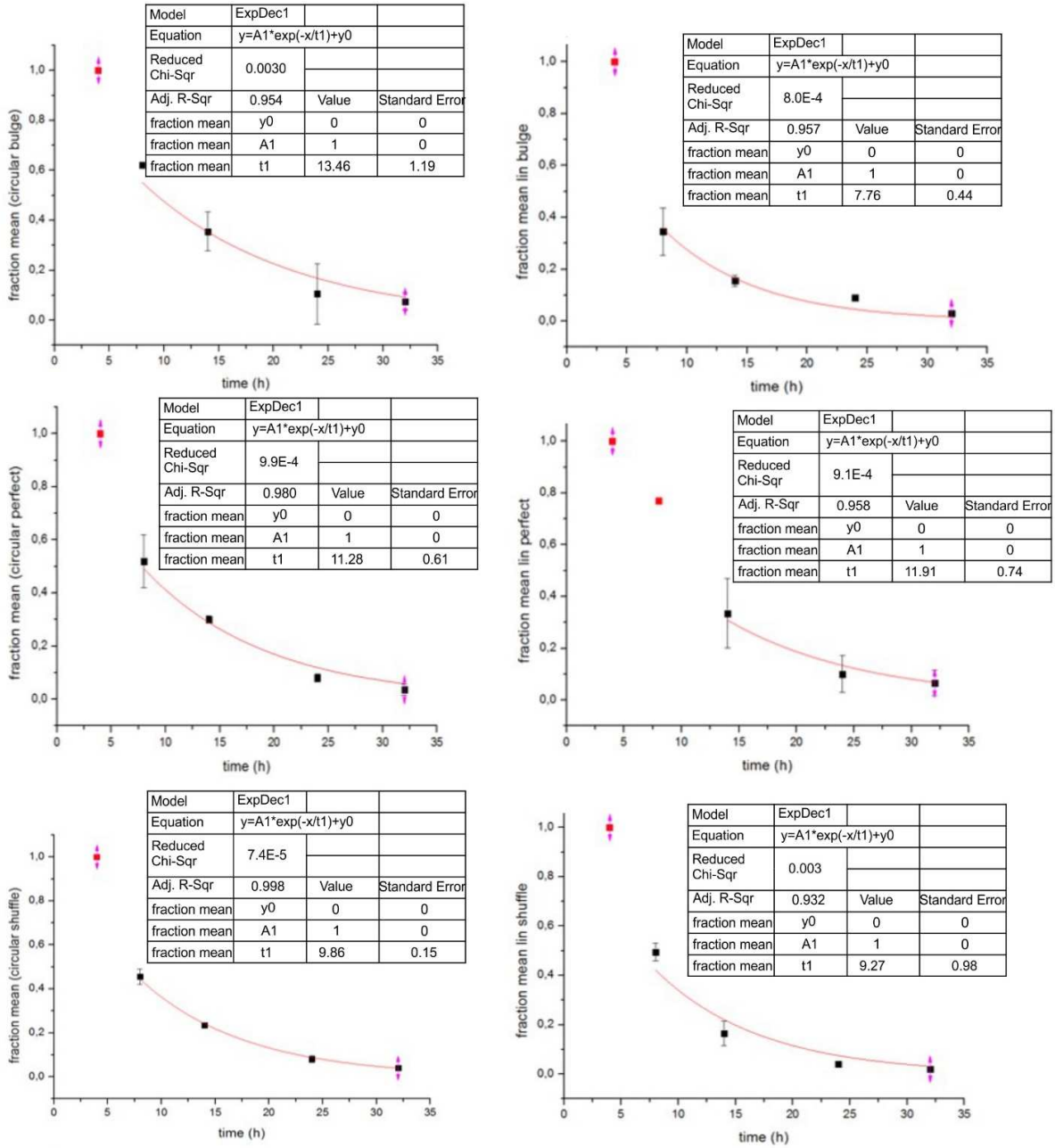

Figure A5 Half-life determination

The linear and circular RNAs (*bulge*, *perfect* and *shuffle*) were transfected into Huh7.5 cells. Total RNA was isolated at time points 4, 8, 14, 24, and 32 h. 30% of the linear RNAs and 20% of the circRNAs were subjected to northern blot analysis using ^{32}P labelled probes. The signals were quantified by phosphor imaging. Each graph is based on two experimental replicates (error bars SD). The values were normalized to the 4 h time point.

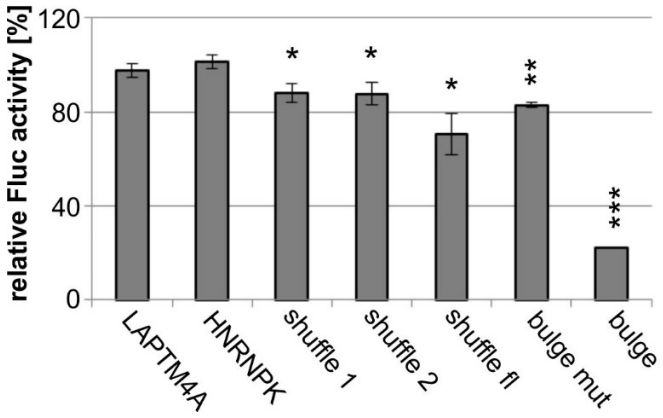

Figure A6 *Shuffle* negative control in comparison to the *bulge* miR-122 target site.
Huh7.5 cells were transfected with the pmirGLO Dual-Luciferase reporters, containing insertions in the 3'UTR derived from the first, or second part of the *shuffle* negative control sequence (*shuffle* 1, *shuffle* 2) or the full length *shuffle* sequence (*shuffle* fl). Firefly luciferase activity was compared to the negative controls *LAPTM4A*, *HNRNPK* and the *bulge* seed mutant. The *bulge* miR-122 binding site served as positive control. Firefly luciferase activity was measured, normalized to Renilla luciferase activity and to *LAPTM4A* negative control. Error bars represent SD from three replicates *p<0.05; **p<0.01; ***p<0.001.

7 LIST OF ABBREVIATIONS

%	percent
℃	degree Celsius
µ	micro
A	adenosine
Å	Ångström
AEC	anion exchange chromatography
AGO	argonaute
ALU	family of repetetive elements in human genomes
antagomiR	microRNA antagonist
APS	ammonium persulfate
b-actin	β-actin
BGH	bovine growth hormone
bp	base pairs
BP	branch point
BSA	bovine serum albumin
BVDV	bovine viral diarrhea virus
C	cytosine
C. elegans	*Caenorhabditis elegans*
cDNA	complementary DNA
CDR1as	cerebellar degeneration-related protein 1 antisense
circRNA	exonic circular RNA
ciRS-7	circular RNA sponge for miR-7
CLIP	crosslinking and immunoprecipitation
CMV	Cytomegalovirus
CTD	carboxy-terminal domain
DAA	direct acting antivirals
DAPI	4',6-diamidino-2-phenylindole
DIG	Digoxygenine
DMEM	Dulbecco's Modified Eagle Medium
DMF	Dimethylformamide
DMPC	Dimethyl pyrocarbonate
DNA	Deoxyribonucleic acid
dNTPs	Deoxynucleotides
DTT	dithiothreitol
E. coli	*Escherichia coli*
EDTA	Ethylenediaminetetraacetic
EGTA	Ethylene glycol tetraacetic acid
EM	electron microscopy
ER	Endoplasmatic reticulum
ESE	exonic splice enhancer
ESS	exonic splice silencer
et al	*et alii* (and others)
EtBr	Ethidium bromide
EtOH	Ethanol

EV	empty vector
FBS	fetal bovine serum
FF	Firefly
fw	forward
g	gram
G	guanosine
GAPDH	glyceraldehyde-3-phosohate dehydrogenase
GTP	guanosine triphosphate
h	hour
H. sapiens	*Homo sapiens*
HCC	hepatocellular carcinoma
HCV	Hepatitis C virus
HCV-FL	Hepatitis C virus Firefly luciferase reporter
I	inosine
IF	immunofluorescence
IGF1R	insuline-like growth factor 1 receptor
IRES	internal ribosome entry site
ISE	intonic splice enhancer
ISS	intronic splice silencer
k	kilo
kb	kilobase
KD	knockdown
kDa	kilo Dalton
KO	knockout
l	liter
LCL	lower confidence level
LNA	locked nucleic acid
lncRNA	long non-coding RNA
LS	large scale
M	marker
m	milli
M	molar
m	mock
m^7G	7-methylguanosine
mA	milliampere
MBL	muscleblind
MCMV	Mouse Cytomegalovirus
MCS	multiple cloning site
min	minutes
miRNA	microRNA
miR-x	microRNA-x
mRNA	messenger RNA
mut	mutant
n	nano
nm	nanometer
NPC	nuclear pore complex

nt	nucleotides
NTC	nineteen complex
NTP	nucleoside triphosphate
oligo	oligonucleotide
ORF	open reading frame
PAA	polyacrylamide
PAGE	polyacrylamide gel electrophoresis
PAS	polyadenylation signal
PBS	phosphate buffered saline
PCR	polymerase chain reaction
PIE	permuted inton-exon structure
PK	proteinase K
PPT	polypyrimidine tract
pre-miRNA	precursor-microRNA
pre-mRNA	precursor-messenger RNA
pri-miRNA	primary microRNA transcript
qPCR	quantitative PCR
RBP	RNA binding protein
RCR	reverse complementary repeat
RdRp	RNA-dependent RNA polymerase
RISC	RNA-induced silencing complex
RN	Renilla
RNA	ribonucleic acid
RNAP	RNA polymerase
RNP	ribonucleoprotein particle
rRNA	ribosomal RNA
rrnC	*E.coli* rRNA operon
RT	reverse transcription
RT	room temperature
RT-qPCR	quantitative reverse transcription-PCR
rv	reverse
s	seconds
S.cerevisiae	*Saccharomyces cerevisiae*
scaRNA	small Cajal-body associated RNA
SD	standard deviation
SDS	Sodium-Dodecyl-Sulfat
SEM	standard error of the mean
SL	stem loop
snoRNA	small nucleolar RNA
snRNA	small nuclear RNA
SRY	sex determination region Y
ss	splice site
t	time point
$t_{1/2}$	half-life
T4 PNK	T4 polynucleotide kinase
TDMD	target-directed miRNA degradation

TEMED	Tetramethylethylenediamine
Tris	tris(hydroxymethyl)aminomethane
tRNA	transfer RNA
TS	target site
TSS	transcription start site
TTN	titin
txt	transcript
u	Units
UCL	upper convidence level
UTR	untranslated region
UV	ultraviolet
V	volt
W	Watt
WHO	Wold Health Organisation
WT	wildtype
xg	times gravity
α	alpha
β	beta
γ	gamma

8 SCIENTIFIC ACHIEVEMENTS

Publications

Starke S, **Jost I**, Rossbach O, Schneider T, Schreiner S, Hung L-H & Bindereif A (2015) Exon circularization requires canonical splice signals. *Cell reports* **10:** 103–111

Jost I*, Shalamova L*, Gerresheim GK, Niepmann M, Bindereif A, Rossbach O. (2017) Functional sequestration of microRNA-122 from Hepatitis C Virus by circular RNA sponges. *RNA biology*. (manuscript under revision)
* These authors contributed equally to this work.

Poster presentation

The Non-Coding Genome EMBL Symposium
October 18th to October 21th 2015 Heidelberg, Germany
Jost I, Shalamova L, Aulbach L, Niepmann M, Bindereif A, Rossbach O. Functional sequestration of microRNA-122 from Hepatitis C Virus by circular RNA sponges.

9 ACKNOWLEDGEMENTS

An dieser Stelle möchte ich mich bei den Personen bedanken, die mir diese Arbeit ermöglicht haben, mich gefördert und unterstützt haben.

Mein Dank gilt:

…Prof. Dr. Albrecht Bindereif für die hervorragende Betreuung während meiner Arbeit, fachliche Ratschläge, anregende Diskussionen in den Labmeetings und die Begutachtung meiner Arbeit.

…Dr. Oliver Rossbach für die Bereitstellung eines interessanten Themas, für stetige Ansprechbarkeit, Motivation und die ausgeklügelten Lab Hacks.

…Prof. Dr. Michael Niepmann als Kooperationspartner bei dem circRNA/HCV Projekt, für fachlichen Rat bei den viralen Reportersystemen und für die Anfertigung des Zweitgutachtens.

…meinen Kollegen, Mitstreitern und den ehemaligen Kollegen.
Christian, Tim, Silke, Henrik, Stefan, Heinrich und Patrick. Ich danke euch für die tolle Arbeitsatmosphäre, Gespräche, Ratschläge, die Kaffeepausen ;)…..und noch vieles mehr. Es war eine schöne Zeit mit euch!

…Lyudmila und Gesche für die Experimente und den Einsatz bei der Revison. Im Besonderen danke ich Lyudmila für die Durchführung der Experimente im S3 Labor-das wäre ohne dich nie möglich gewesen.

…Prof. Dr. Peter Friedhoff für die Ratschläge bei der Bestimmung der Halbwertszeiten.

…Christina und Lena, die durch ihre tolle Arbeit während der Masterthesis das Projekt durch Vorexperimente maßgeblich vorangebracht haben.

…Tom, Lennart und Bernhard aus der Mibi für die Ratschläge zur Expression und Aufreinigung von circRNAs in *E.coli*.

…natürlich meinen Freunden ;D

…und nicht zuletzt meinen Eltern und meiner Familie. Ihr habt mich immer unterstützt =) Vielen Dank dafür!

10 EIDESSTATTLICHE ERKLÄRUNG

Hiermit versichere ich, die vorgelegte Thesis selbstständig und ohne unerlaubte fremde Hilfe und nur mit den Hilfen angefertigt zu haben, die ich in der Thesis angegeben habe. Alle Textstellen, die wörtlich oder sinngemäß aus veröffentlichten Schriften entnommen sind, und alle Angaben die auf mündlichen Auskünften beruhen, sind als solche kenntlich gemacht. Bei den von mir durchgeführten und in der Thesis erwähnten Untersuchungen habe ich die Grundsätze guter wissenschaftlicher Praxis, wie sie in der ‚Satzung der Justus-Liebig-Universität zur Sicherung guter wissenschaftlicher Praxis' niedergelegt sind, eingehalten. Gemäß § 25 Abs. 6 der Allgemeinen Bestimmungen für modularisierte Studiengänge dulde ich eine Überprüfung der Thesis mittels Anti-Plagiatssoftware.

Datum	Unterschrift